POLITECNICO DI MILANO

M.Sc. in Civil Engineering for Risk Mitigation

3D Model Generation and FEM analysis of Santa Maria Novella

Supervisor

Dr. Alberto Taliercio

Thesis by

Sepehr Beheshti

799066

September 2015

POLITECNICO DI MILANO

3D Model Generation and FEM analysis of Santa Maria Novella

A Master thesis submitted to Department of Civil and Environmental Engineering in partial fulfillment of the requirements for the degree of Master of Science in Civil Engineering for Risk Mitigation.

Submitted by:

Sepehr Beheshti
Student ID: 799066

Supervised by:

Dr. Alberto Taliercio
Dept. of Civil Engineering
Politecnico di Milano
Piazza L. da Vinci, 32, I-20133 Milan

Abstract (English)

Santa Maria Novella can be considered as a Masonry gothic church including different types of arches, vaults, pillars and walls. One of the most effective methods for structural analyzing of such a masonry building is implementing finite elements model analysis methods. In the procedure of the FEM analysis, the geometrical model must be developed then by considering various parameters such as elements type, materials, element connection properties, element interaction definition and support and constraint assignment then the finite elements model will be developed. For FEM analysis there are two possible methods for developing geometrical model, the first method is generating of 3D model of mono or bi-dimensional elements which will be 3D model without thickness of the parts and the second method is the generation of complete 3D geometrical model according to the real tri-dimensional elements of the structure then by defining other parameters the finite elements model will be developed. In this project by taking the data of geometrical survey and precise geometrical details of the element into consideration, the 3D model of the tri-dimensional elements of the structured is generated and by assigning 3D linear elements type, the meshing model through all over the assembled model is done and then by defining materials, boundary conditions and static loading system the final FEM is achieved and finally the structural analysis is done by using Abaqus software. After completing the analysis the maximum and minimum principal stress and also the displacements are demonstrated and they are compared with the previous project results.

Author keywords: Santa Maria Novella, masonry, geometrical survey, finite elements model, 3D geometrical model, tri-dimensional elements.

Sommario

Santa Maria Novella a Firenze è una chiesa gotica in muratura che comprende diversi tipi di archi, volte, pilastri e pareti. Uno dei metodi più efficaci per l'analisi strutturale di un edificio in muratura di questa complessità è sviluppare un modello a elementi finiti. Nella procedura di analisi FEM, il modello geometrico deve essere sviluppato considerando elementi diversi per le varie parti della struttura e tenendo conto dei diversi materiali presenti, del tipo di interazione fra gli elementi strutturali e delle condizioni al contorno cinematiche e statiche. Per l'analisi FEM ci sono due possibili metodi per lo sviluppo del modello geometrico: il primo consiste nel generare un modello 3D composto da elementi mono- o bidimensionali, di trave e di guscio; il secondo metodo consiste nella generazione di un modello realmente 3D, che riproduca fedelmente la geometria della struttura. In questo lavoro di tesi, partendo dai dati di un rilievo mediante laser scaner di alcune parti della chiesa e da piante e sezioni disponbili, è stato generato un modello 3D estremamente accurato della struttura. Utilizzando elementi finiti tetraedrici lineari, è stata svolta l'analisi strutturale della chiesa sotto il peso proprio utilizzando il software Abaqus. L'analisi fornisce in particolare gli sforzi principali minimi e massimi, che vengono confrontati con i risultati ottenuti in precedenti lavori con modelli formati da travi e gusci e con il quadro fessurativo rilevato nella chiesa.

Parole chiave: Santa Maria Novella, muratura, rilievo geometrico, modello a elementi finiti, modello geometrico 3D, elementi tridimensionali.

Acknowledgments

I would like to express my sincere gratitude to my advisor, Prof. Alberto Taliercio, who was so supportive and always available to help me to come up with some solutions for any kind of problems. Cause of his patience, kindness, respect to the students, and immense knowledge, I have got lots of support and encouragement to accomplish my project, so it was a great pleasure to do my final thesis with him. I am so grateful to him for being my supervisor.

Sepehr Beheshti

Politecnico di Milano

September 2015

Contents

Chapter 1

INTRODUCTION

[*This chapter is taken from "Final Project Report Santa Maria Novella, Florence, Italy prepared by: Thomas E. Boothby Department of Architectural Engineering the Pennsylvania State University 104 Engineering Unit at University Park, PA 16803-1416, USA"*]

1.1. Santa Maria Novella

1.1.1. Introduction

Figure 1 Santa Maria Novella in Florence

Santa Maria Novella is a church in Florence, Italy, which chronologically, it is the first great basilica in Florence, and is the city's principal Dominican church. This church was called Novella (New) because it was built on the site of the 9th-century oratory of Santa Maria delle Vigne. The church was designed by two Dominican friars, Fra Sisto Fiorentino and Fra Ristoro da Campi. The church is 99.2 long and it is about 28.3 meters in width in nave part and 61.54 meters in width in transept part. Building of the church began in 1279 and was finished in 1360 under the supervision of Friar Iacopo Talenti with the completion of the Romanesque-Gothic bell tower and sacristy. At that time, only the lower part of the Tuscan gothic facade was finished. The three portals are spanned by round arches, while the rest of the lower part of the facade is spanned by blind arches, separated by pilasters, with below Gothic pointed arches, striped

in green and white, capping noblemen's tombs. This same design continues in the adjoining wall around the old churchyard. The church was consecrated in 1420.

Like their counterparts in other regions of Europe, Italian builders of the Gothic era experimented with new types and methods of construction, such as the domical vaults of Santa Maria Novella raised high on slender shafts, so much more daring than the domical vaulted churches of Romanesque and Gothic Lombardy, and achieved without the aid of the iron tie rods so often seen in Italian Gothic buildings. In so doing, the builders of Santa Maria Novella created that airy interpenetration of space that would come to characterize Tuscan Gothic architecture.

Figure 2 Main nave of the church

1.1.2. Chronology of Interventions at the Site

There is no record of major interventions to the vaulting or to any element of the basic structural system of Santa Maria Novella. Documented and identifiable interventions on the building include the removal of the tramezzo (screen) that extended across the entire interior of the nave and the changing of the shape of the windows in the side aisles in the 16th century under the direction of Giorgio Vasari. The aisle windows were again changed in the 19th century, back to a Gothic lancet shape, the floor was relaid, and a new roof replaced the old one, also in the 19th century. In the 20th century, work was largely restricted to restoration and maintenance of the interior plasterwork and fresco decorations and consolidation of the 15th century marble veneer on the façade. This same facade is currently undergoing a cleaning process, a project carried out by the Commune of Florence.

1.1.3. Measured Drawings

The church of Santa Maria Novella was constructed in an unusual orientation, with the main facade 'oriented' to the south. The construction of the nave proceeded from the crossing to the main facade, that is, towards the south. As such, we have numbered the bays 1 through 6 beginning with the bay closest to the crossing. Bays 1 and 2 are clearly rectangular. The remaining four bays, variable in length, are closer to square in plan. The aisle bays are designated by a number reflecting the bay number and E or W, to identifying their location to the east or the west of the nave. Figure 1 shows a key plan, illustrating the orientation of the nave and the numbering scheme adopted for the bays.

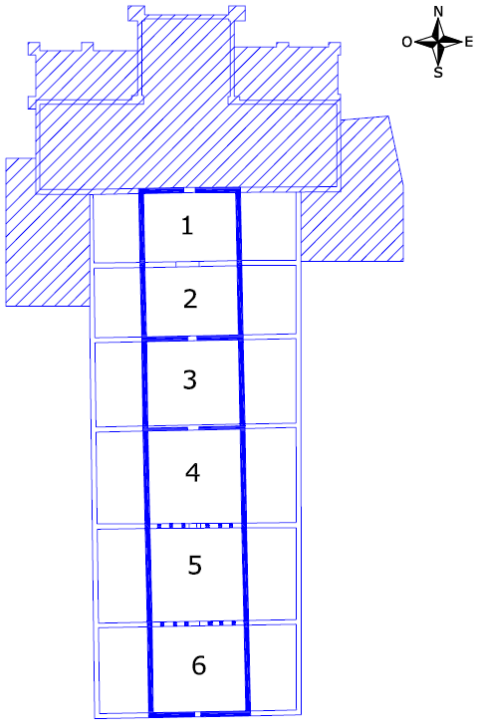

Figure 3 Key plan of nave of Santa Maria Novella

Two sets of measured drawings have been produced for the nave of Santa Maria Novella. The first set was produced by a team from The Pennsylvania State University in summer 2002, using funding from the Kress Foundation and others, and has remained largely unmodified since then. In the present project. Small corrections have been made to these drawings, including corrections to the height of the column bases, and to the shape of the nave. These drawings were produced by establishing a baseline along the length of the nave, taking x-y-z measurements at specific points in the nave with a reflector less total station, and transferring the measured coordinates manually to written notes. The notes were used to generate drawings, using the computerized drafting software AutoCAD. Detailed elevation measurements were taken in Bay 2 and 5 only. This drawing set includes detailed plan information, a longitudinal section, and detailed transverse sections in bays 2 and 5. It also includes a rudimentary drawing of the layout above the nave vaults.

The second set of drawings were taken directly as part of the present project in July and September 2006. These are detailed drawings of features above the vaults. The information collected includes highly detailed computer models of the surface of the extrados of the vaults in Bays 2 and 5 (See Figure 4), detailed surveys of the transverse walls above the nave vaults, and surveys of the

transverse walls above the aisle vaults. A set of drawings representing a thorough summary of the survey of cracking in the vaults and walls above the nave and aisles is done for comparing with the analysis results.

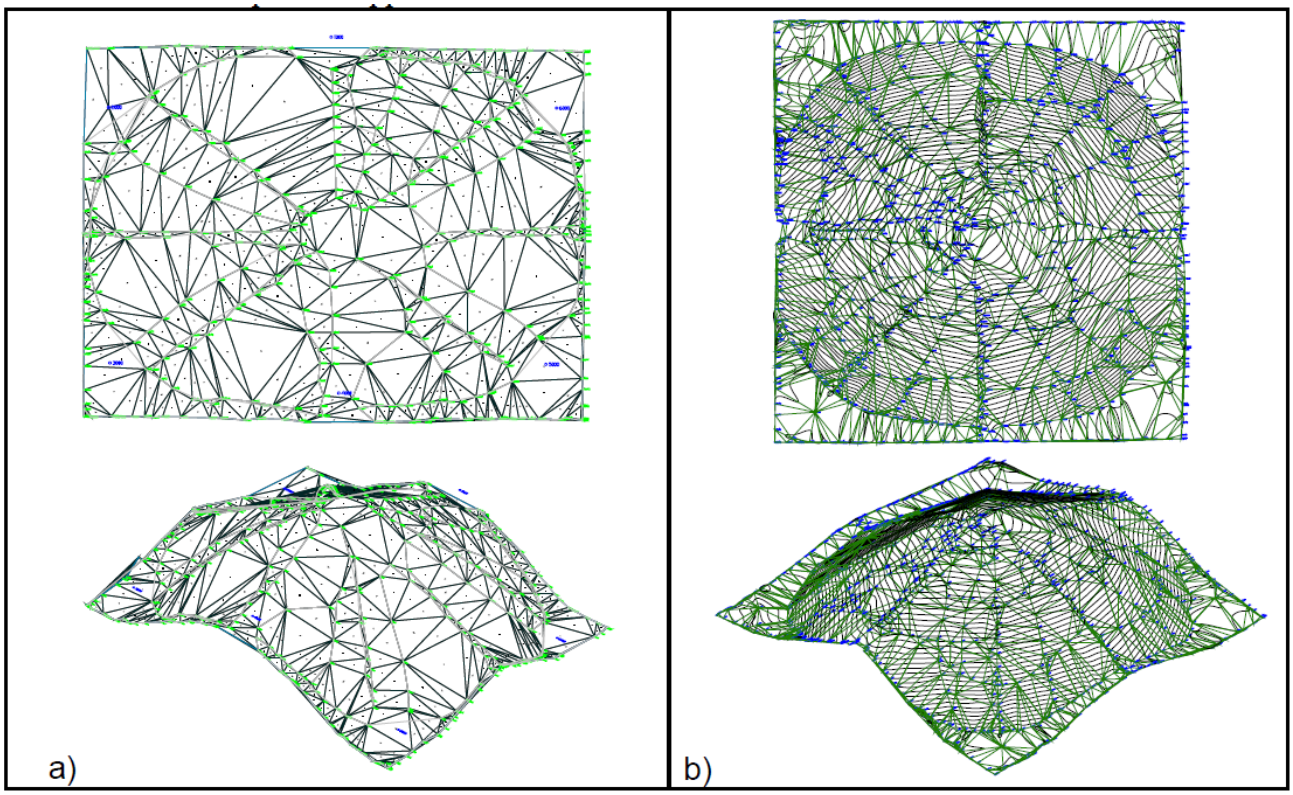

Figure 4 the network used to survey the extrados of the vaults (a) Bay 2 of Nave and (b) Bay 5 of nave

A further effort has gone into the measurement of the plan and elevation dimensions of the pier and pilaster bases in the nave. This study has been particularly important, as there is substantial variation in these features, which is suggestive of a construction sequence for the nave.

1.1.4. Typology

The bases of the nave are not all alike but can roughly be divided into three groups, based on their forms.

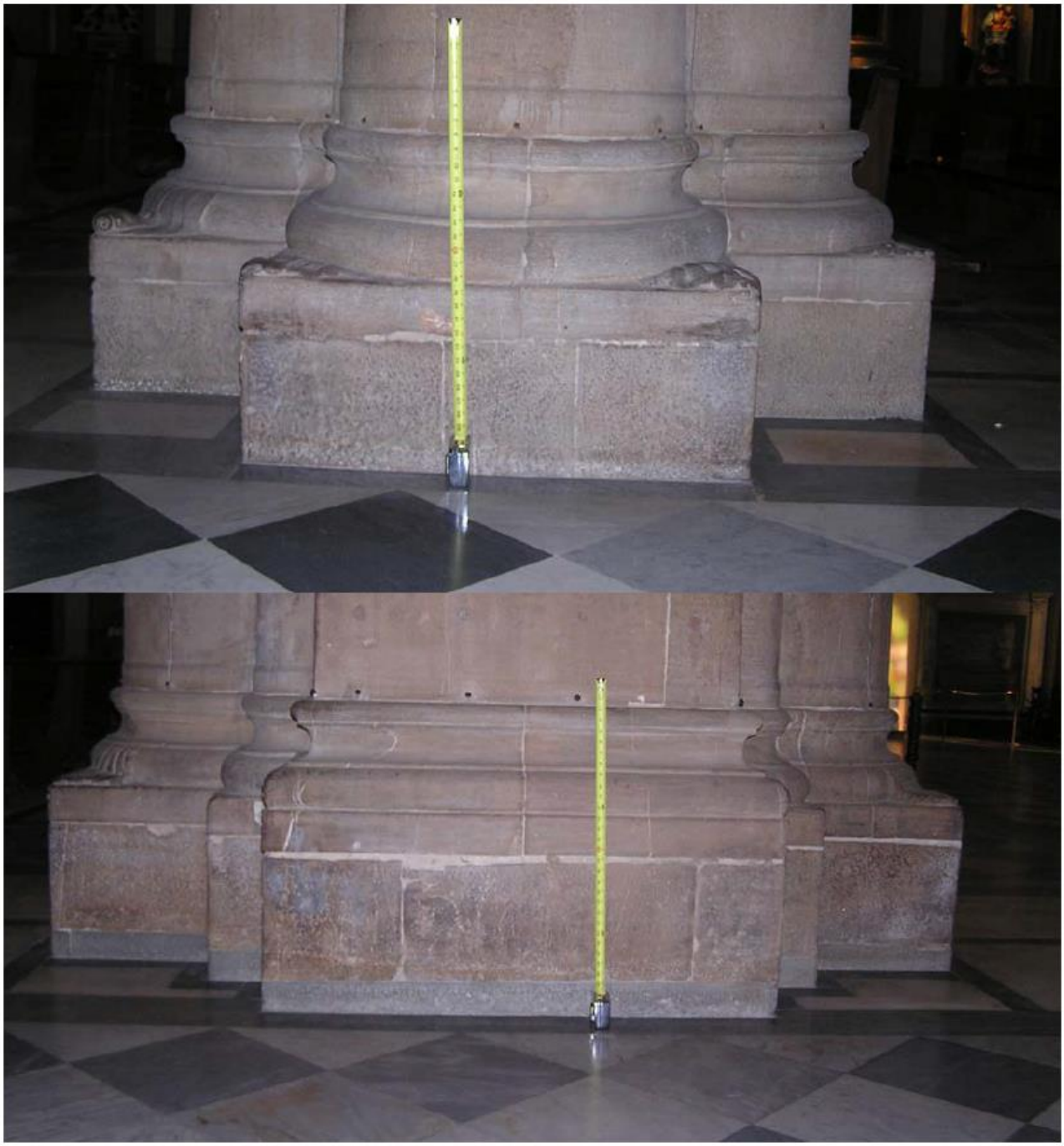

Figure 5 Base Group 1, light pier (2 West), and heavy pier (3 West)

Group 1:

The first two bays adjoining the crossing are markedly different from the four other bays, being built on a rectangular plan. The piers in these bays are alternately heavy and light, with the diagonal vault ribs springing from round colonnettes in the angles of the heavy compound piers,

while they simply disappear into the impost blocks of the main columnar element on the light piers, whose bases give no indication of being intended to support cross vaults. In addition, all the ribs in the aisles of these two bays also spring directly from the tops of the piers rather than from colonnettes. Also to be included in this group are the bases of the two pilasters of the façade wall whose placement is in line with the main piers of the nave. Like the pilasters of the first two nave bays, the bases on the façade wall have no colonnettes, so that the cross ribs of the aisle vaults spring directly from their impost blocks while those of the high vault above them spring instead from corbels keyed into the façade wall. All of the bases in this group share a similar molding profile and many of them have decorative spurs on the corners, usually of a foliate design.

Figure 6 Vault ribs over 4-lobed pier

Group 2:

This comprises the bases of the pilasters along the perimetral wall in the east aisle of the nave extending to the façade. These bases are characterized by moldings similar to those in Group 1 and by the presence of corner spurs, again like the bases in Group 1. However, they also have octagonal colonnettes on either side of the main columnar section of each pilaster, intended to support the diagonal ribs of the cross vaults over the aisles. These octagonal ribs are a characteristic of Group 3.

Group 3:

The rest of the bays in the four southernmost bays of the nave and aisles all share a similar design. Like the bases of Group 2, they are compound piers with octagonal colonnettes in the angles to support the diagonal ribs of the vaulting. They differ, however, in the molding profile and in the way the corners of the bases have no spurs but instead are cut off and beveled down at an angle.

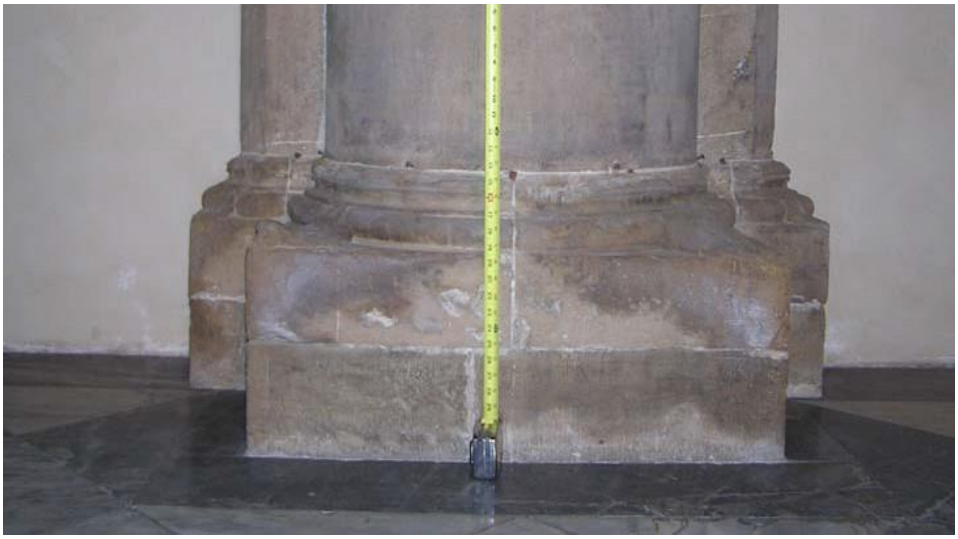

Figure 7 Base Group 2, (5 East)

Figure 8 Base Group 3 Pier (5 West)

Measurements:

While similar in plan, the bases are not all of the same height. For example, in bay 5, the base of Pier 6W (39 cm above floor) is higher than that of Pier 6E (31 cm above floor) by 8 cm, while Pilaster 6W along the west aisle wall (62 cm above floor) is 31 cm higher than Pier 6E. Pilaster 6E is 32 cm above the floor, similar to Pier 6E.

Questions and Tentative Hypotheses to be derived from the Evidence of the Bases

1) The first two bays appear to have been designed for sexpartite vaulting, often constructed on alternately light and heavy supports. The design of the other four bays is consonant with four-part domical vaulting. Yet the entire nave is covered with four-part domical vaults. Medieval domical vaults were usually erected over square bays, better suited to them structurally. Why then do we find domical vaults also over the two rectangular bays of the nave? Was their presence the result of a change in design?
2) The bases along the aisle walls in the first two bays and on the facade wall do not make any provision for the support of ribbed vaulting, whereas the rest of the bases have either round or octagonal colonnettes from which the cross ribs ultimately spring. Does this indicate that the original design did not call for vaults at all? Were the heavy piers of the first two bays originally intended to support transverse walls across a timber-roofed nave, as in the 12th c. Florentine church of San Miniato al Monte?
3) Does the fact that the two bases on the façade wall as well as those along the outer wall of the east aisle differ in design from the rest of the bases in the four southernmost nave bays indicate a difference in building campaign? Can one deduce from the fact of their similarities to those in the first two bays that these bases, and hence these walls, were put in place before the west aisle wall and the main piers of the nave in this section?
4) Do the variations in height have any significance for our understanding the sequence and process of construction? Again, can they be interpreted as deriving from different building campaigns, perhaps with different master masons?

1.2. Structural Problem

1.2.1. Crack and Defect Documentation

Cracks and defects have generally been documented by visual inspection and production of drawings illustrating the observed conditions. The observations have concentrated on three main areas, the back of the vaults, the transverse walls above the nave vaults, and the transverse walls above the aisle vaults. The extrados of the vaults has a cement plaster coating in many locations. Although this makes the observation of the configuration of the bricks used in vaulting difficult, it makes the existence of cracks quite apparent. Based on locations of diagonal ribs, which are also easy to locate on the vaults, the location and general size information on visible cracks have been noted. The transverse walls between bays above the nave permit two types of observations: general construction details and condition information. General construction details include patterns and coursing of stonework, the frequency and type of ties to the nave wall, the location of corbels and truss seats, and the evidence in the wall of different phases of construction.

Condition information collected on these walls includes the location and size of cracks, missing stonework, and evidence of prior repairs.

Cracking in vaults:

The nave vaults are subject to cracking along diagonal ribs. The cracks vary in size from less than 1 mm to 1 cm. In Bay 3, the cracks are stitched with iron bars, while repairs to the cracks in the other bays are not in evidence. The most severe cracking is evident in Bays 2, 3, and 4. (See Figure 9).

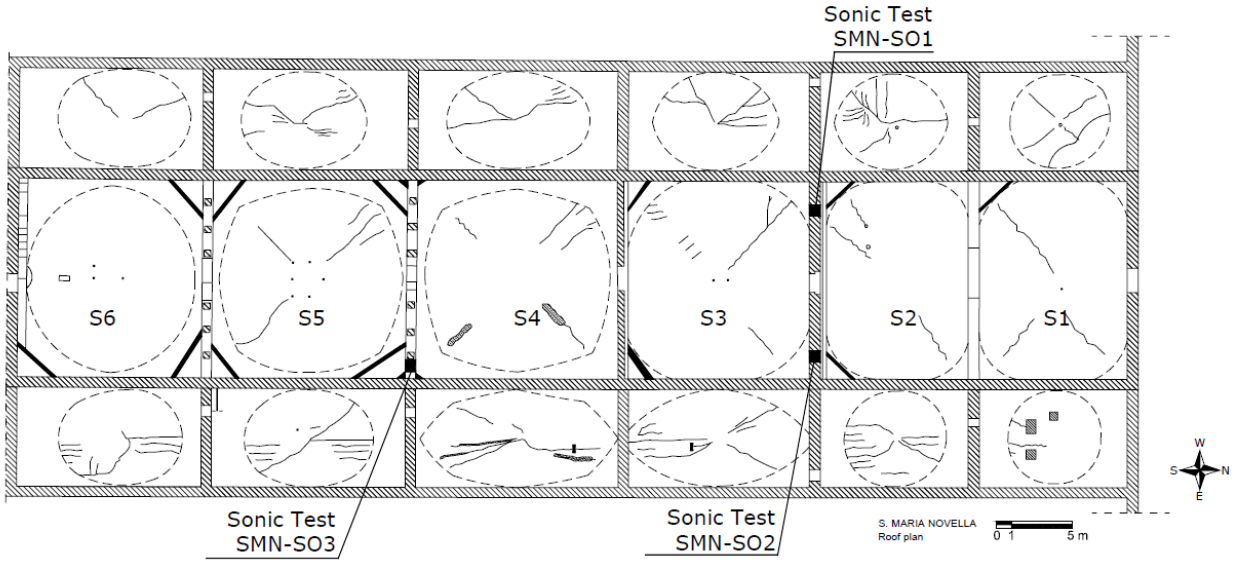

Figure 9 Summary of main cracks in nave vaults (looking upwards, east and west reversed)

The vaults in the west aisle show a high level of cracking and deformation. Some of the cracks are over 2 cm and extend through the entire thickness of the vault. In addition, relative deformation on the two sides of the cracks may be close to 5 cm in two of the vaults. The east aisle vaults have much less visible damage, but include some small (1-2 mm cracks) in a similar pattern.

Cracking in nave transverse walls

Significant cracking has been observed in the transverse walls that separate nave bays, particularly the full-height walls between bays 2-6. The cracks tend to be vertical or near vertical, to initiate approximately at the surcharge intersection of the filling and the vault extrados, and to propagate upwards towards the ridge line. An example of such a crack, between bays 3 and 4, is shown in Figure 10.

Figure 10 Cracks and repaired cracks on the transverse wall between Bays 3 and 4

A severe level of cracking has been noted in the transverse walls in the west aisle. The cracks display two similar patterns. They either extend from the surcharge adjacent to the west exterior wall upwards toward the east, usually passing through the opening into the adjacent vault, or they form between the transverse wall and the west exterior wall, taking advantage of the lack of interlocking between the transverse wall and the exterior wall/buttress. In the walls between bays 3/4, 4/5, and 5/6, the total movement on the two sides of the cracks exceeds 15 cm. Similar patterns of cracking have not been noted in the east aisle.

Figure 11West Aisle: transverse wall between Bays 3 and 4. Cracking and shifting of the stonework of up to 20 cm has been noted

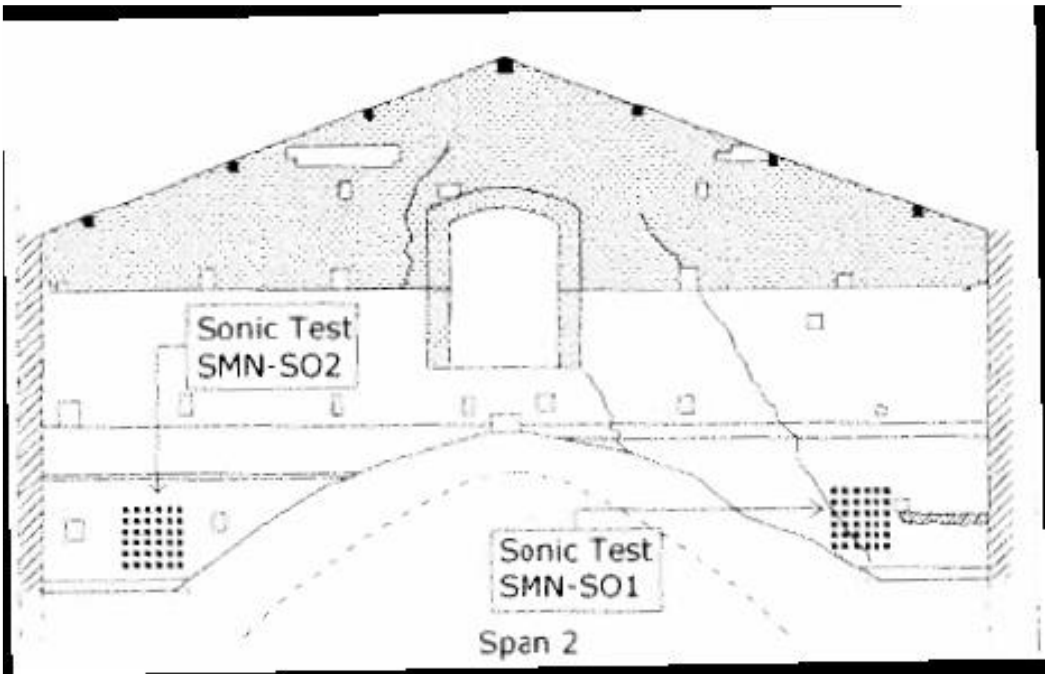

Figure 12 Summary of main cracks in the wall in transept part

The following construction irregularities have been noted.

Form of vaults:

The shape of the nave vaults results in almost flat expanses of masonry between diagonal ribs, particularly in nave bays 3-5. In some cases the extrados of the vaults can be observed to be observed to be concave, particularly in Bays 3 and 5 to the east and west of the central axis. It is unknown whether this anomaly in the shape of the vaults results from the original construction or is a result of long-term deformations of the vaults.

Similarly, in the west aisle, the extrados of the vaults is nearly flat along a line running east and west from the apex of the vault. In some cases, particularly in bays 2 and 3, this line is concave, with a visible sag. In Bays 2, 3, and 4, a north-south crack is evident in the west aisle vaults, with relative (north-south) horizontal displacements of up to 6 cm across the crack. Since these patterns is not repeated in the other vaults of the west aisle, and the vaults of the east aisle, this is considered to be an effect of the general structural problems observed in the west aisle.

Tying of transverse walls to nave walls:

A detailed survey of the tying of transverse walls to transverse walls was undertaken by a student from Polytechnics o Milan and summarized in the Marenda thesis referenced in the Appendix.

In general, significant efforts were found to interlock masonry between the transverse walls and the nave walls, especially in the rectangular bays towards the north end of the nave. However, as shown in the detailed diagrams, this connection between nave wall and transverse wall appears to be an afterthought, with the tying accomplished by removing stones from the nave wall, and projecting stones from the transverse wall into the connecting stonework. The nave walls and transverse walls have inconsistent coursing, and stone sizes, and the appearance of the corners is very irregular.

Figure 13 Wall between nave bays 4 and 5

Also present are two types of ties, appearing to date from the original construction of the basilica: single interlocking stones at the intersection, and diagonal wood ties, which connect to internal wood ties embedded in the wall.

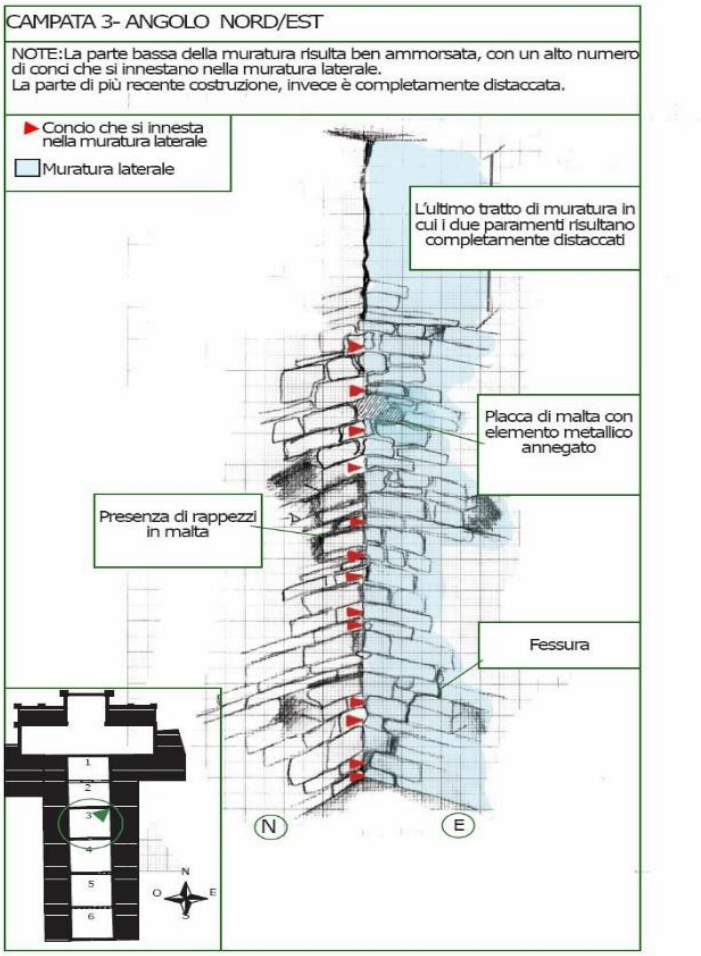

Figure 14 Detailed drawing of connection of nave wall

Tying of transverse walls to west aisle walls

There is little evidence of tying of the transverse walls to the exterior walls above the aisle vaults, on either the east or the west side of the nave. In general, the construction of these two features appears to be independent, with entirely different coursing, and only occasional, very shallow penetration of the masonry from the transverse wall into the exterior wall. This has facilitated the separation between these two features, described above. (See Figure 14)

Figure 15 Junction between transverse aisle wall between Bays 3 and 4 and west wall of church

In view of this evidence, it appears that the transverse walls were conceived after the nave and aisle walls had been constructed to approximately their full height. The role that these walls were meant to play is much more difficult to discern. Previous modeling efforts (see Erdogmus dissertation, referenced in publications list) have focused on the influence of the walls on the transverse lateral thrusts of the nave. Two key elements have not yet been considered, and will receive significant attention as the work progresses.

First, Rocchi asserts that the transverse wall, between the transept and Bay 1, and between Bay 2 and Bay 3, at least, are meant, in conjunction with the nave walls to function as a rectangular 'tower' and assist in resisting the lateral thrust from the transept vaults. This outlook would assign to these walls a date approximately similar to the vaulting of the transept, much later than the vaulting of the nave, and would still leave the question of the intended purpose of the remainder of the transverse nave walls unanswered.

Second, given our inclination to believe that the transept vaulting is much later than the nave vaulting, based on observation of the type of moldings used in the ribs and the generally lighter construction of the transept vaults, it is necessary to consider a hypothesis concerning the transverse walls that does not depend on the presence of the transept vaulting. In the previous study, the walls were considered in the absence of the elaborate system of tying the transverse walls to the nave walls. As such, the conclusion, as outlined in the Erdogmus dissertation, was that the transverse walls simply add dead weight to the transverse arches without contributing to their resistance to transverse thrust.

However, in considering the evidence of significant efforts to tie the two walls together, especially the unusual system of diagonal timber ties connecting to timber ties embedded into the walls, it becomes apparent that such transverse walls *can* contribute significant lateral resistance to the overall masonry assembly. This may be simply illustrated by the two diagrams shown in Figure 13, where the failure mechanism of an arch/buttress/wall system without transverse tying is compared to the failure of a similar system tied through transverse walls. The primary mechanism

is the rotation of each half of the arch ring, with the crown descending, and the springing rotating outwards. This mechanism is driven by the descent of the center of gravity of the arch ring. Where ties are not provided (Figure 15), the transverse wall splits in two parts and rotates about the same center as the arch, adding to the effect of the failure mechanism.

Where ties are provided (Figure 15), the transverse walls tend to be retained in a vertical position, and only a small part of the wall breaks off and descends with the arch ring. As a result, the vertical load on the pier is increased, and the energy driving the failure mechanism is reduced. The crack patterns illustrated in Figure 16 show that this tying to the transverse walls may be more or less effective.

Figure 16 Crack patterns suggestive of influence of wall ties on transverse nave walls

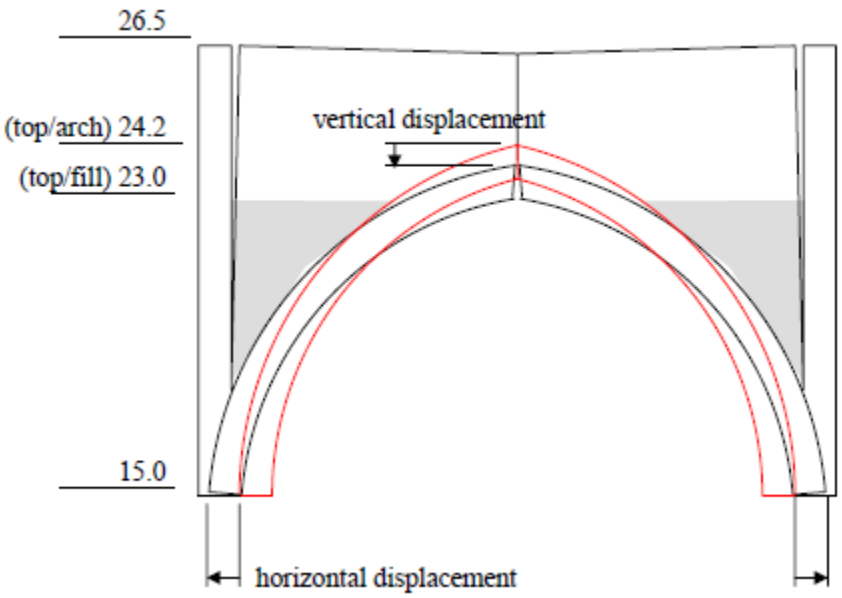

Figure 17 basic mechanism of sagging of the nave vaults and horizontal yielding of the support piers

The elevation of the embedded timber ties, compared to the transverse arches is also very noteworthy in this case, as the timber ties are placed in general at the top of the rubble fill, and practically coinciding with the elevation of the intrados of the transverse arch at the crown. So, the transverse walls, in combination with the embedded timber ties may be seen as a means of providing additional weight onto the piers, and mitigating the horizontal thrust produced by the nave vaults, as well as providing some tying together of the nave walls.

Historically, the connection of the use of transverse walls above the nave vaults to a similar practice observable in the aisles at San Galgano also needs to be considered.

1.2.2. Non-destructive evaluation

Georadar

A limited scope georadar investigation was undertaken on two separate occasions. The objectives of these georadar investigations above the vaults were:

- To check the homogeneity of the vault structure (texture and thickness)
- To detect the presence of timber beams embedded inside the walls that exist between the vaults of the central nave and inside the lateral walls of the central nave.

The measurements were conducted working above the vaults of the central nave (vaults 2 and 5 where vault 1 is the one near the façade, west side) and above the aisles of the left lateral nave. A further investigation was conducted on the floor of the basilica, in an effort to locate possible traces of foundations that might indicate a different bay system, as hypothesized, that was later abandoned in favor of the current system.

Findings above the vaults

The georadar equipment that was used is a Ground Penetrating System produced by IDS Spa (Pisa, Italy). A GPR is a very high frequency electromagnetic equipment that works on the principle of echo graphic methods, i.e., it generates a short pulse that propagates through the medium and is reflected back by the inhomogeneities of the medium. The system consists of a two channel central unit connected by a network cable to a notebook that runs the acquisition software and saves the data and connected by a coaxial cable to a shielded 600MHz antenna. The antenna of 600MHz is appropriate for these measurements being an optimal tradeoff between the needed penetration (1m for the thicker walls) and the resolution (between 5 and 8 cm).

For the measurements above the vaults of the central nave, a calibration test was performed on vault 1, near the façade where a large opening exists so that a metal target can be inserted to create a moving target just below the vault. Further tests of the construction of the vaults were conducted along the lines shown in Figure 17. An examples of a profile collected over vault 2 is presented in Figure 18. The reflection from the lower side of the vault is observed at about 36cm. This is the measured thickness of both the vaults. From the radar data, the thickness of the vaults does not vary along the profiles. So, the conclusion is that these vaults present a constant thickness of about 36cm and a homogeneous masonry texture.

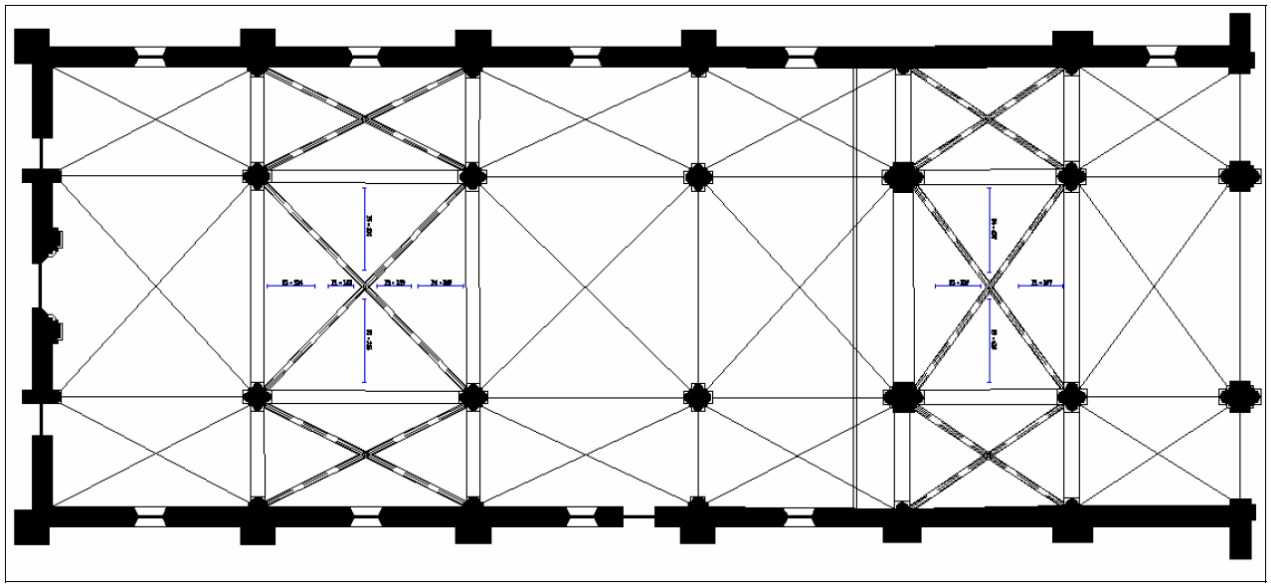

Figure 18 summary of georadar testing program on nave vaults

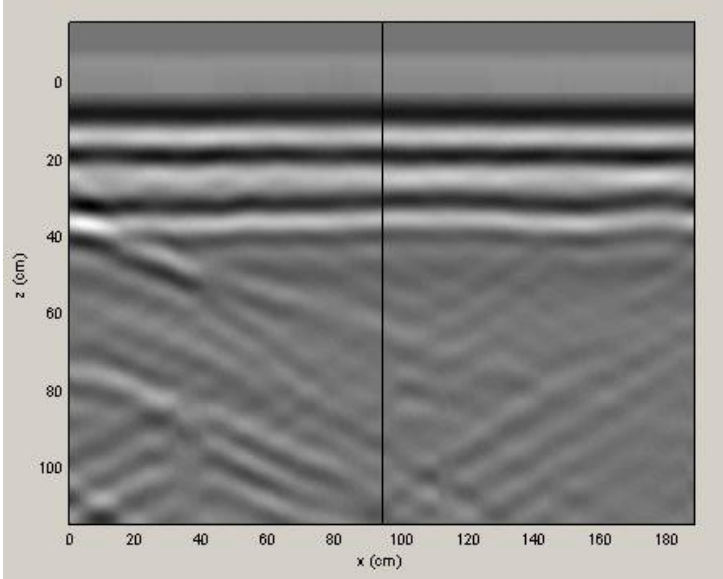

Figure 19 Example of georadar vault profile, Vault 2

Portions of a number of walls, including the transverse wall between Bays 4 and 5 were subdivided into a rectangular grid for a radar investigation of the construction of the wall. A typical result is illustrated in Figure 20 below, which shows two of approximately ten profile lines taken at this location. In general, the survey of the nave transverse walls showed a regular masonry texture with a constant thickness.

This method was also used in some of the aisle walls, where glimpses of wooden tie beams are visible, in an attempt to determine the extent of the wooden tie beams. In every case the presumed tie beam location corresponded to the location of an electrical conduit, and the results of this investigation, although suggestive of a continuous wooden time beam, were inconclusive.

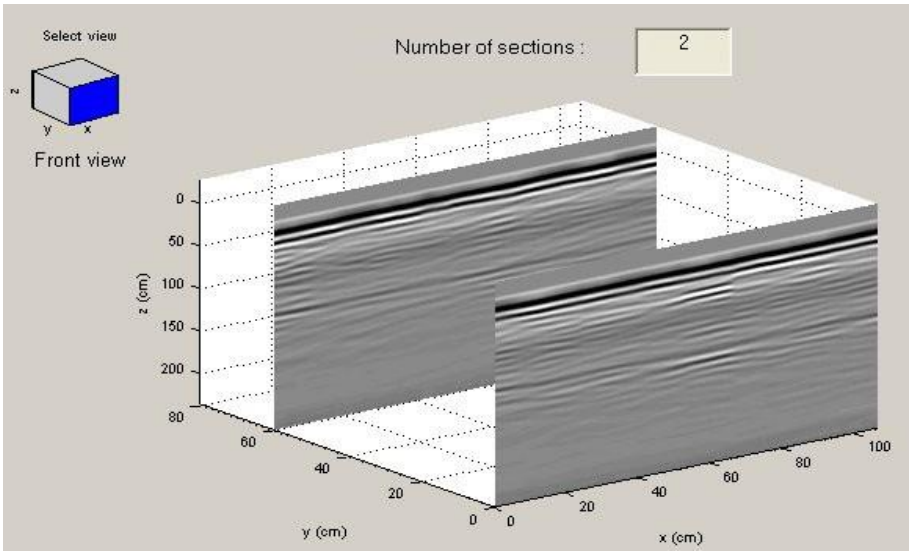

Figure 20 Georadar investigation results for transverse nave wall between Bay 4 and 5

1.2.3. Findings on the nave floor

The georadar equipment that was used is again the Ground Penetrating System produced by IDS Spa (Pisa, Italy). A 600MHz shielded antenna was used. The in-line position of the traces was regularly spaced by using a standard triggering wheel while the cross-line position of the parallel profiles was ensured by using a laser positioning system.

Figure 21 Georadar system in operation

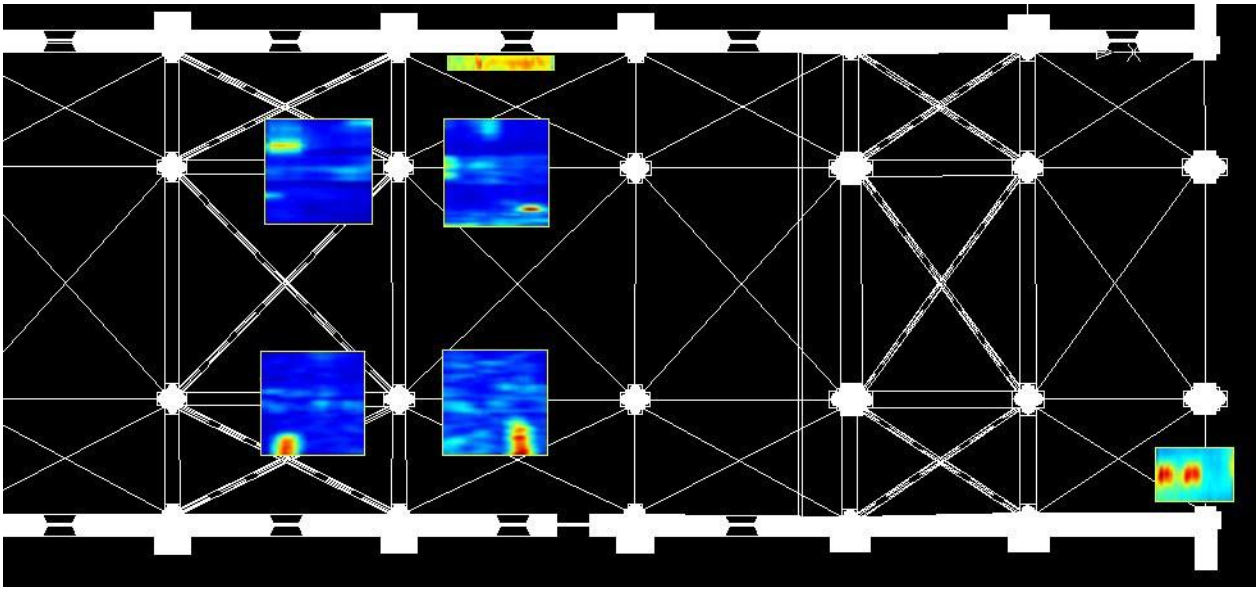

Figure 22 Plan of and Results of Acquisition of Georadar Data

The preliminary results are summarized in Figure 22 where a constant depth section from each survey is shown in the respective position. Red and yellow colors indicate high reflected energy while blue indicates absence of radar return. The depth of the images is around 30-40cm except the

narrow survey executed close to the wall where the depth section is only a few centimeters below the ground level.

By exploring the whole 3D volumes of the processed data, the conclusion is that there is no evidence of additional foundations. Instead, there are some consistent correlations of the radar images as expected from tomb locations. The energy observed close to the floor level in the Novella 5 position is associated with a distortion of the radar background signal generated by a small level variation of the pavement that was also observed during the survey.

1.2.4. Sonic Pulse Transmission

The testing technique is based on the generation of elastic waves in the frequency range of sound (20 Hz-20 kHz), by means of mechanical impulses at ~~a~~ points of the structure. In a homogeneous and isotropic solid the pulse velocity is related to the modulus of elasticity and the density. The relationship is independent on the frequency of the vibrations. In the case of masonry, due to its heterogeneity, the pulse velocity only qualitatively represents the characteristic of the masonry.

Figure 20 shows the execution of a sonic test in the Basilica of Santa Maria Novella. A signal is generated by percussion with an instrumented hammer (transmitter) and is received by means of an accelerometer (receiver), which can be placed in various positions. The data processing consists of measuring the transit time between the transmitter and the receiver and of calculating the pulse velocity equal to the distance between the devices divided by the transit time. Signals are stored by a waveform analyzer coupled with a computer for further processing. Three types of tests can be carried out:

(1) Direct (or through-wall) tests in which hammer and accelerometer~~s~~ are placed in line on opposite sides of the masonry element;

(2) Semi-direct tests in which hammer and accelerometer~~s~~ are placed at a certain angle to each other, and

(3) Indirect tests in which hammer and accelerometer are both located on the same face of the wall in a vertical or horizontal line. Generally a grid of acquisition points is investigated.

Figure 23 Carrying out a sonic test on the transversal walls of the Basilica of St. Maria Novella

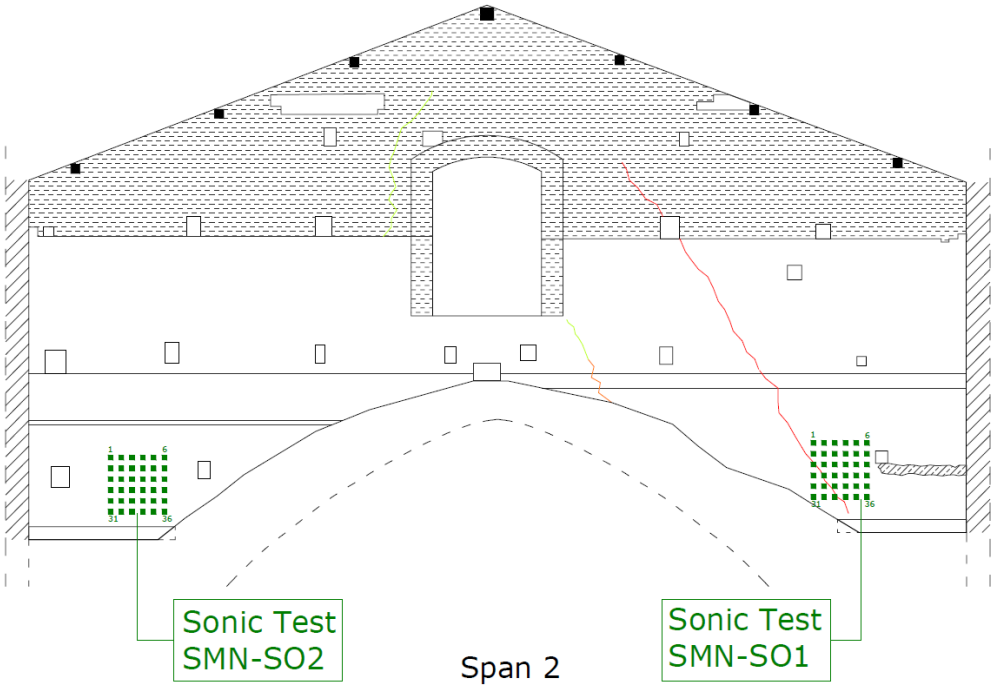

Figure 24 Position of the sonic grids on the transversal wall between Bay 2 and 3

Figure 24 shows a typical testing configuration used on the transverse walls above the nave vaults. A similar test, designated SO3, was conducted on the wall between bays 4 and 5. The velocities represent generally homogeneous masonry construction, however, it is evident that the later wall is of superior construction, reflected by its greater average ultrasonic pulse velocity. The 1900 m/s average velocity of the second wall represents an approximate modulus of elasticity of 7.2 GPa, a relatively high value for masonry, and the 1400 m/s velocity of the first wall represents an approximate modulus of elasticity 4.9 GPa. The homogeneity of the walls is consistent with the findings of the georadar investigation.

Some further tests were done on a column base in order to determine the homogeneity of the construction of the piers. Velocities in the range of 3000 m/s were found on trajectories through the base of the pier, while the transmission velocities degraded to approximately 1500 m/s at a point 140 cm above the floor. The velocities at the base are undoubtedly indicative of solid masonry construction, while the readings taken above the base suggest that solid facing and a rubble core are employed.

Chapter 2

Generation of 3-D Geometrical Model

2.1. Existing Geometrical Model of the Church

In previous thesis project [*Basilica di Santa Maria Novella a Firenze: Modellazione Geometrica e Analisi strutturale del Transettoproject, Relatore: Prof. Alberto Taliercio, Correlatrice: Arch. Paola Condoleo, Candidato:Andrea Manini*]the 3D model of the church was generated by considering the obtained information from survey and the 2D plans of the church. In the previous method the generated 3D model consists of mono or bi-dimensional elements. Consequently, all the elements in the previous model are mono-dimensional elements like pillars and arches and the bi-dimensional element like vaults and interior and exterior walls.

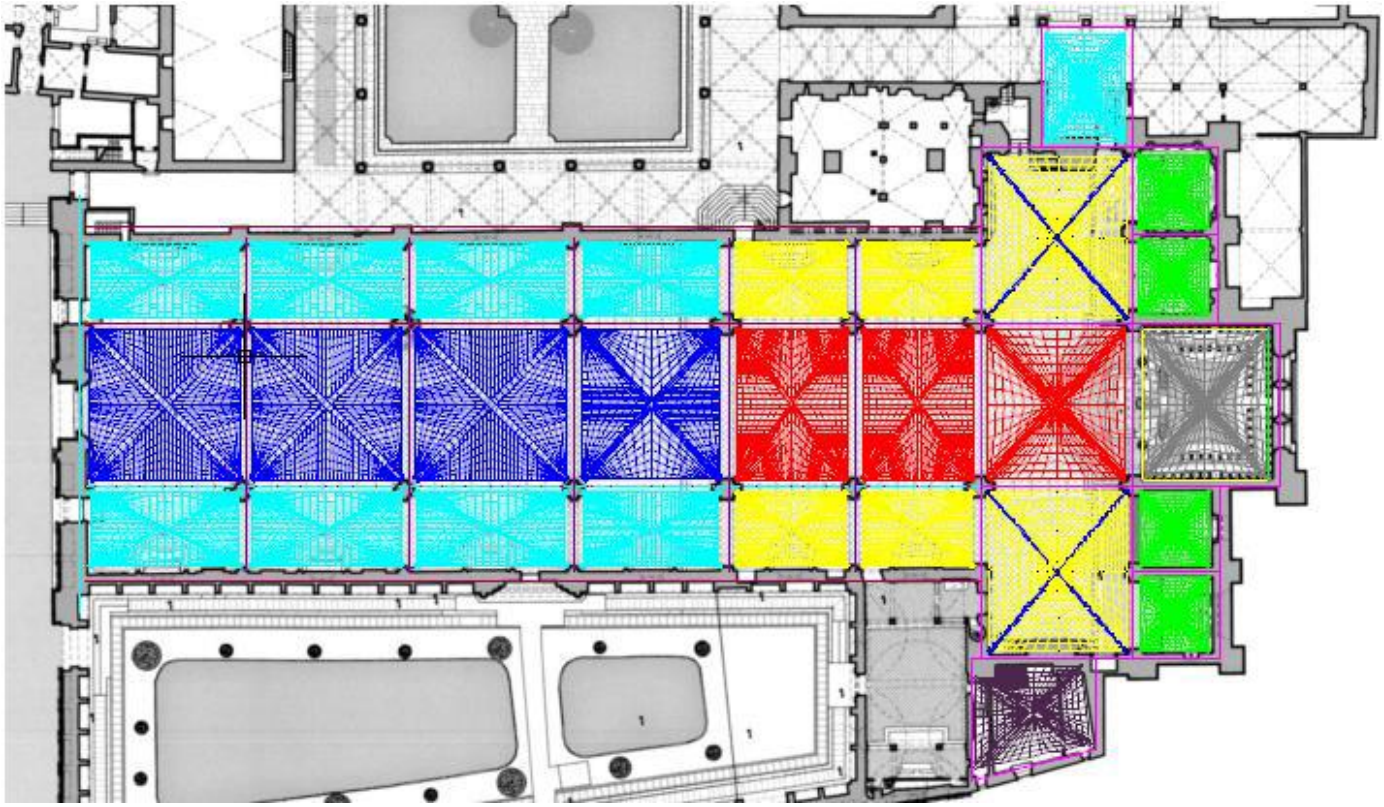

Figure 25 2D plan of the church

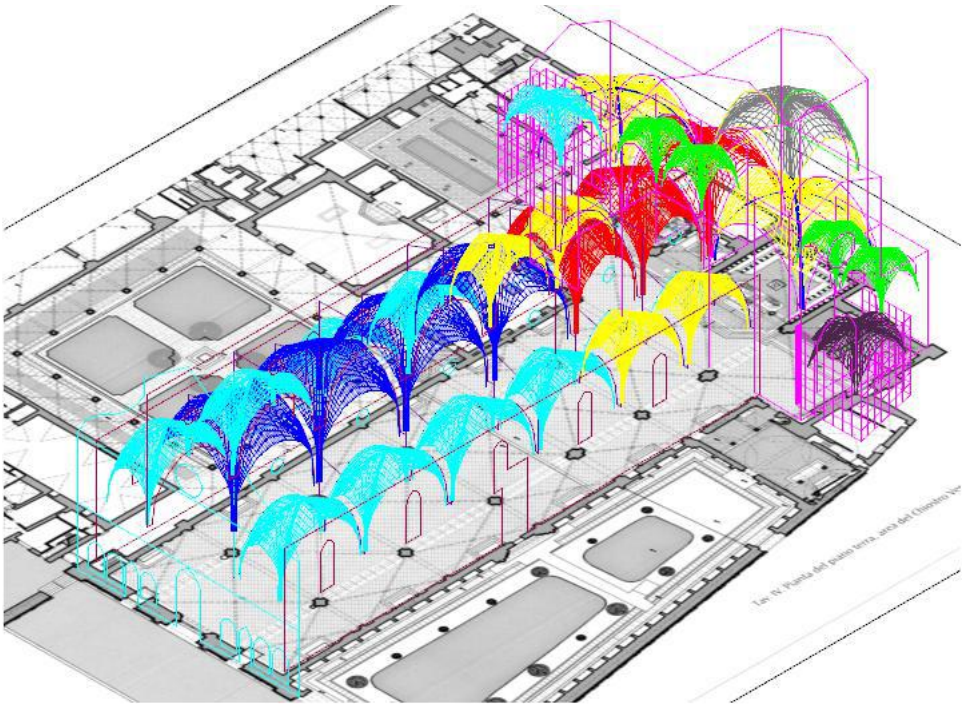

Figure 26 3D model on the 2D plan

Mono-dimensional elements:

Figure 27 Mono-dimensional element (arches, ribs and pillars)

Arches, ribs and pillars are designed as mono-dimensional elements of the model which represent just the guidelines of these elements for the future operations in analysis procedure.

Types of the vaults:

In this model, different types of vault are defined according to the curvature of the diagonal arches and also the data and position of the sample point which are measured by surveying the vaults and arches.

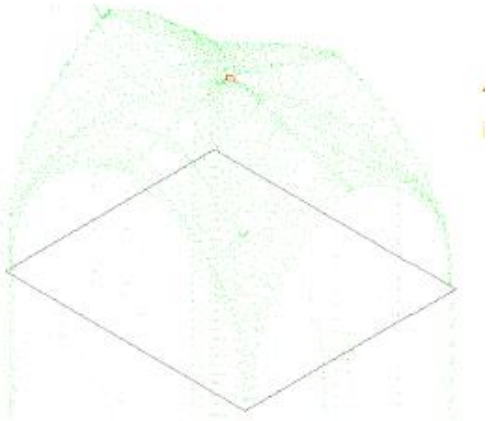

Through the available information it is determined the plane of the pillars and the position of the connection point of the ribs in the center of vault.

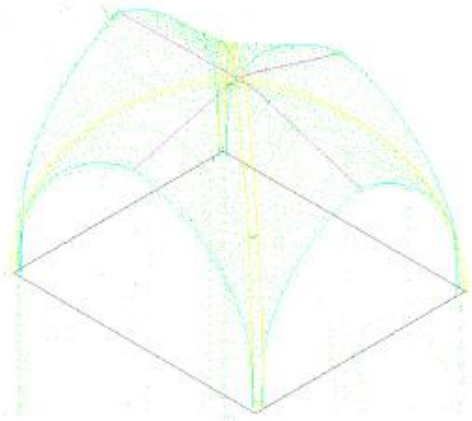

The Peripheral arches and ribs are modeled through guidelines.

The arches are connected to the outer ribs, finally the surfaces of the vaults are created through the command "loft" by considering the guidelines of the peripheral arches and ribs.

The ribs are represented by thin strips besides the vaults and in the corners of the plane are connected to the top of the pillars.

This process needs a continuous comparison with the information available to define a satisfactory geometry.

Figure 28 Creation process of the surfaces of the vaults

Figure 29 Different types of the vaults

Finally the 3D model is generated from elements without thickness so, in one point of view it was not realistic model according the geometry of the church.

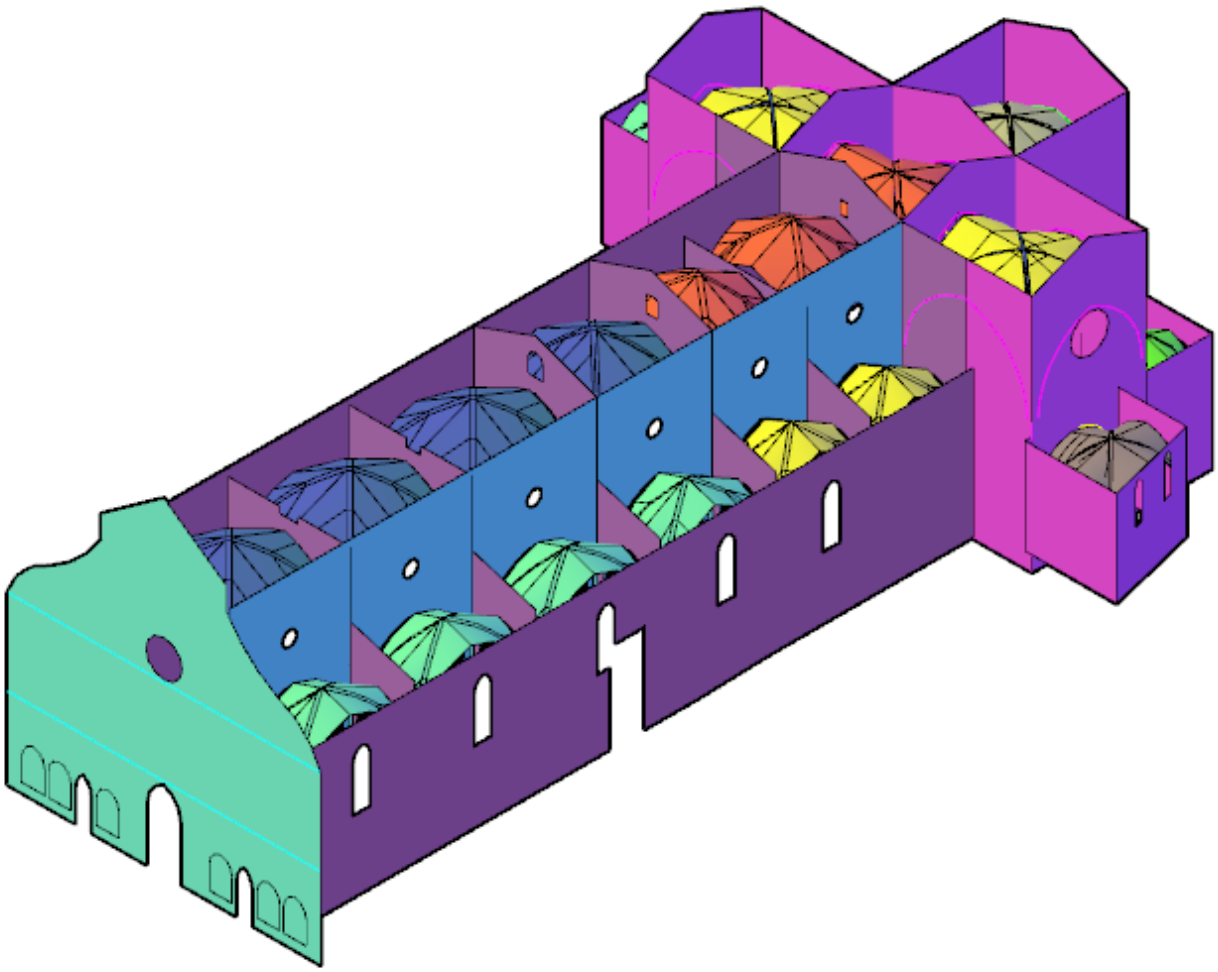

Figure 30 3D model consist of mono and bi-dimensional elements

2.2. Assumptions and Hypothesis for new 3D model

In this project the new approach is studied for generating the more realistic 3D complete geometrical model consisting of three-dimensional elements according to geometry of the church's parts and elements. As there is not very precise information about the geometrical data of the different members of the church and also there is no exact idea about the construction procedure of the church, so we have to suppose some hypothesis to create the complete 3D assembled model by all the 3D element.

In this procedure these hypothesis are considered:

- The cross sections of the ribs, longitudinal and transversal arches are rectangular.
- The base points of all the pillars are in the same level.
- All the lateral arches have the same base level.
- Arches of the transept part and also central arches have the same starting level.
- All the diagonal, longitudinal and transversal arches are connected to top of the pillars on the same surface.
- All the arches are symmetric and the church is also symmetric according to central longitudinal axis passing through the nave.
- For creation of the new vaults with thickness, the geometry of the vaults in the previous project are considered as reference surfaces and their thickness are created toward the outside of the vaults.
- The thickness of all the vaults is 35cm and it is same for all the vaults in all bays.
- The vaults are put on the diagonal arches and then they are moved vertically 10cm toward ground to assembly the vaults and arches for not having any gap between diagonal arches and vaults.

2.3. Modeling of Pillars

Designing of the model is done in AutoCAD software. For designing the pillars, the 2D plan of the church is used to determine the position of the columns. The pillars are modeled on the plane below and according to the measurement of the pillars (Figure 33 and Figure 34), the cross sections are defined.

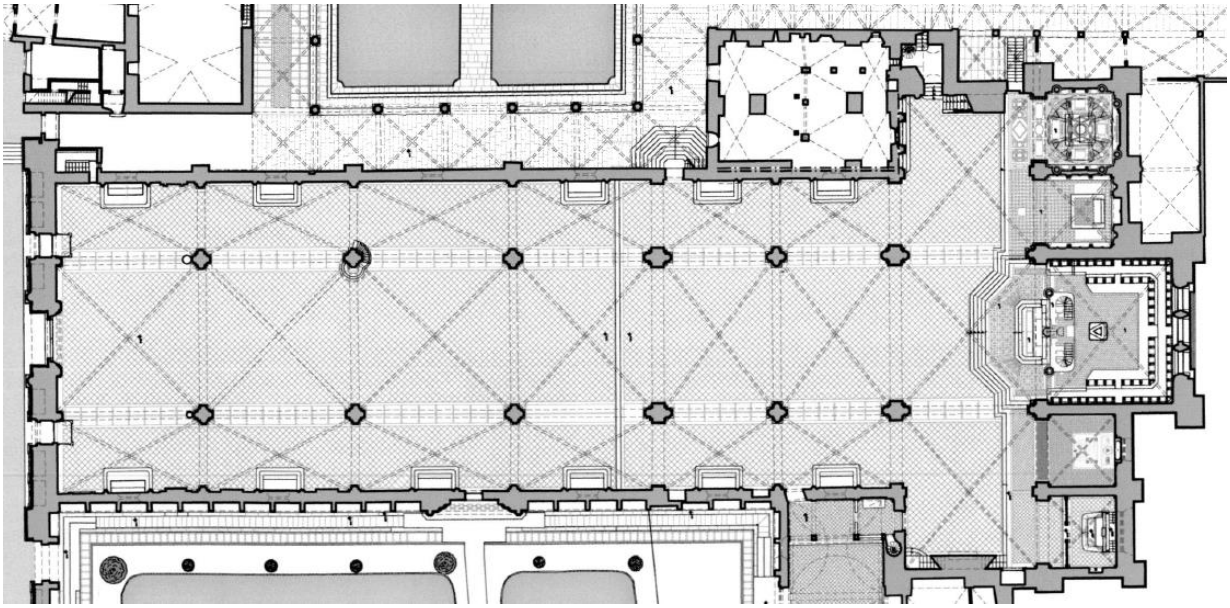

Figure 31 2D plan of the church for determining pillars position

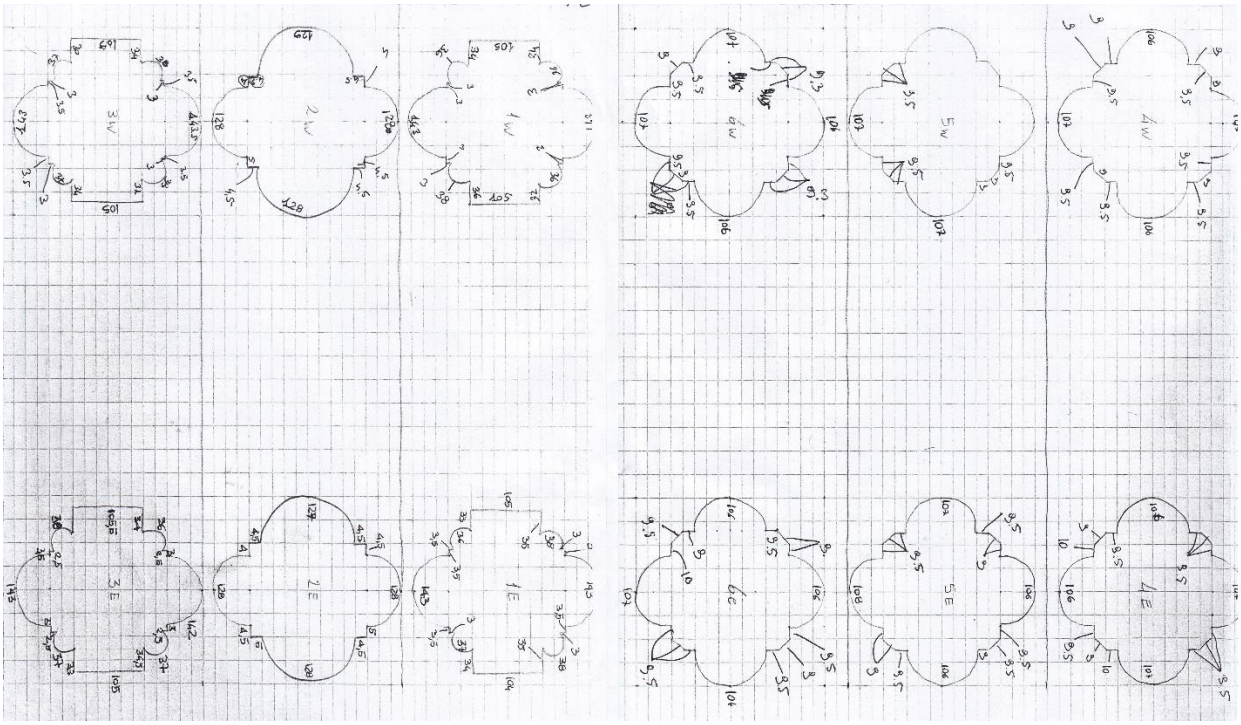

Figure 32 the measured cross section of the central pillars

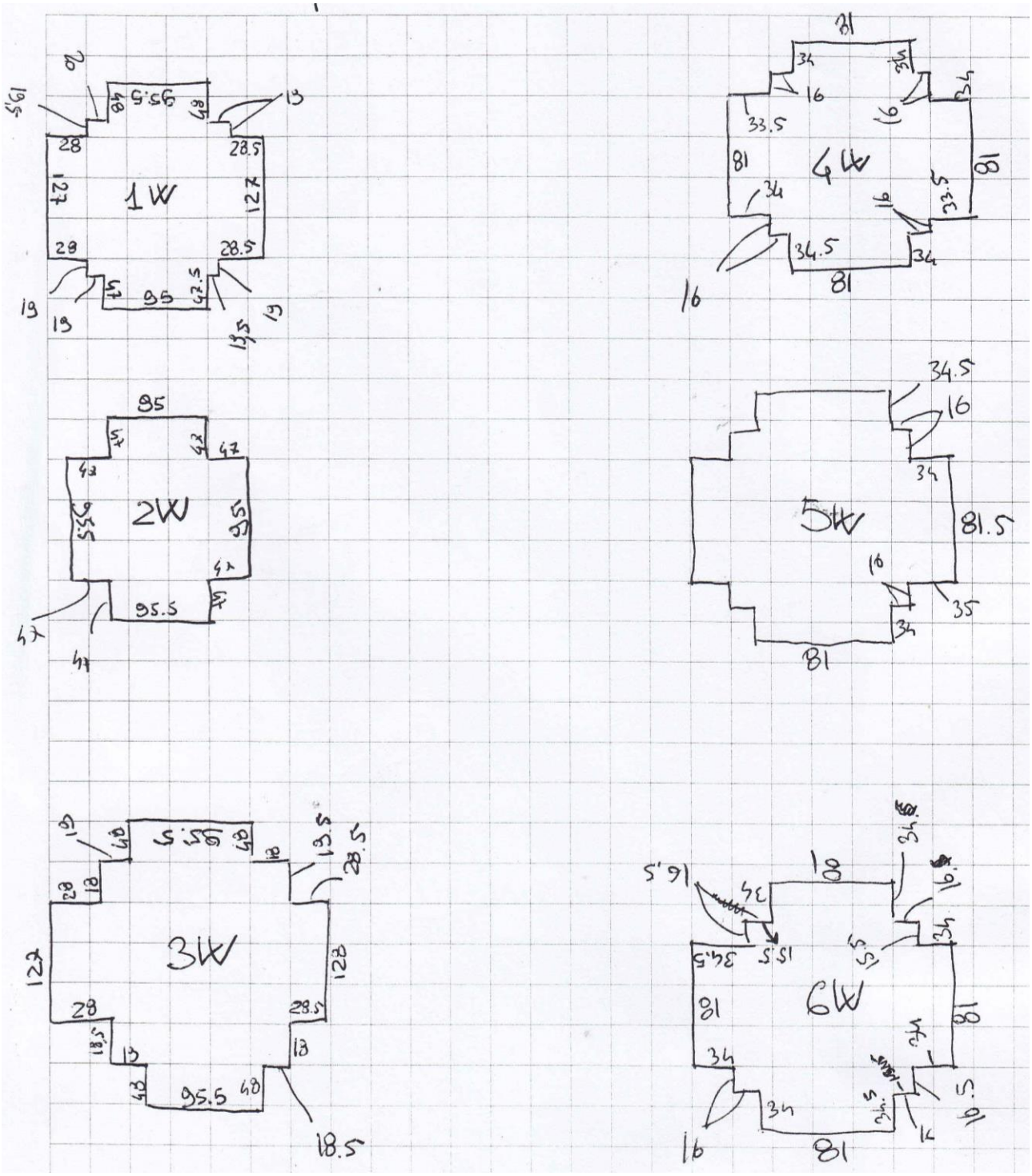

Figure 33 base cross section of the west central pillars

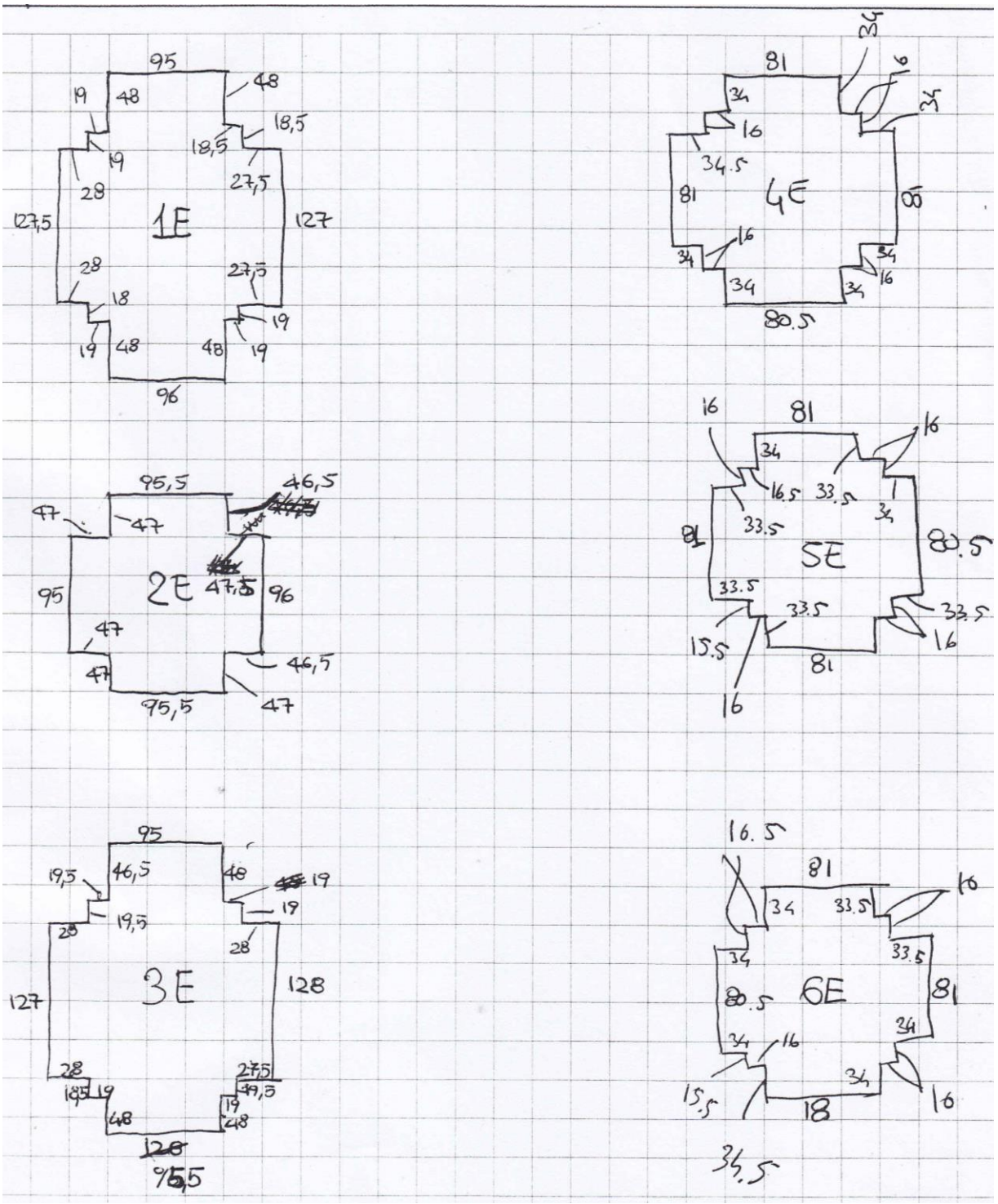

Figure 34 base cross section of the east central pillars

The designed pillars are presented in the plane below:

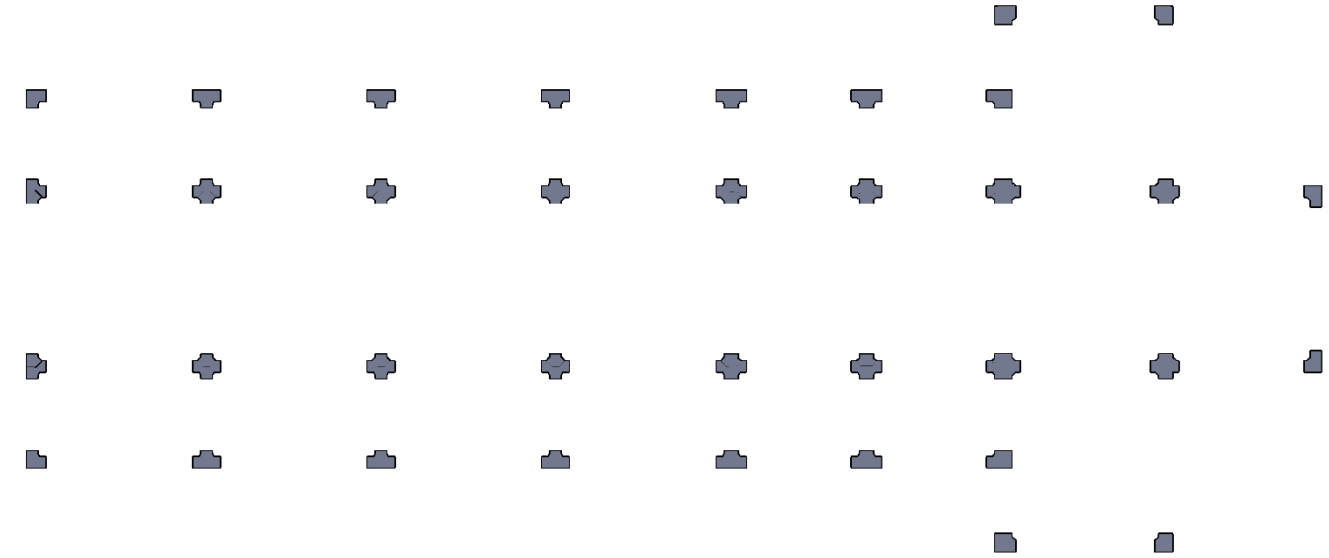

Figure 35 2D plan of the pillars

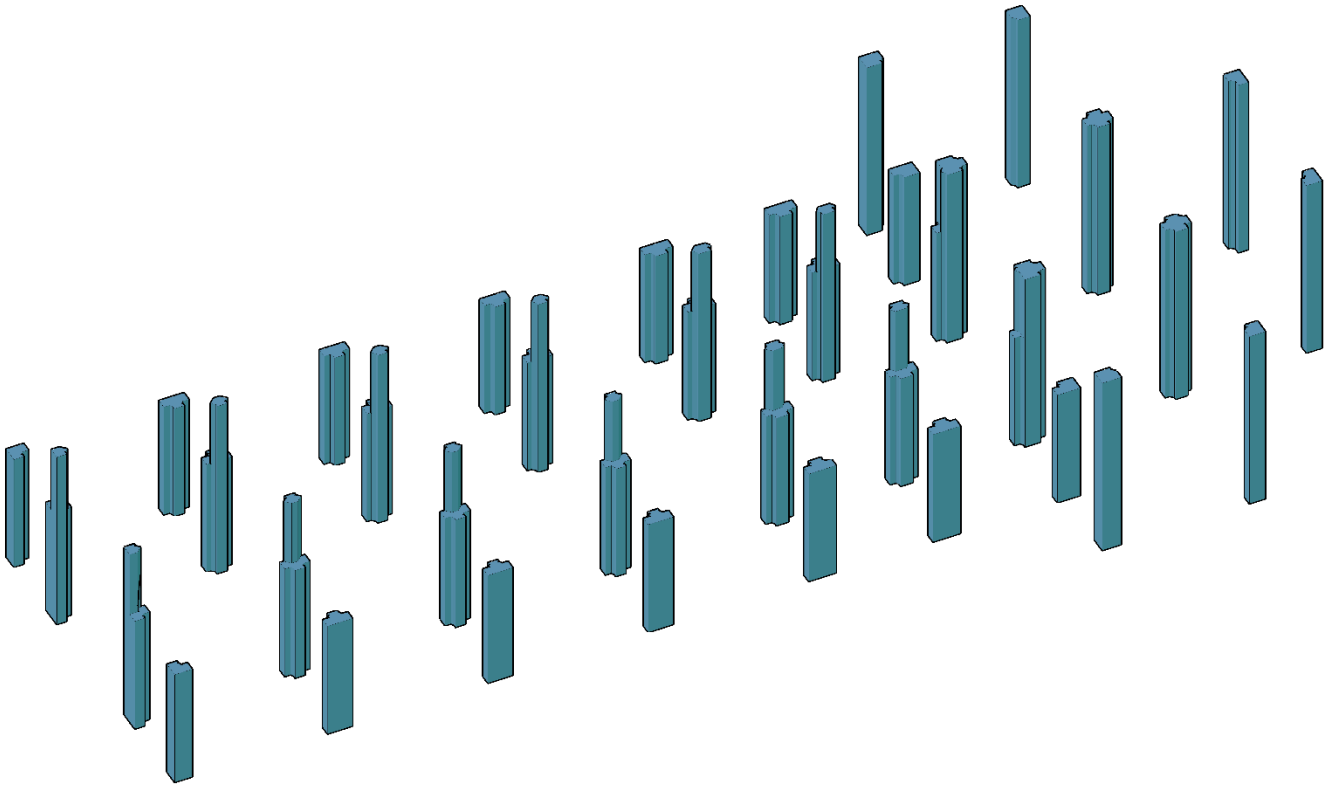

Figure 36 Presentation of the modeled pillars in 3D space

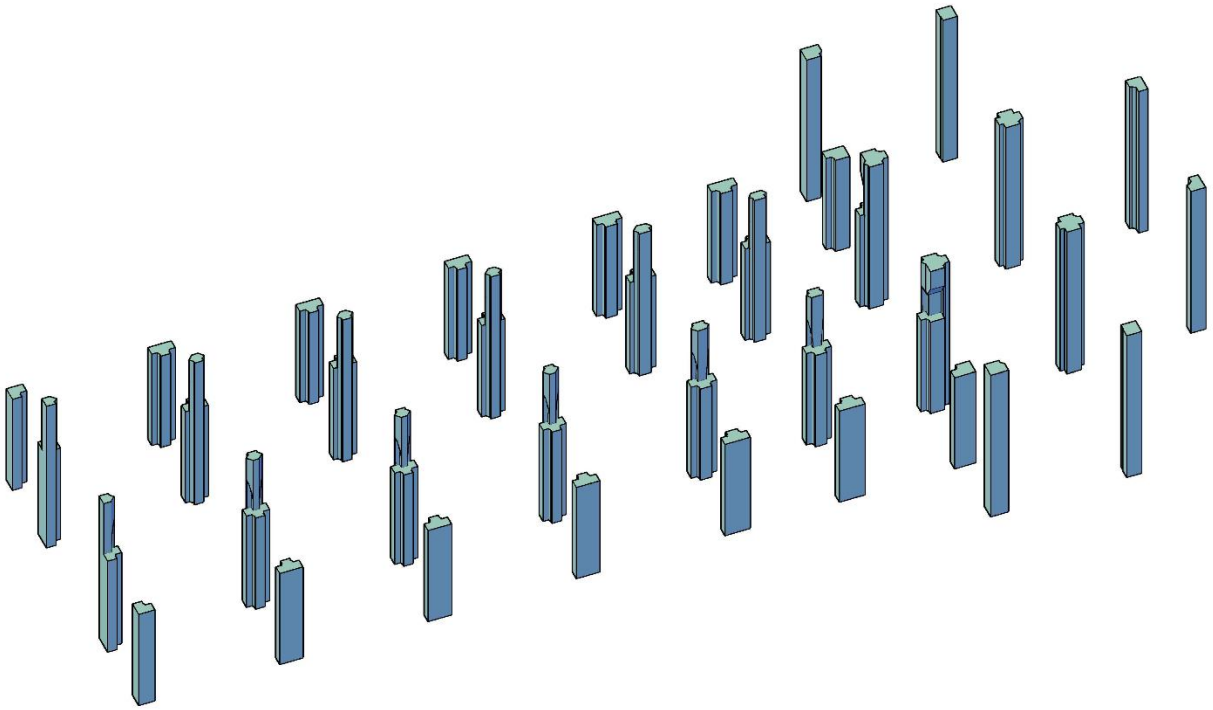

Figure 37 the final shape of the pillars after cutting out the interferences with arches and ribs

2.4. Modeling of Arches

All the arches are designed by defining the reference arch from previous project model. For some parts two arches are combined to each other to create the more precise arches for the elements according the real geometry. In the simplest arches, it is used just three point to define the arch and for some other arches they are used spline curves with 5-6 point instead of 3-point arch.

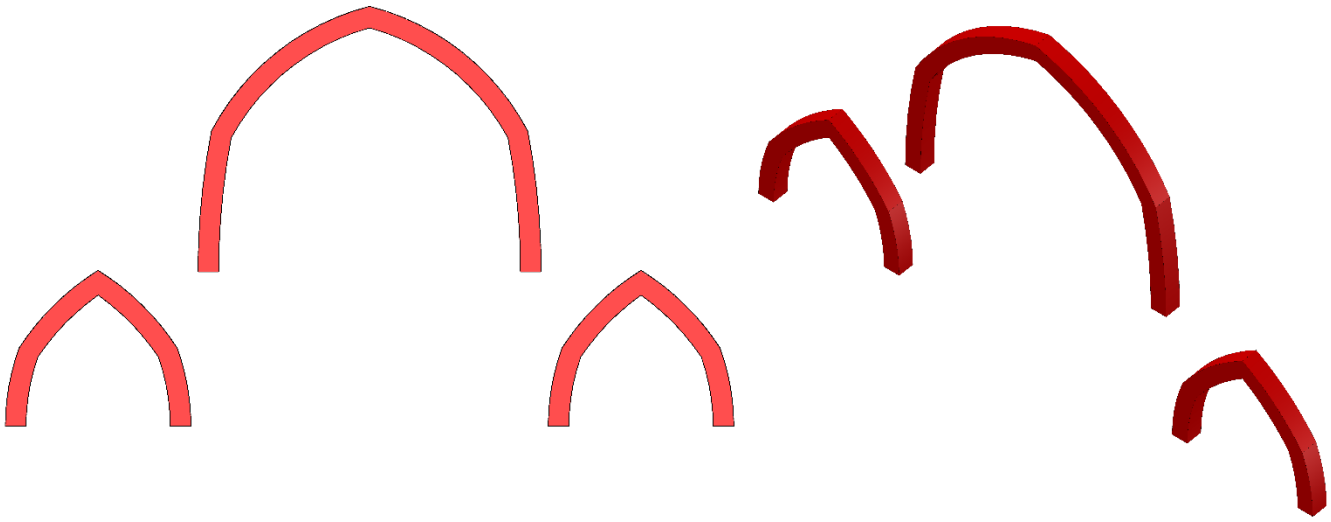

Figure 38 central and lateral transversal arches

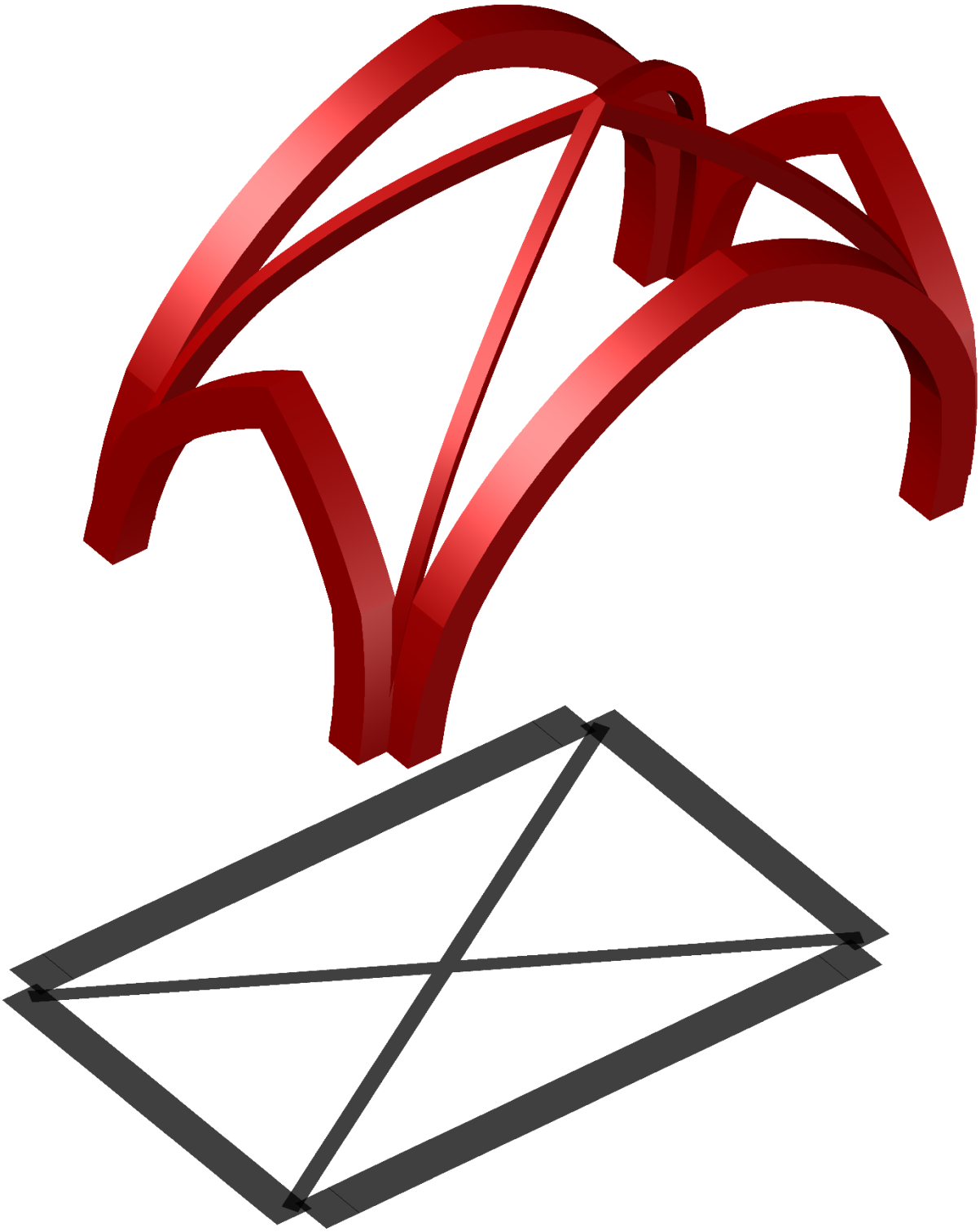

Figure 39 Lateral bay 6, 5, 4 and 3 arches and ribs

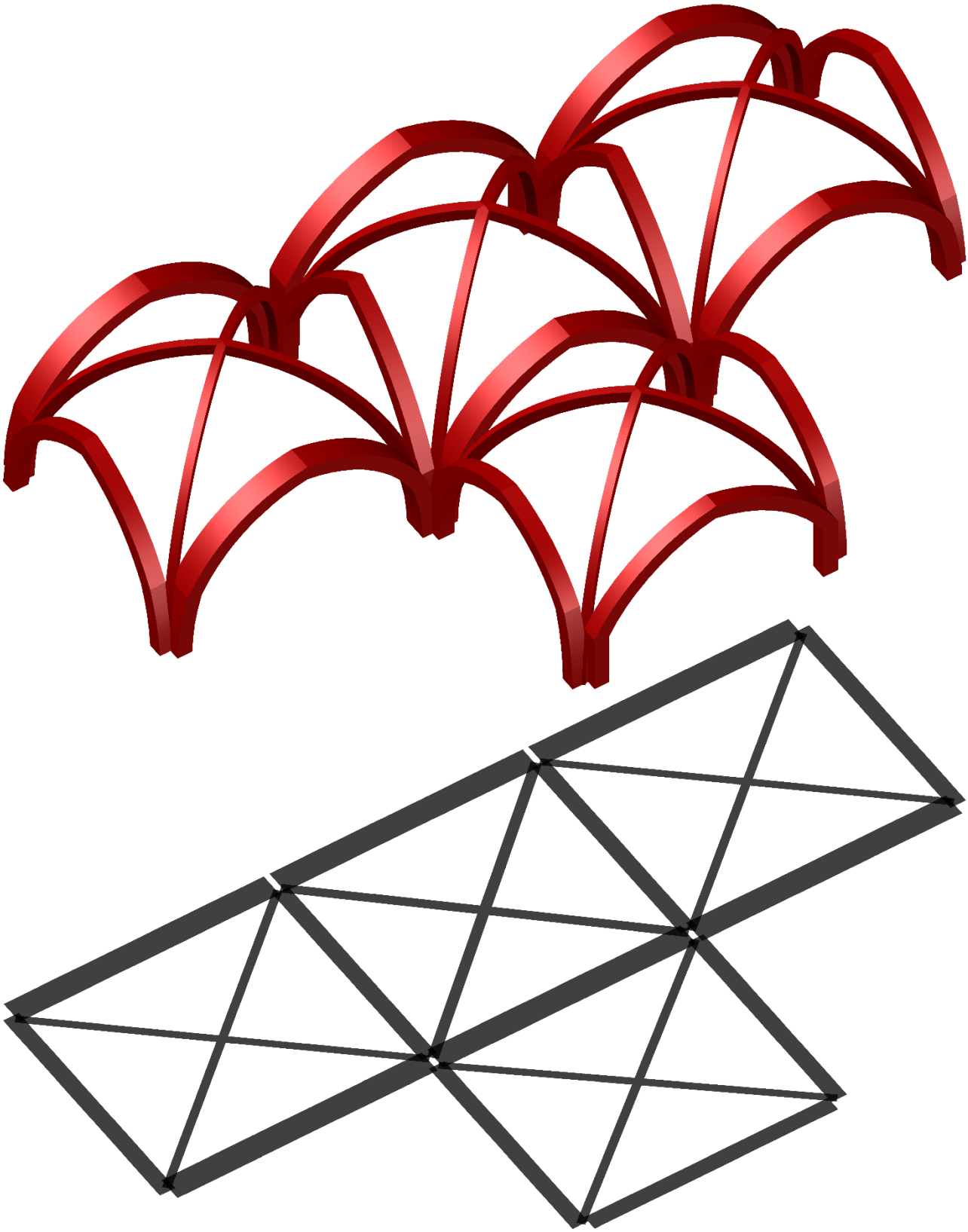

Figure 40 arches and ribs of transept part

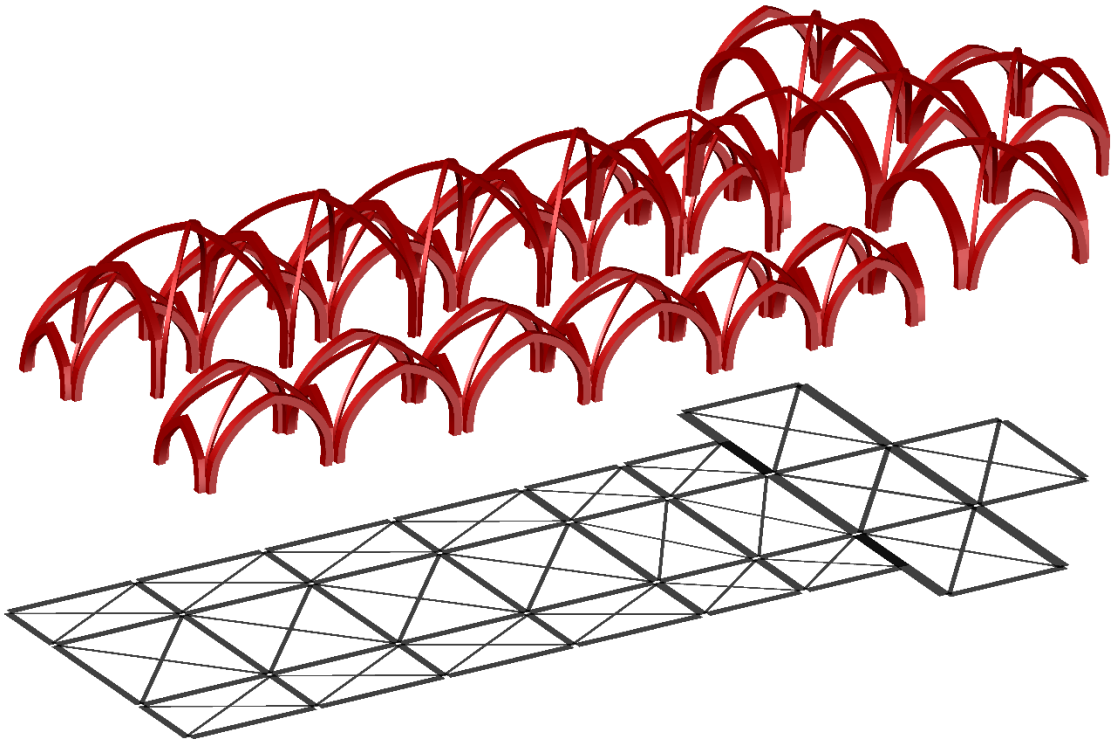

Figure 41 all arches and ribs of the church

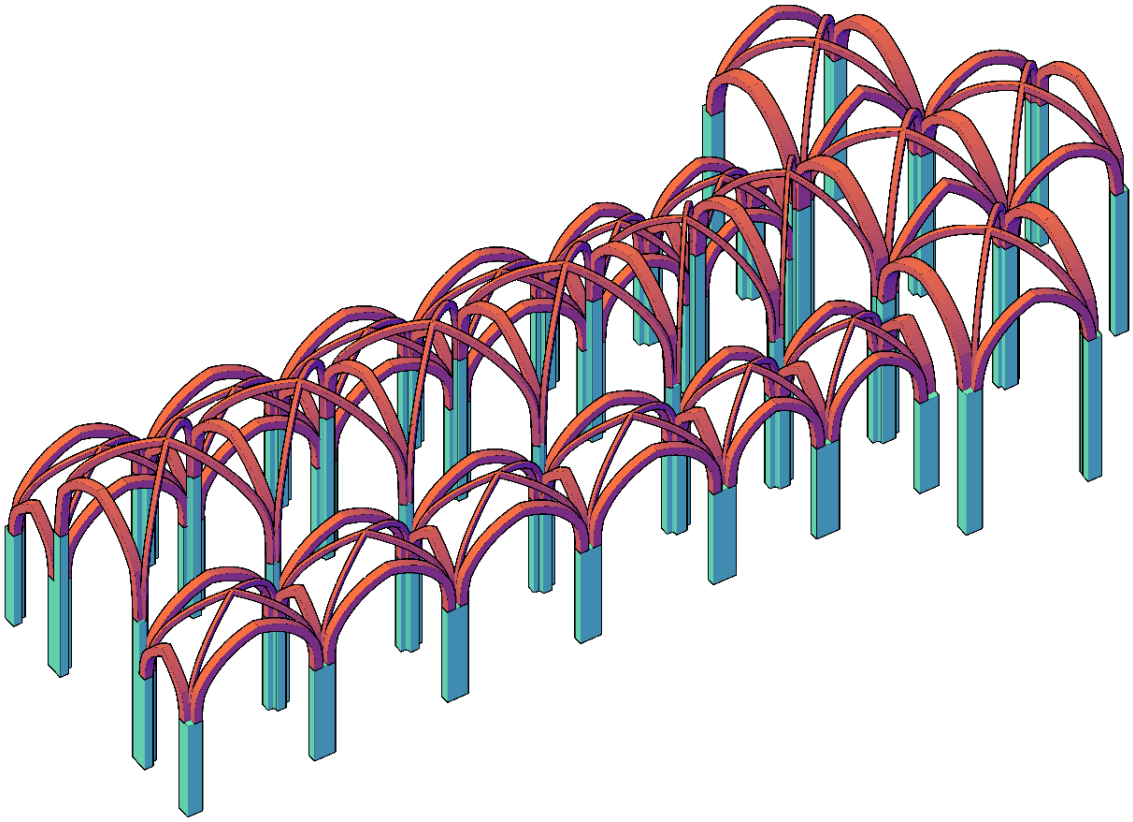

Figure 42 pillars and arches

2.5. Modeling of internal walls

All the internal walls have thickness 0f 80cm. They are built on the longitudinal and transversal arches and they are connected to the external walls in lateral zones and also façade.

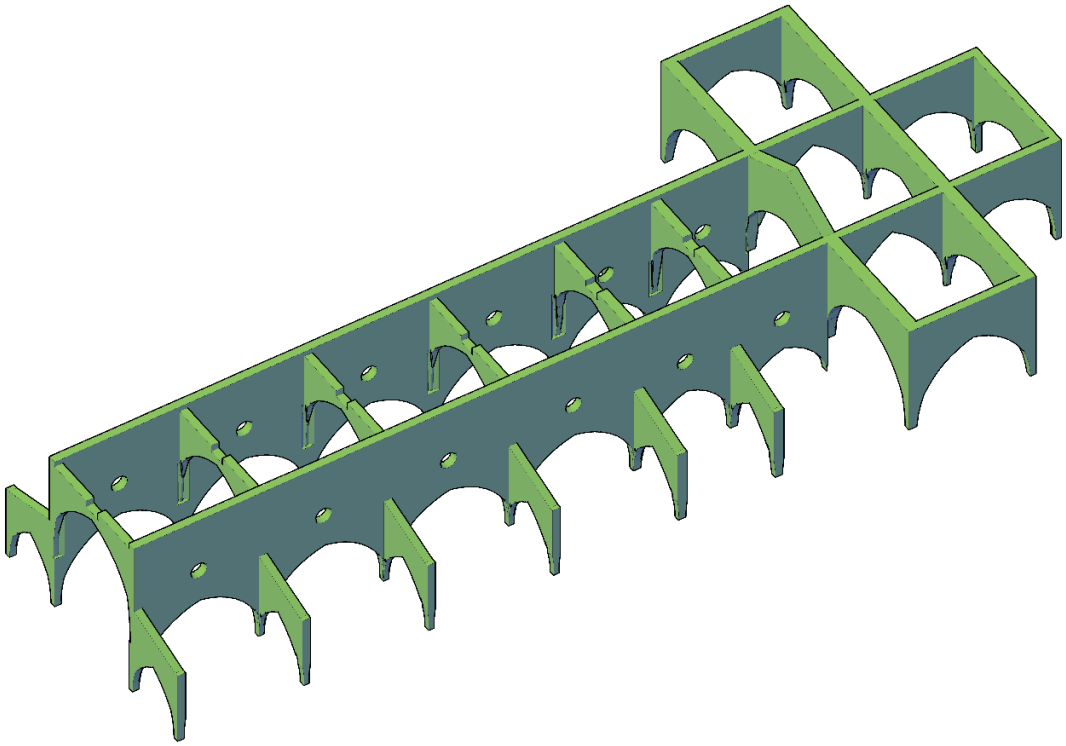

Figure 43 internal walls

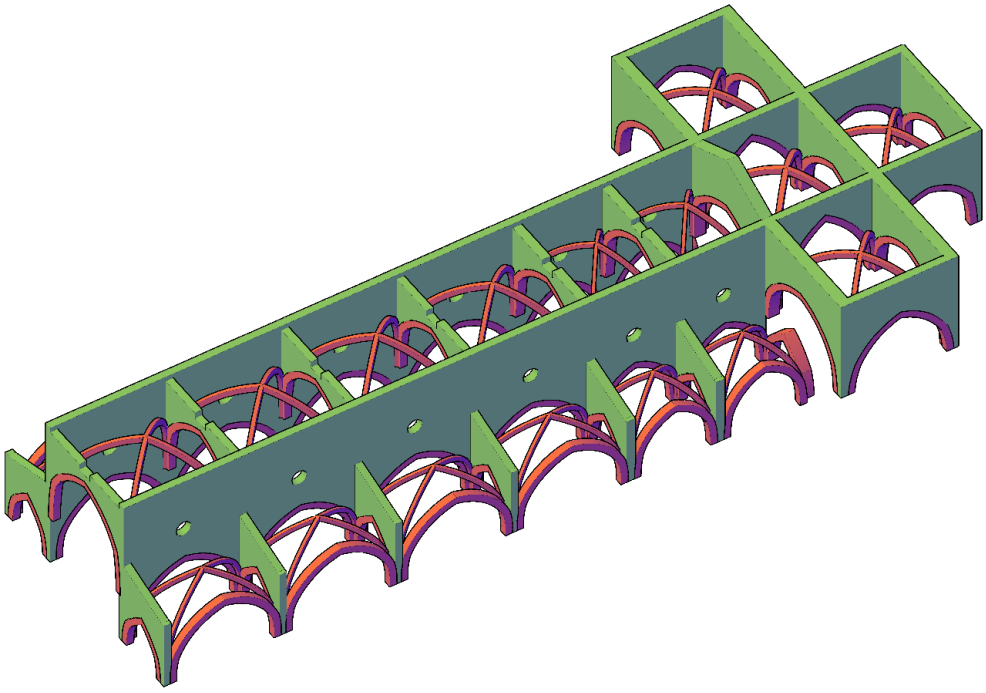

Figure 44 Arches and internal walls

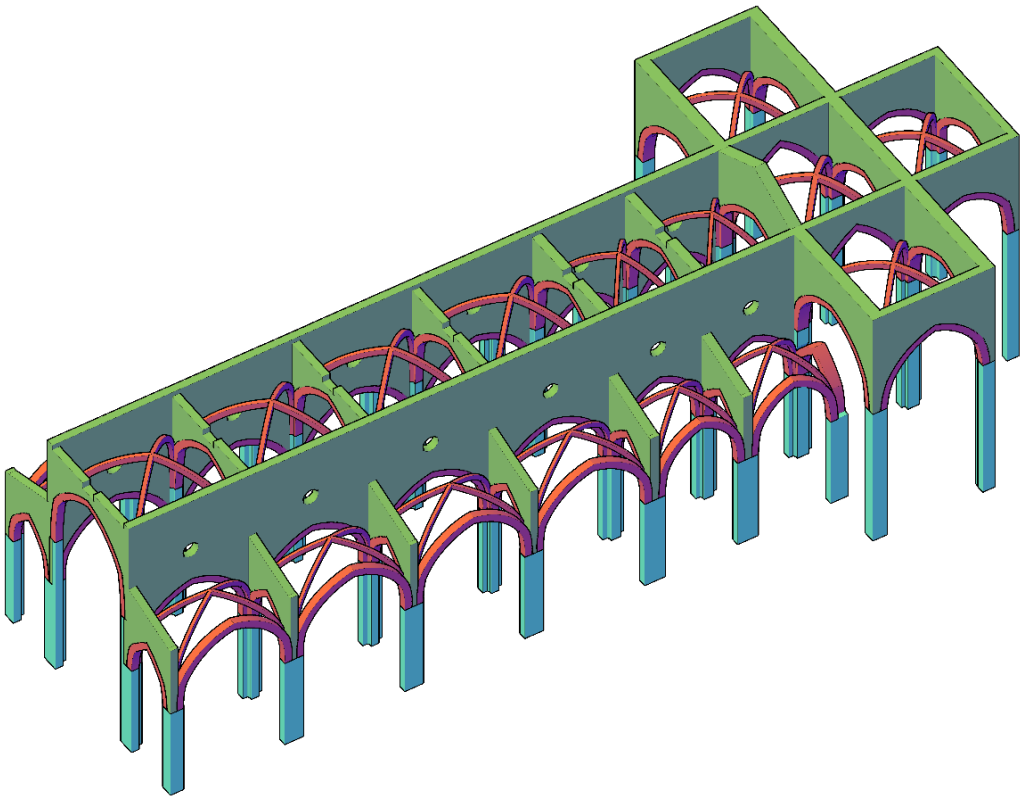

Figure 45 Arches, pillars and internal walls

2.6. Modeling of vault

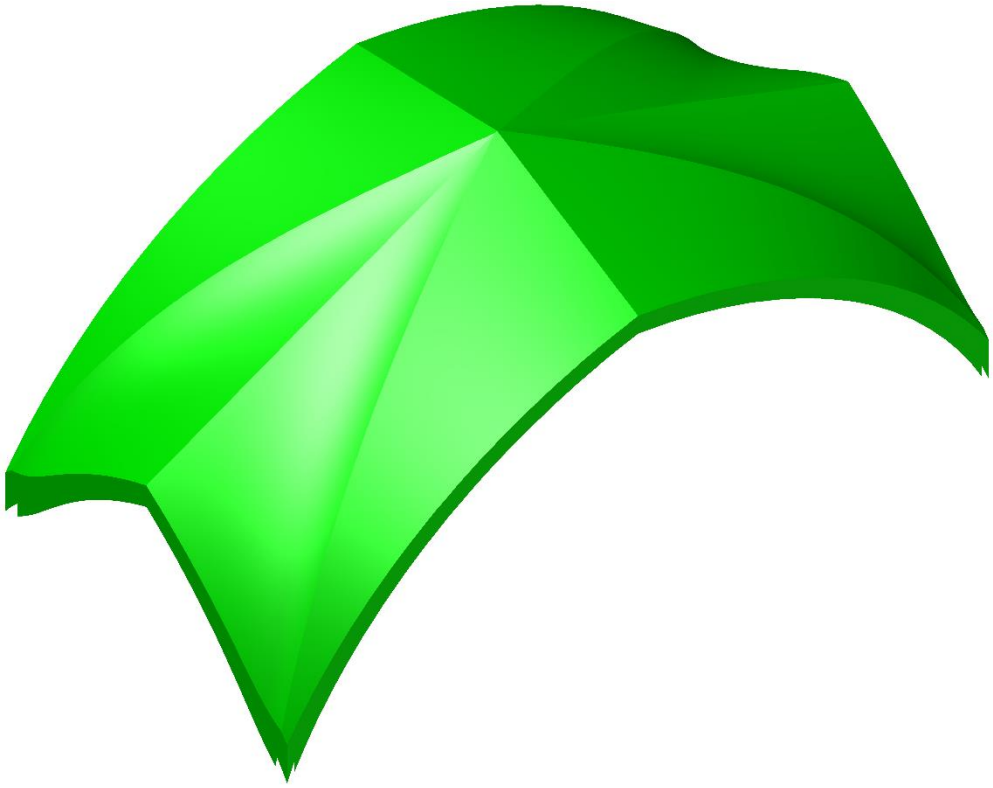

Figure 46 Lateral bay 3,4,5,6 vault

Figure 47 central bay 3,4,5,6 vault

Figure 48 central and lateral bays vaults

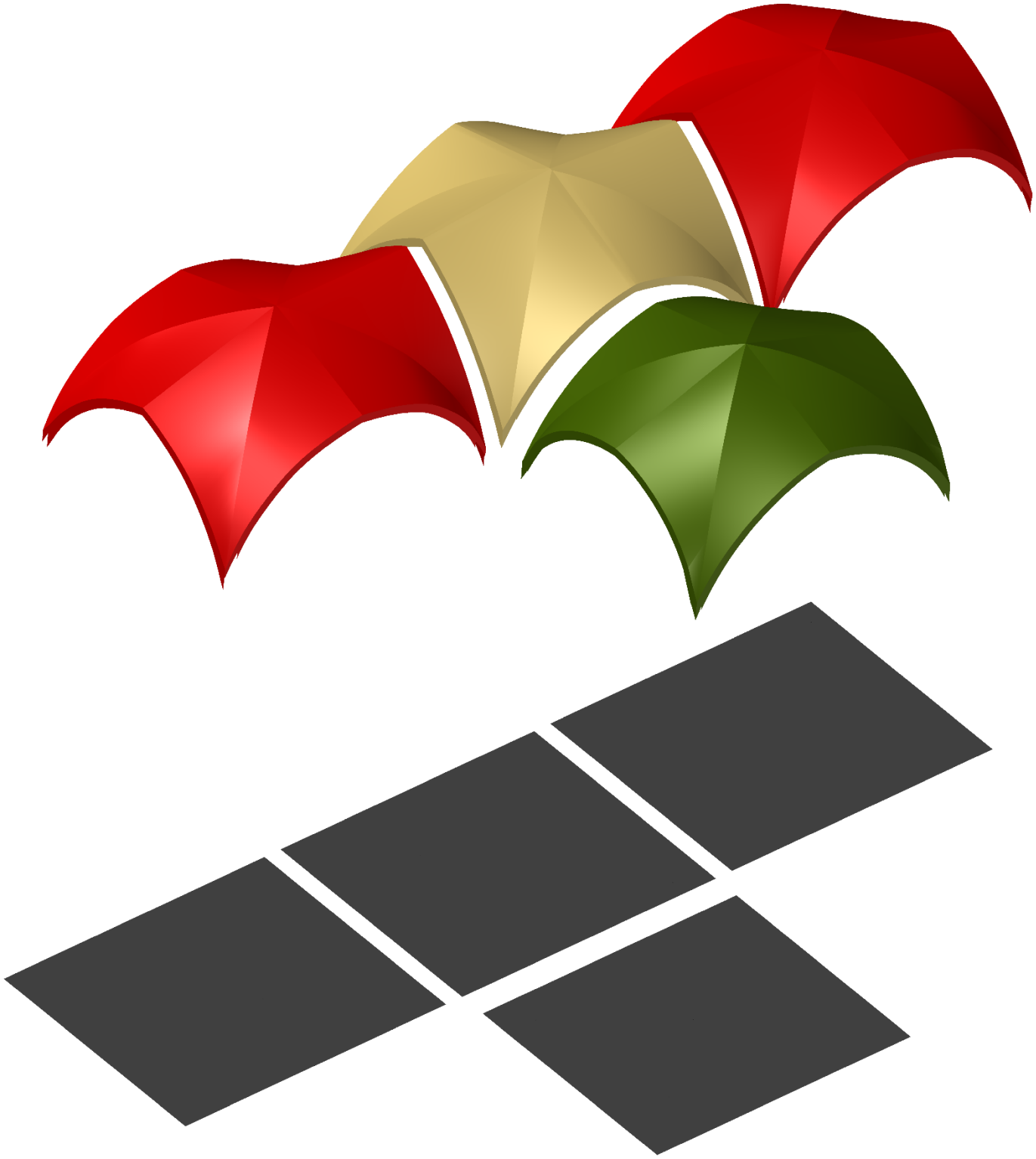

Figure 49 vaults of the transept

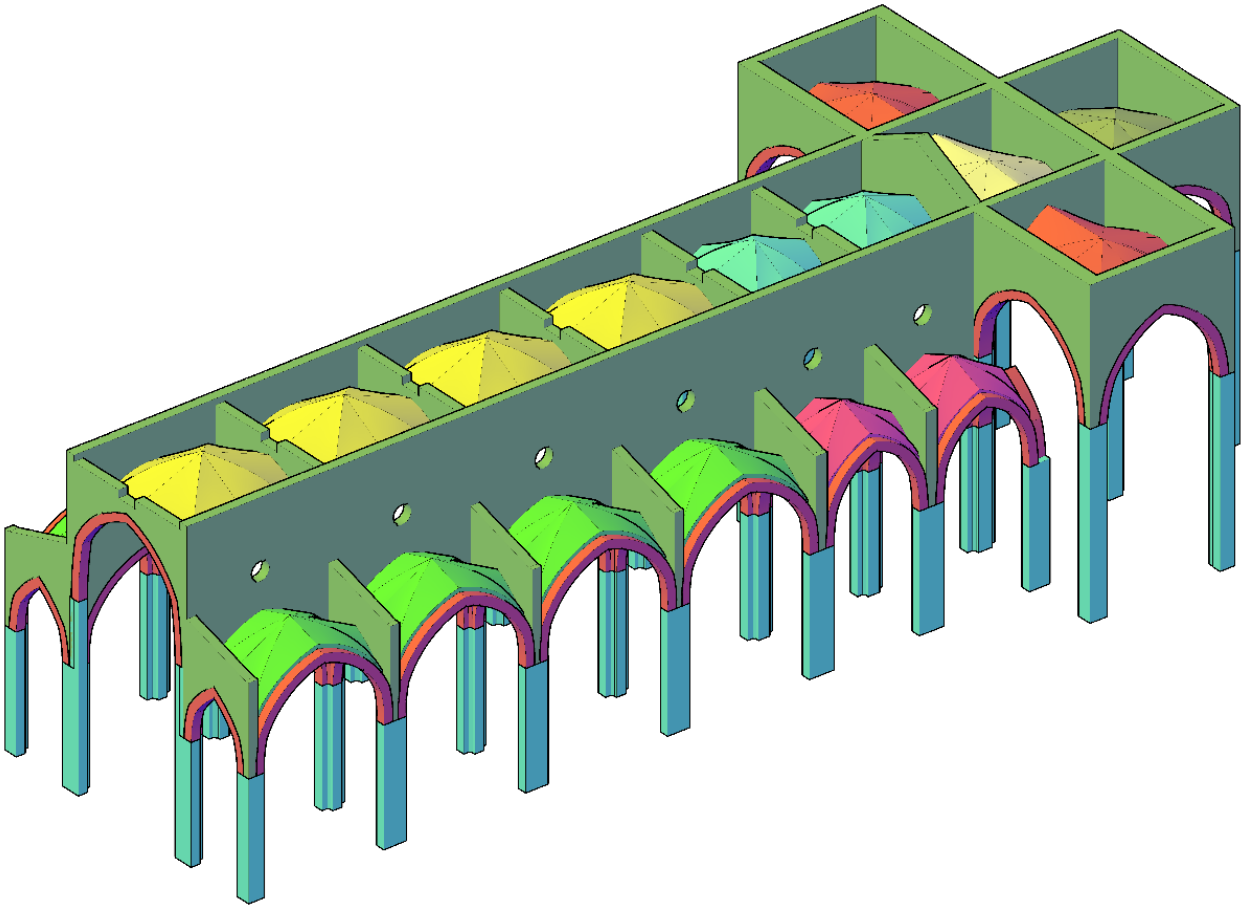

Figure 50 Arches, pillars, vault and internal walls

2.7. Modeling of external walls

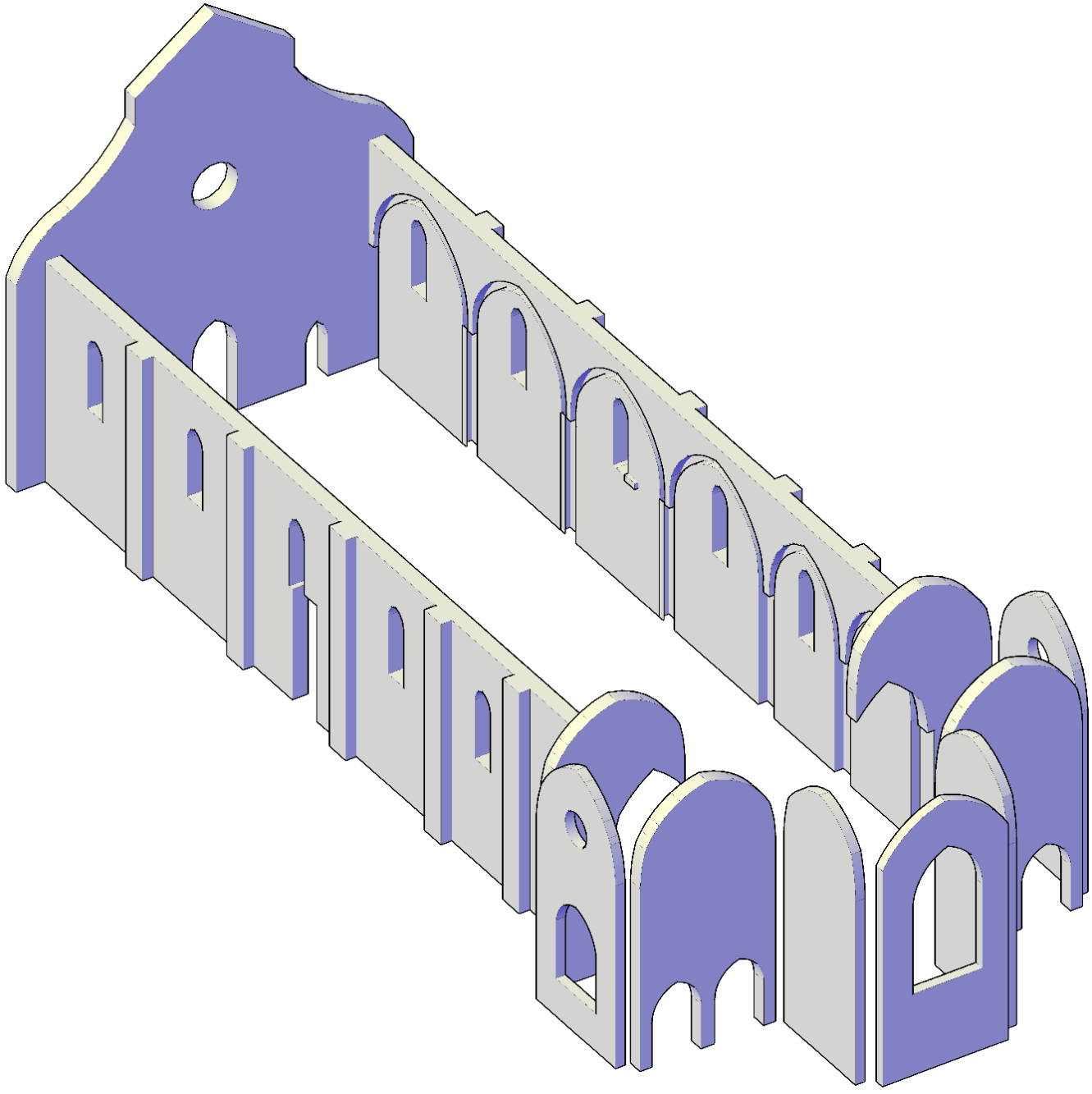

Figure 51 External walls

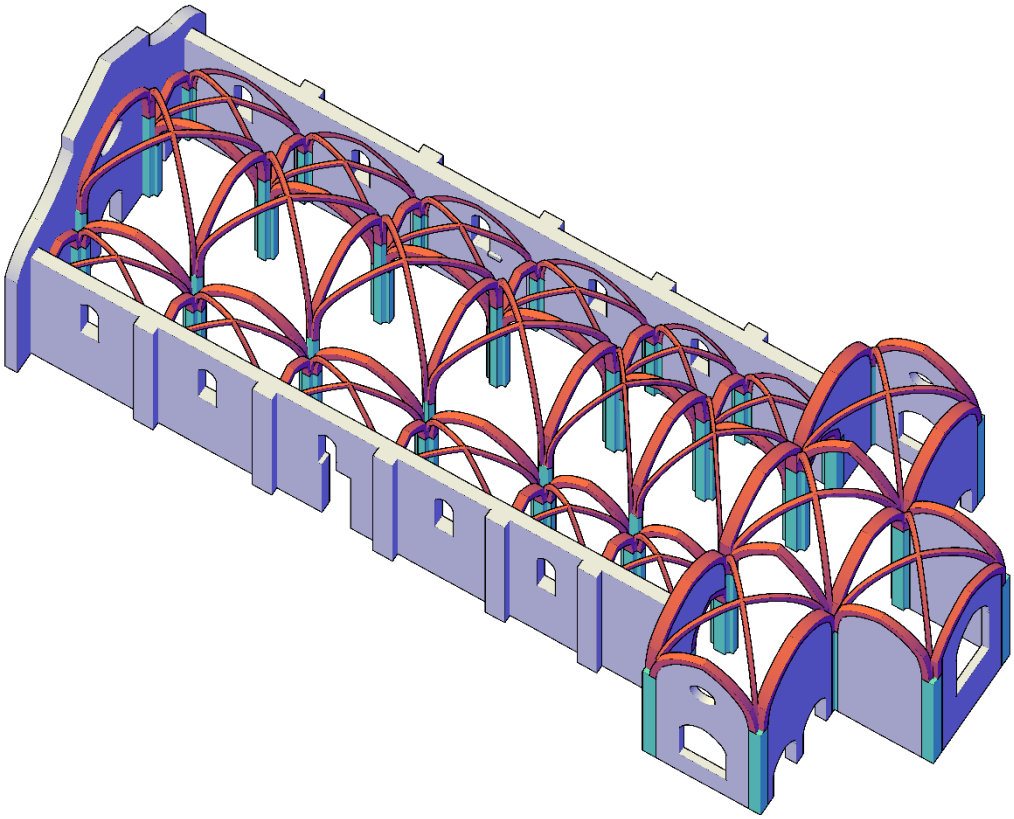

Figure 52 Arches, internal and external walls, pillars

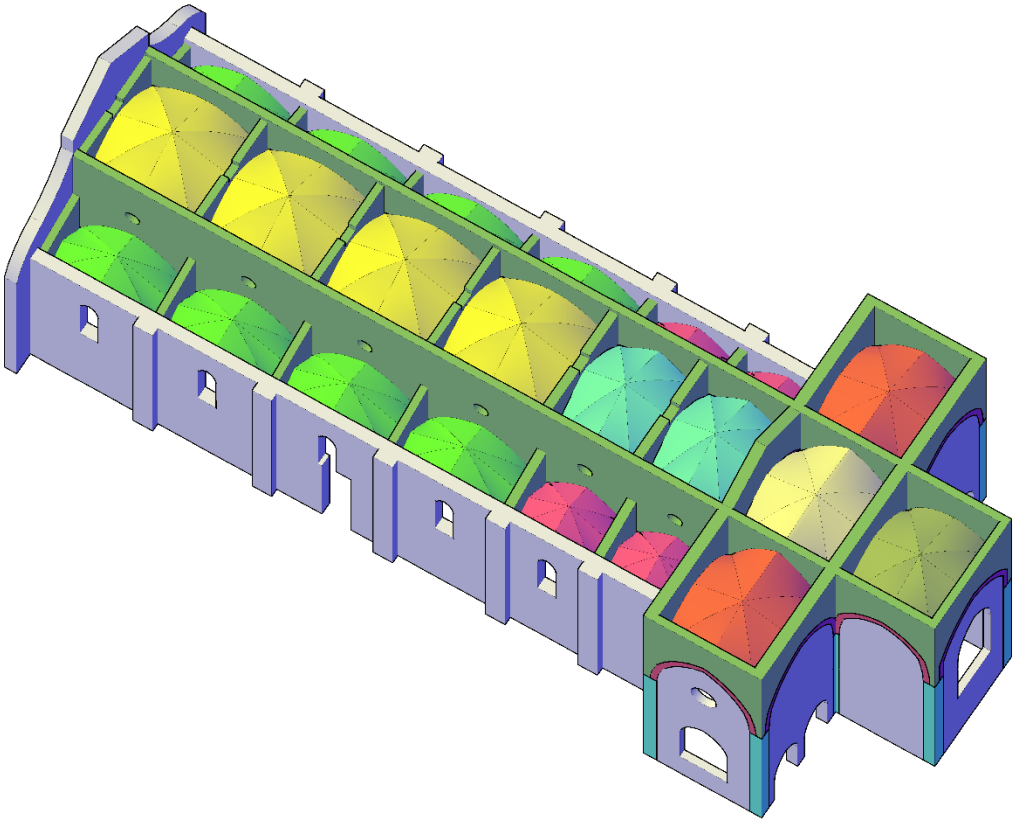

Figure 53 Final model

2.8. Generation of 3-D Complete Model

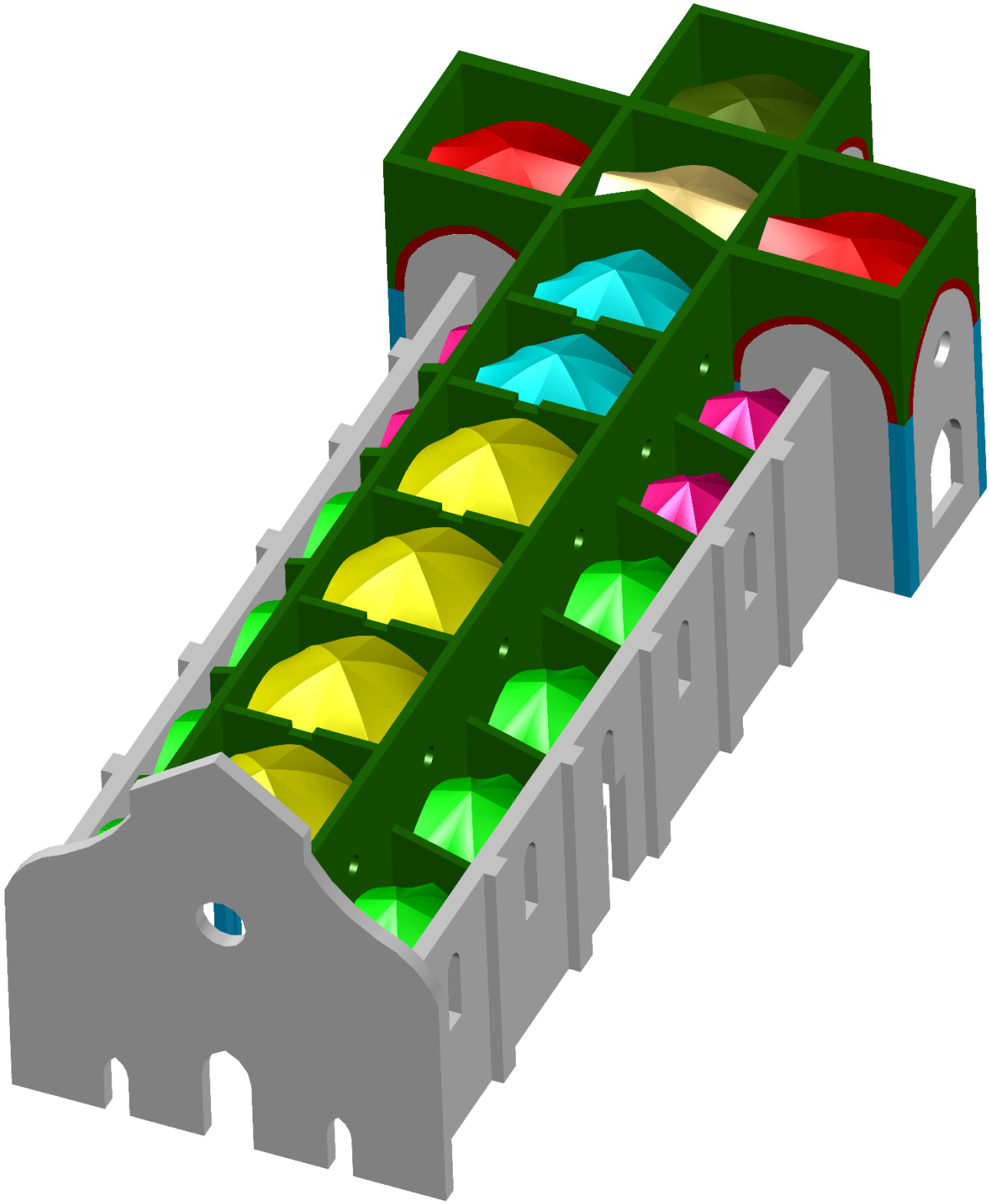

Figure 54 3D geometrical model from southern view

CHAPTER 3

Finite Element Modeling

3.1. Introduction

[*This part is taken from "Maple: Programming, Physical and Engineering Problems Paperback – February 2, 2006 by Victor Aladjev (Author), Marijonas Bogdevicius (Author), chapter 2: Application of Maple for solution of engineering-physical problems*]

The finite element method (FEM), or finite element analysis (FEA), is a computational technique used to obtain approximate solutions of boundary value problems in engineering. Boundary value problems are also called field problems. The field is the domain of interest and most often represents a physical structure. The field variables are the dependent variables of interest governed by the differential equation. The boundary conditions are the specified values of the field variables (or related variables such as derivatives) on the boundaries of the field.

Finite Element Analysis (FEA) was first developed in 1943 by R. Courant, who utilized the Ritz method of numerical analysis and minimization of variational calculus to obtain approximate solutions to vibration systems. Shortly thereafter, a paper published in 1956 by M. J. Turner, R. W. Clough, H. C. Martin, and L. J. Topp established a broader definition of numerical analysis. The paper centered on the "stiffness and deflection of complex structures".

FEA consists of a geometrical model of a material or design that is stressed and analyzed for specific results. It is used in new product design, and existing product refinement. Modifying an existing product or structure is utilized to qualify the product or structure for a new service condition. In case of structural failure, FEA may be used to help determine the design modifications to meet the new condition.

There are generally two types of analysis: 2-D modeling, and 3-D modeling. While 2-D modeling conserves simplicity and allows the analysis to be run on a relatively normal computer, it tends to yield less accurate results. 3-D modeling, however, produces more accurate results while sacrificing the ability to run on all but the fastest computers effectively. Within each of these modeling schemes, the programmer can insert numerous algorithms (functions) which may make the system behave linearly or non-linearly. Linear systems are far less complex and generally do not take into account plastic deformation. Non-linear systems do account for plastic deformation, and many also are capable of testing a material all the way to fracture.

FEA uses a complex system of points called nodes which make a grid called a mesh. This mesh is programmed to contain the material and structural properties which define how the structure will react to certain loading conditions. Nodes are assigned at a certain density throughout the material depending on the anticipated stress levels of a particular area. Regions which will receive large amounts of stress usually have a higher node density than those which experience little or no stress. Points of interest may consist of: fracture point of previously tested material, fillets, corners, complex detail, and high stress areas. The mesh acts like a spider web in that from each node, there extends a mesh element to each of the adjacent nodes.

Each FEA program may come with an element library.

Some sample elements are:

- Rod elements
- Beam elements
- Plate/Shell/Composite elements
- Shear panel
- Solid elements
- Spring elements
- Mass elements
- Rigid elements
- Viscous damping elements

Different types of finite element analysis

Structural analysis consists of linear and non-linear models. Linear models use simple parameters and assume that the material is not plastically deformed. Non-linear models consist of stressing the material past its elastic capabilities. The stresses in the material then vary with the amount of deformation.

Vibrational analysis is used to test a material against random vibrations, shock, and impact. Each of these incidences may act on the natural vibrational frequency of the material which, in turn, may cause resonance and subsequent failure.

Fatigue analysis helps designers to predict the life of a material or structure by showing the effects of cyclic loading on the specimen. Such analysis can show the areas where crack propagation is most likely to occur. Failure due to fatigue may also show the damage tolerance of the material.

Heat Transfer analysis models the conductivity or thermal fluid dynamics of the material or structure. This may consist of a steady-state or transient transfer. Steady-state transfer refers to constant thermo properties in the material that yield linear heat diffusion.

A GENERAL PROCEDURE FOR FINITE ELEMENT ANALYSIS

• Preprocessing

- Definition of the geometric domain of the problem
- Definition of the element type(s) to be used
- Definition of the material properties of the elements
- Definition of geometric properties of the elements (length, area, and the like)
- Definition of element connectivity (mesh the model)
- Definition of the physical constraints (boundary conditions)

– Definition of the loadings

• Solution

– Computation of the unknown values of the primary field variable(s)
– Computation of values which are used by back substitution to compute additional, derived variables, such as reaction forces, element stresses, and heat flow.

• Post processing

Postprocessor software contains sophisticated routines used for sorting, printing, and plotting selected results from a finite element solution.

– Sort element stresses in order of magnitude.
– Check equilibrium.
– Calculate factors of safety.
– Plot deformed structural shape.
– Animate dynamic model behavior.
– Produce color-coded temperature plots.

Mesh Generation of Finite Element Model

The basic concept in the physical FEM is the subdivision of the mathematical model into disjoint (non-overlapping) components of simple geometry called *finite elements* or *elements* for short. The response of each element is expressed in terms of a finite number of degrees of freedom characterized as the value of an unknown function, or functions, at a set of nodal points. The response of the mathematical model is then considered to be approximated by that of the discrete model obtained by connecting or assembling the collection of all elements.

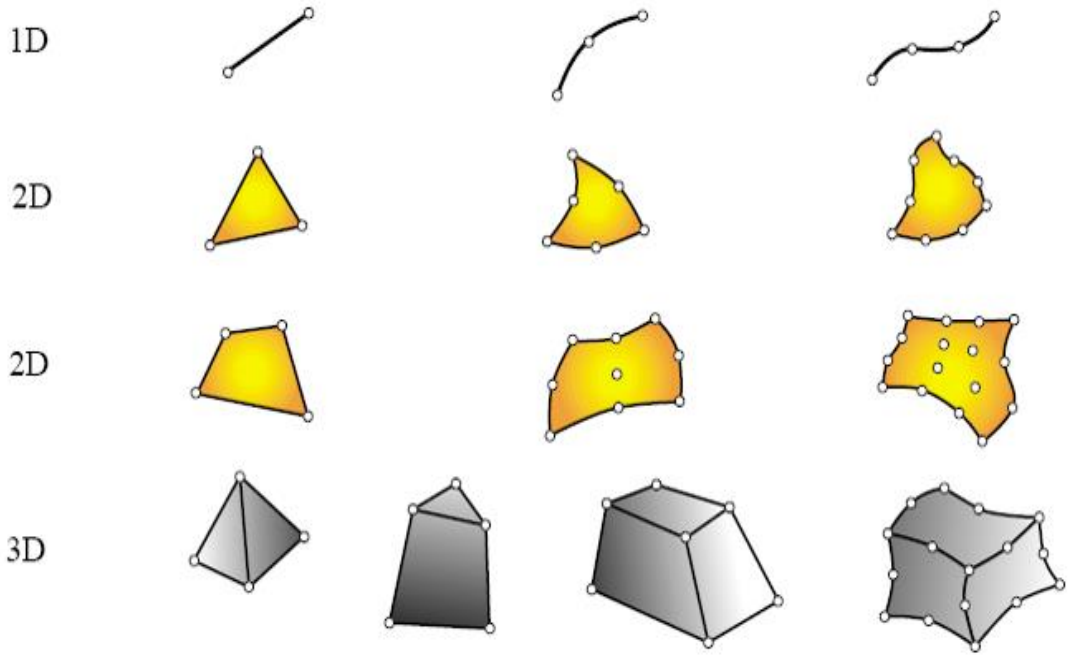

Figure 55 Different mesh elements

A three-dimensional element types

A 3D solid element can be considered to be the most general of all solid finite elements because all the field variables are dependent of x, y and z. An example of a 3D solid structure under loading is shown in Figure 9.1. As can be seen, the force vectors here can be in any arbitrary direction in space. A 3D solid can also have any arbitrary shape, material properties and boundary conditions in space. As such, there are altogether six possible stress components, three normal and three shear, that need to be taken into consideration. Typically, a 3D solid element can be a tetrahedron or hexahedron in shape with either flat or curved surfaces. Each node of the element will have three translational degrees of freedom. The element can thus deform in all three directions in space.

Since the 3D element is said to be the most general solid element, the truss, beam, plate, 2D solid and shell elements can all be considered to be special cases of the 3D element. So, why is there a need to develop all the other elements? Why not just use the 3D element to model everything? Theoretically, yes, the 3D element can actually be used to model all kinds of structural components, including trusses, beams, plates, shells and so on. However, it can be very tedious in geometry creation and meshing. Furthermore, it is also most demanding on computer resources. Hence, the general rule of thumb is, that when a structure can be assumed within acceptable tolerances to be simplified into a 1D (trusses, beams and frames) or 2D (2D solids and plates) structure, always do so. The creation of a 1D or 2D FEM model is much easier and efficient. Use 3D solid elements only when we have no other choices. The formulation of 3D solids elements is straightforward, because it is basically an extension of 2D solids elements. All the techniques used in 2D solids can be utilized, except that all the variables are now functions of x, y and z. The basic concepts, procedures and formulations for 3D solid elements can also be found in many existing topics.

Different 3D element types

- Tetrahedral
- Bricks
- Prisms
- Pyramids

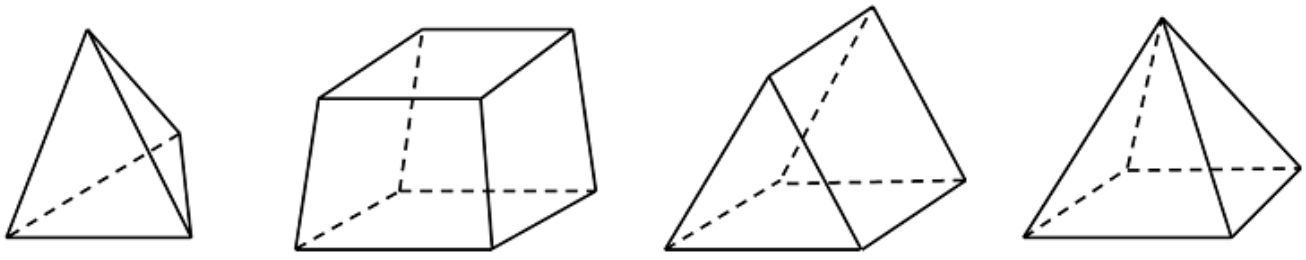

Figure 56 Different 3D element types

3.2. Tetrahedral elements

Tetrahedral is also known as a simplex, which simply means that any 3D volume, regardless of shape or topology, can be meshed with tetra elements. They are also the only kind of elements that can be used with adaptive mesh refinement. For these reasons, tetrahedral elements can usually be the best or may be the only choice for complex geometries.

The other three element types (bricks, prisms, and pyramids) should be used only when it is motivated to do so. It is first worth noting that these elements will not always be able to mesh a particular geometry. The meshing algorithm usually requires some more user input to create such a mesh, so before going through this effort, you need to ask yourself if it is motivated. Here we will talk about the motivations behind using brick and prism elements. The pyramids are only used when creating a transition in the mesh between bricks and tets.

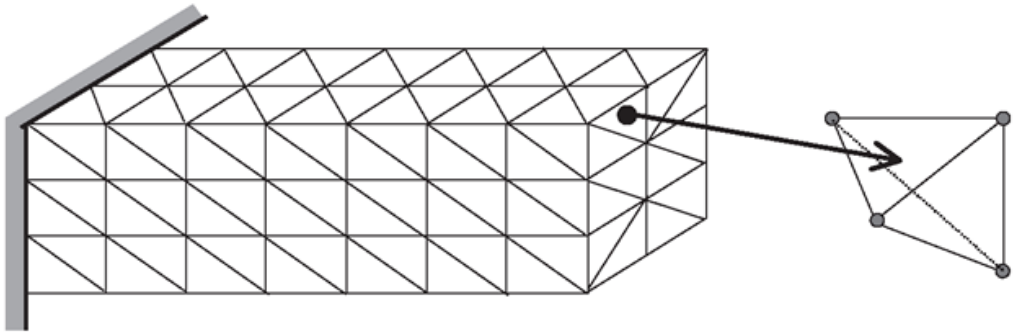

Figure 57 Solid block divided into four-node tetrahedron elements

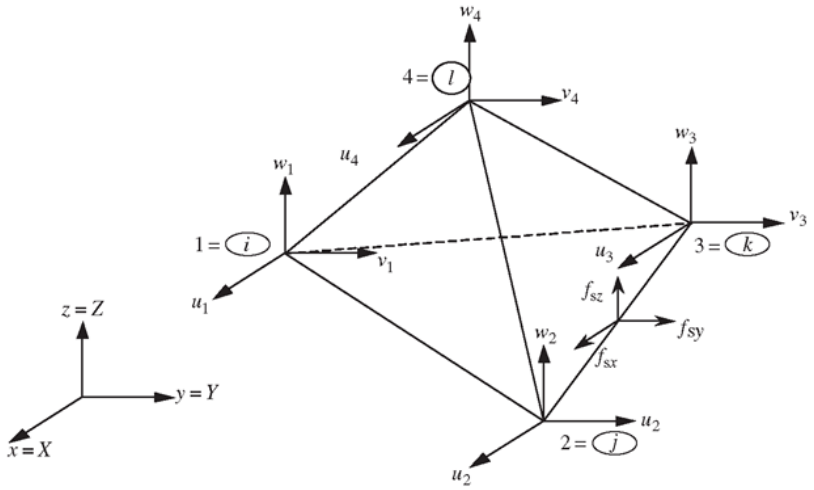

Figure 58 Tetrahedral element nodal displacements

The nodes are numbered 1, 2, 3 and 4 by the right-hand rule. The local Cartesian coordinate system for a tetrahedron element can usually be the same as the global coordinate system, as there are no advantages in having a separate local Cartesian coordinate system. In an element, the displacement vector U is a function of the coordinate x, y and z, and is interpolated by shape functions in the following form, which should by now be shown to be part and parcel of the finite element method

Nodal displacement vector (de)

$$\mathbf{d}_e = \begin{Bmatrix} u_1 \\ v_1 \\ w_1 \\ u_2 \\ v_2 \\ w_2 \\ u_3 \\ v_3 \\ w_3 \\ u_4 \\ v_4 \\ w_4 \end{Bmatrix} \begin{matrix} \\ \\ \\ \\ \\ \\ \\ \\ \\ \\ \\ \\ \end{matrix} \begin{matrix} \left.\begin{matrix} \\ \\ \\ \end{matrix}\right\} \text{displacements at node 1} \\ \left.\begin{matrix} \\ \\ \\ \end{matrix}\right\} \text{displacements at node 2} \\ \left.\begin{matrix} \\ \\ \\ \end{matrix}\right\} \text{displacements at node 3} \\ \left.\begin{matrix} \\ \\ \\ \end{matrix}\right\} \text{displacements at node 4} \end{matrix}$$

Figure 59 Nodal displacement vector (de)

Shape functions Matrix

$$\mathbf{N} = \begin{bmatrix} \overbrace{N_1 & 0 & 0}^{\text{node 1}} & \overbrace{N_2 & 0 & 0}^{\text{node 2}} & \overbrace{N_3 & 0 & 0}^{\text{node 3}} & \overbrace{N_4 & 0 & 0}^{\text{node 4}} \\ 0 & N_1 & 0 & 0 & N_2 & 0 & 0 & N_3 & 0 & 0 & N_4 & 0 \\ 0 & 0 & N_1 & 0 & 0 & N_2 & 0 & 0 & N_3 & 0 & 0 & N_4 \end{bmatrix}$$

Figure 60 Shape functions Matrix

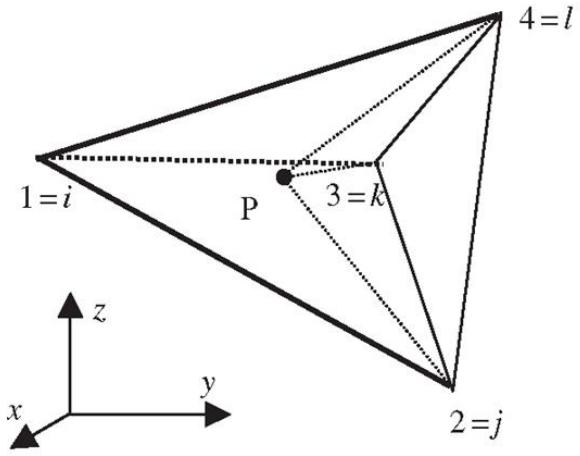

Figure 61 Volume coordinates for tetrahedron elements

3.3. Meshing of the model

After generating the geometrical model in AutoCAD, the model is divided in five parts.

Five different part of the model

1. Arches (which includes, all the longitudinal and transversal arches and ribs)
2. Pillars (which includes just pillars)
3. External walls (which includes all the peripheral walls of the church that are connected to the ground)
4. Internal walls (which includes all the internal walls which are connected to upper surface of the arches)
5. Vaults (which includes all the vaults of the lateral and central vaults)

After defining the parts in AutoCAD, the model is exported as *.sat file, then this files is imported in Abaqus software. We select arches, pillars and external walls parts and they are assembled to an independent assembly model. After assembling these parts, by implementing Merge/Cut instance tab in assembly page of Abaqus, the geometry of the parts are merged by retaining the intersecting interaction of the parts. Then we add other two remained parts (vaults and internal walls) to create the final assembled model.

When the final model including all the parts is assembled, linear 3D solid tetrahedral elements are assigned for all the model by seeding the nodes first time with 80cm in distance and another time with 20cm in distance. After defining all the parameter for elements and meshes, the meshing procedure is done and all the parts in the model are meshed simultaneously, and the result of the meshing is represented in the figures below.

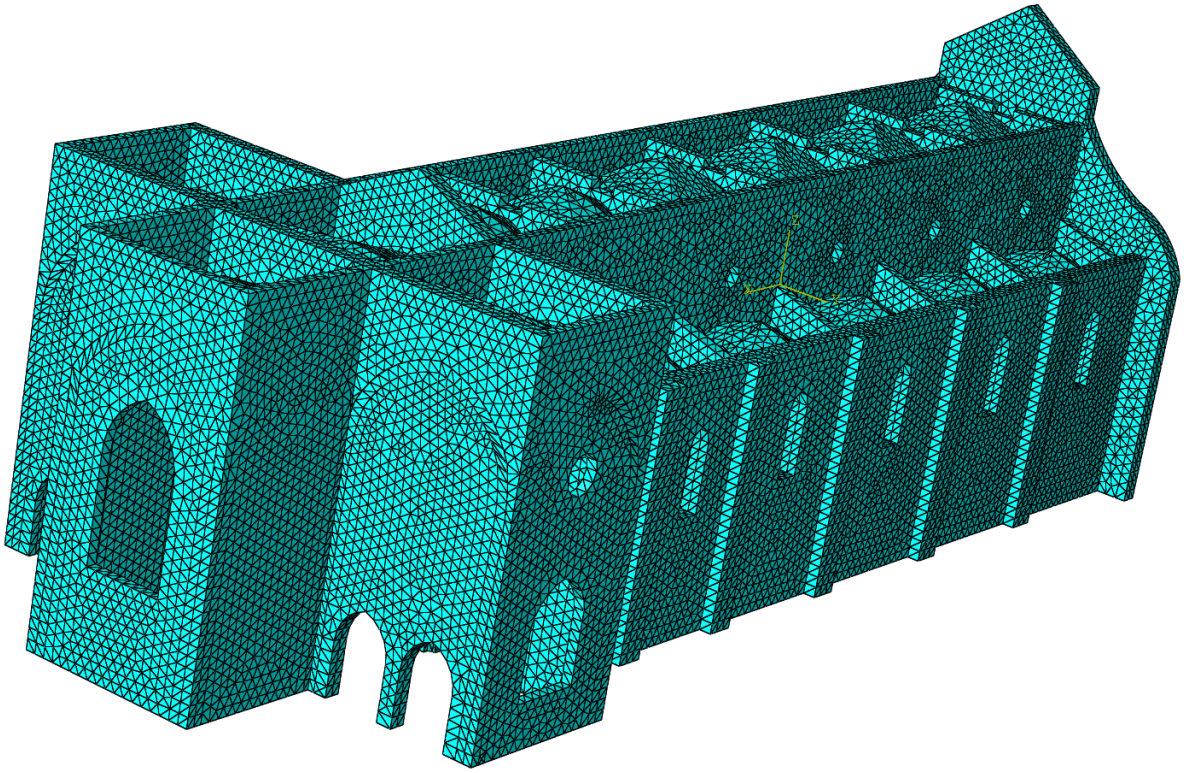

Figure 62 Meshing of the assembled model

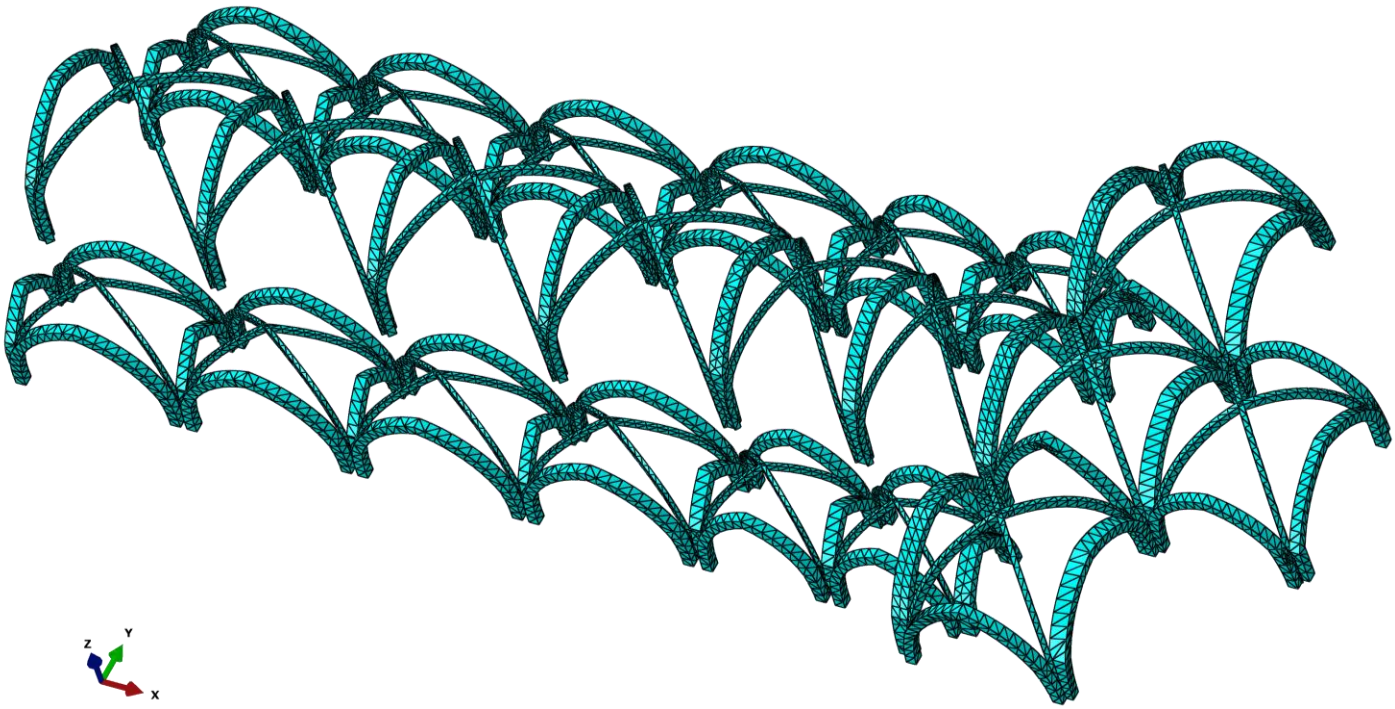

Figure 63 mesh generation for the arches part

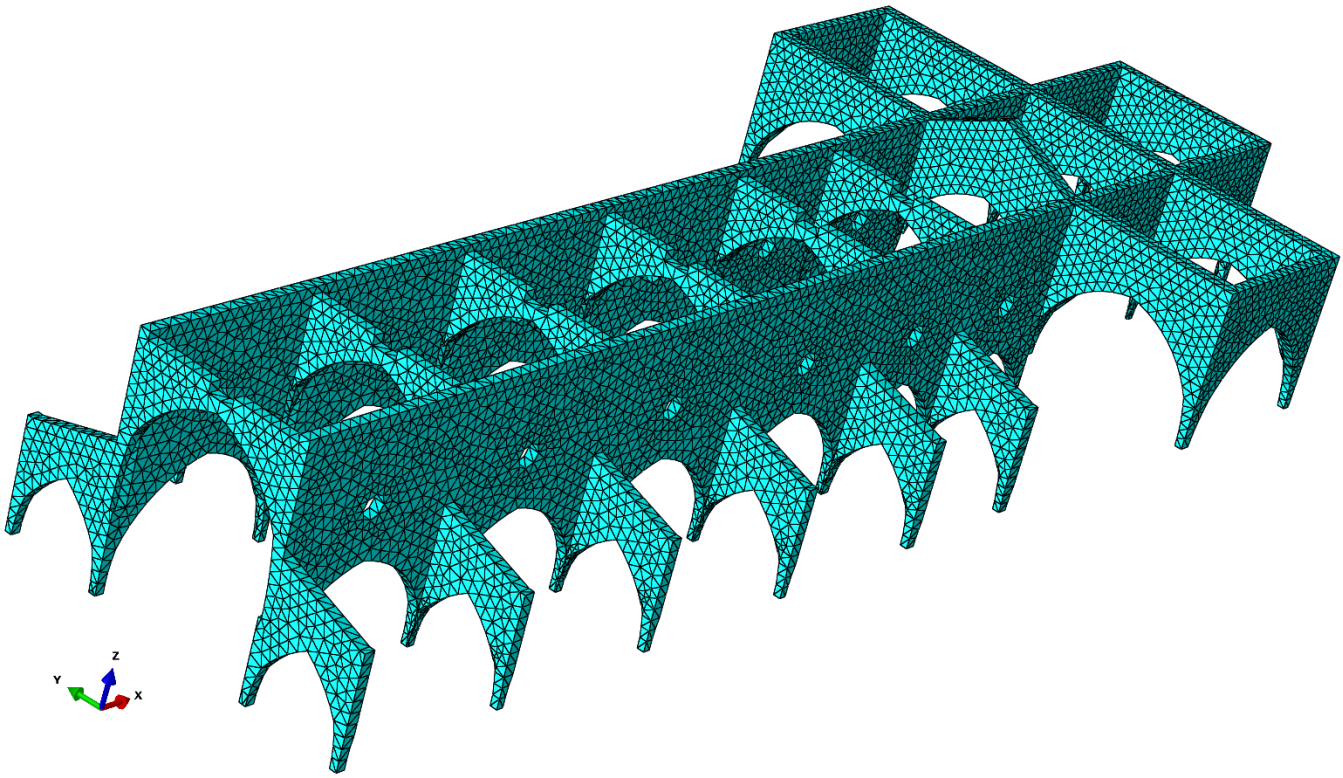

Figure 64 mesh generation for the internal walls part

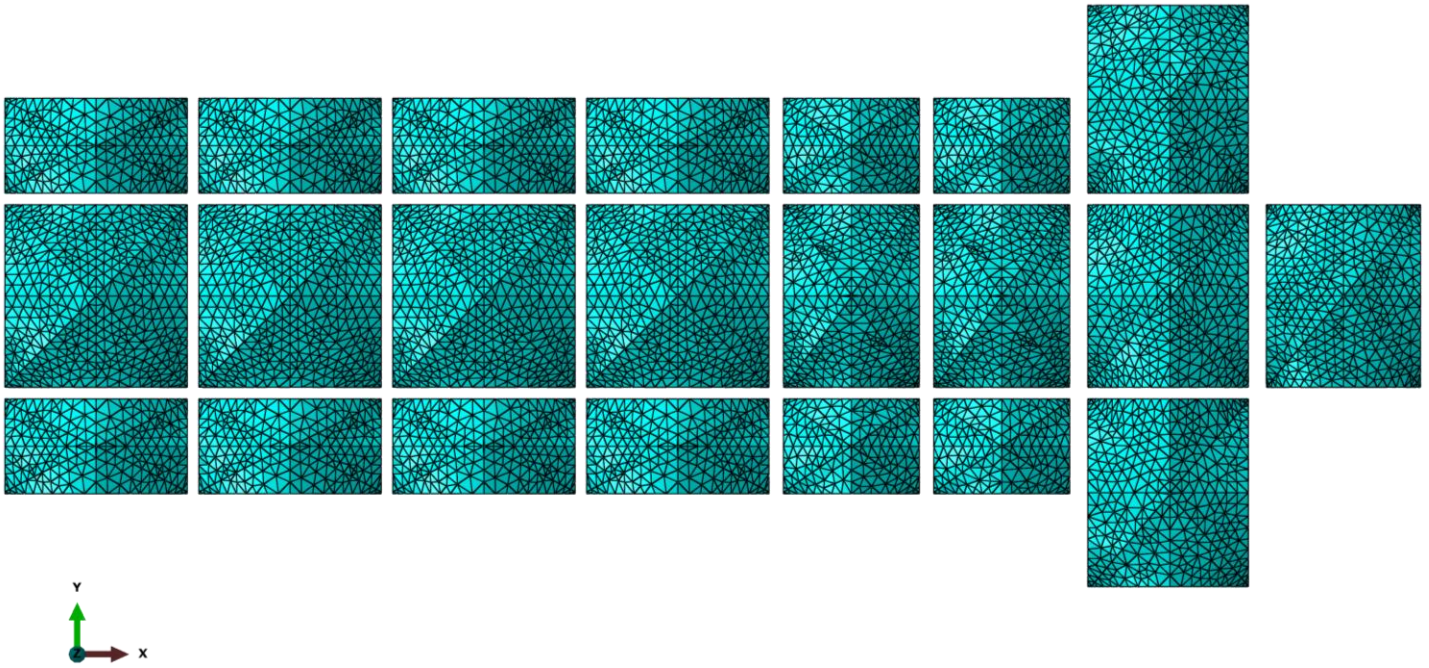

Figure 65 mesh generation for vaults part extrados view

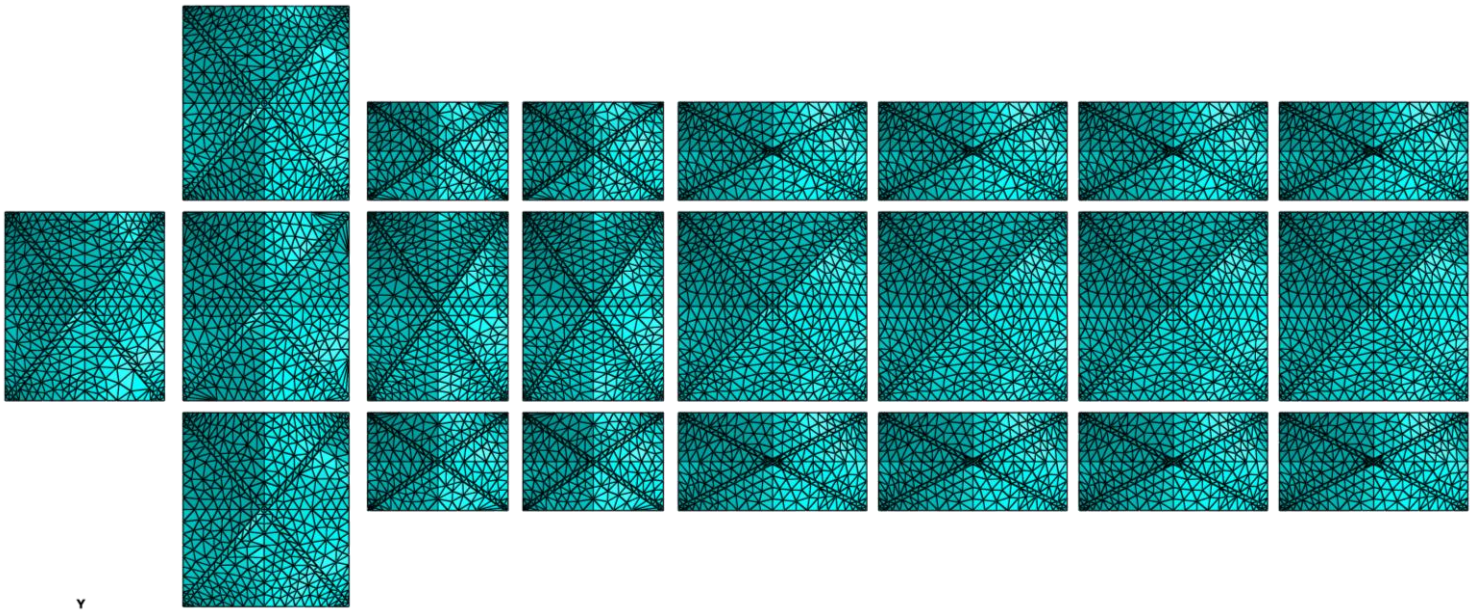

Figure 66 mesh generation for vaults part intrados view

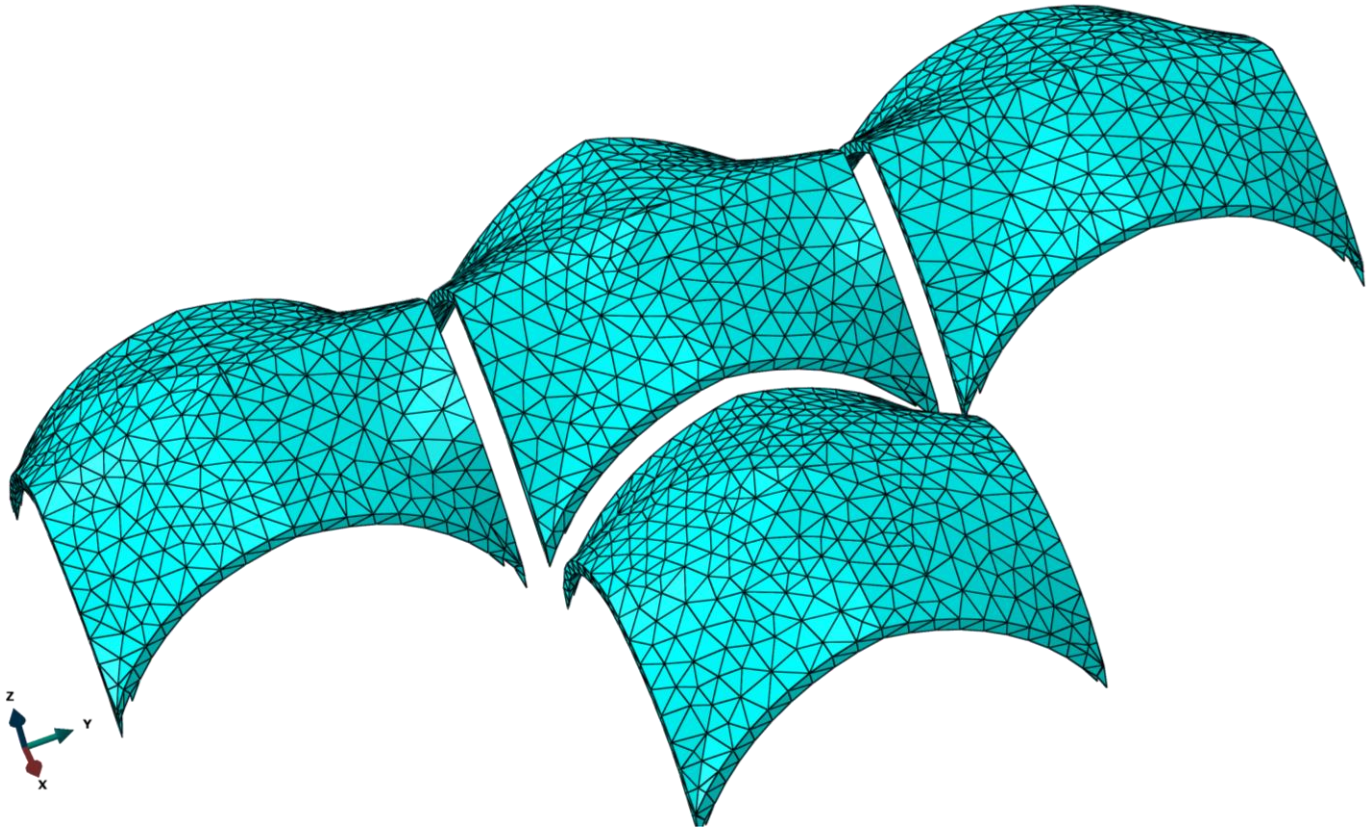

Figure 67 mesh generation for vaults of the transept part

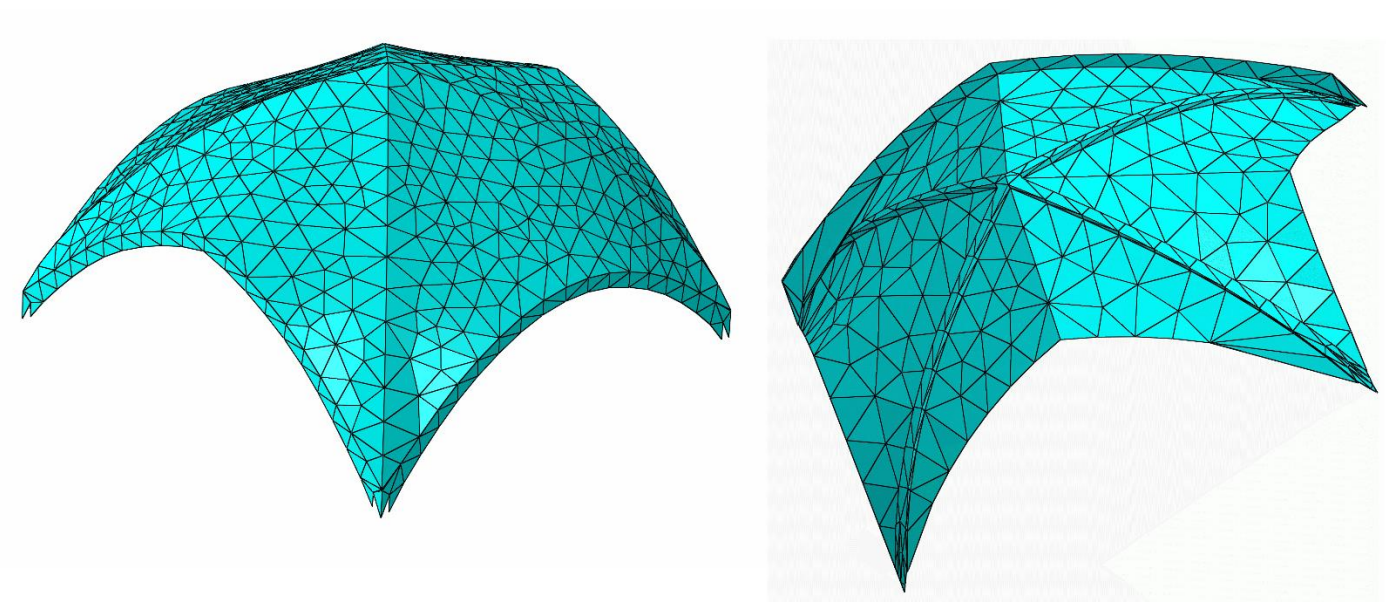

Figure 68 mesh generation for central bay vault from extrados and intrados view

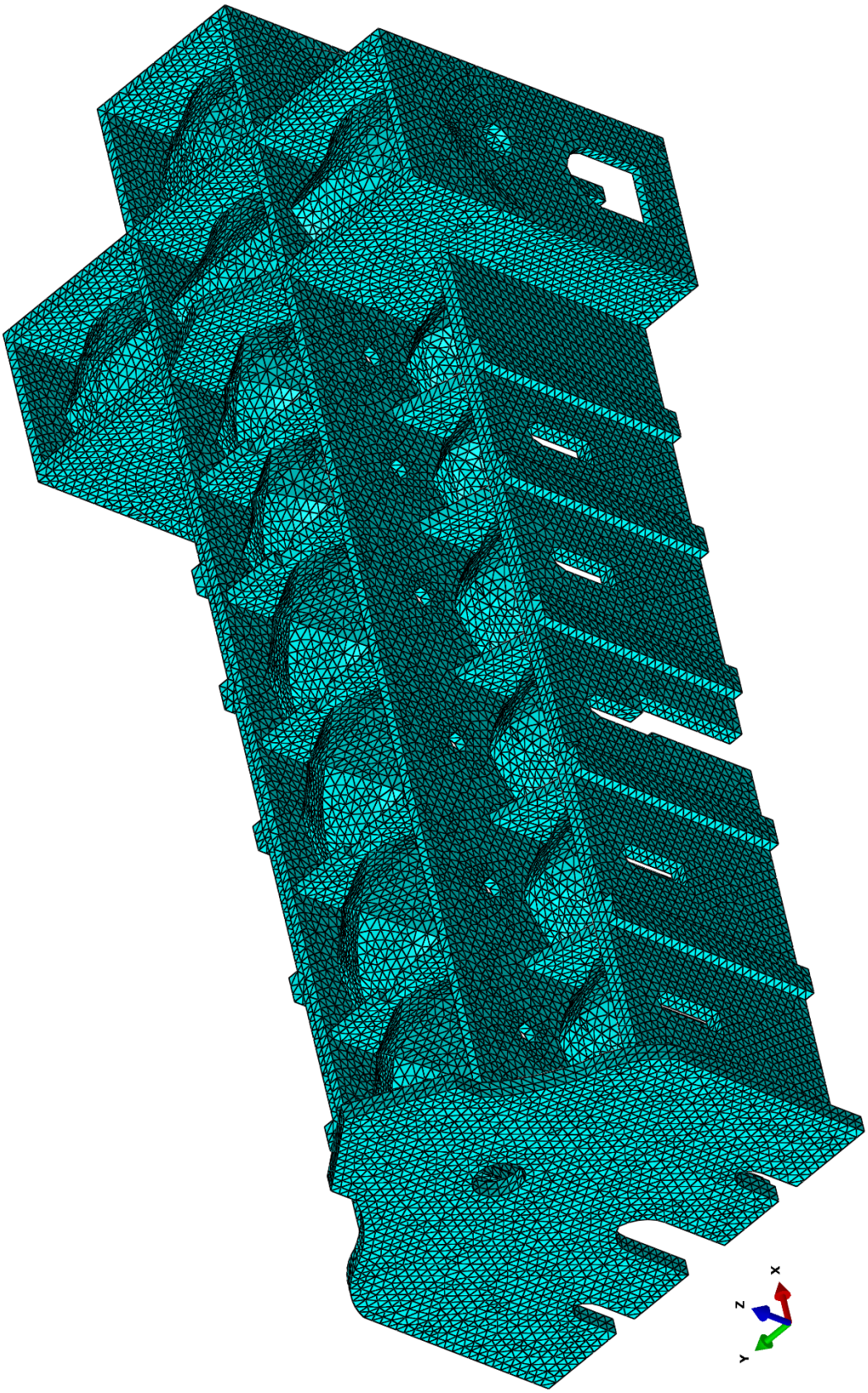

Figure 69 Mesh generation through all the model with 80cm seeding distance

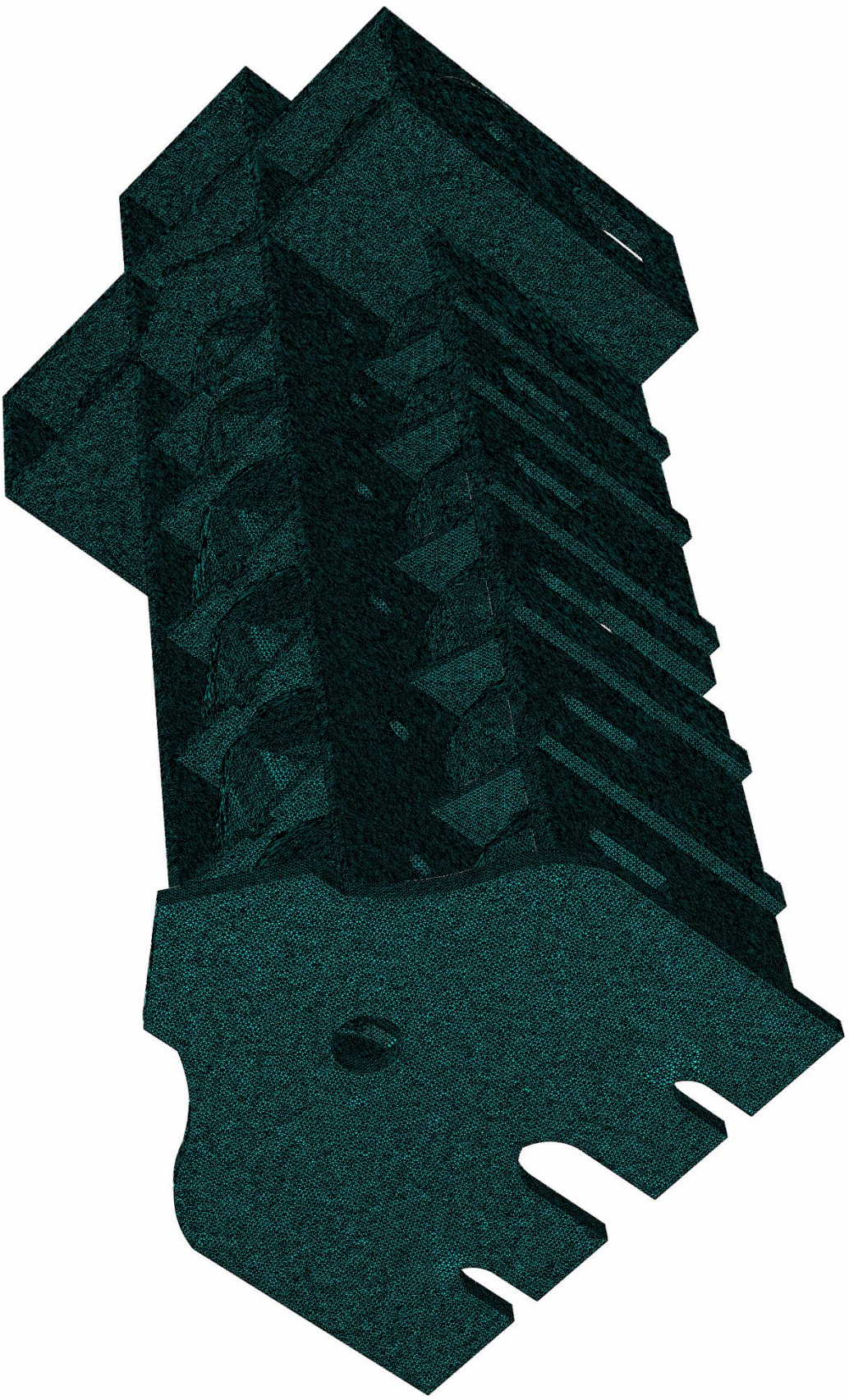

Figure 70 Mesh generation with 20 cm seeding distance

CHAPTER 4

STRUCTURAL ANALYSIS

After generating the mesh model, now the mechanical properties of the materials must be defined and the proper material must be assigned for each part of the model in Abaqus software. Here is the list of materials and their properties.

4.1. Materials and their mechanical properties

Like the previous thesis project [*Basilica di Santa Maria Novella a Firenze: Modellazione Geometrica e Analisi strutturale del Transetto, Candidato: Andrea Manini*] the same materials are considered for the new model. These properties of the defined material are obtained from experimental tests that carried out on samples of different sandstones.

Material	Mass density **Kg/m3**	Young's modulus **MPa**	Poisson's ratio	Assigned parts
sandstone masonry	2000	3800	0.15	Internal and external walls
sandstone rib	2000	18000	0.2	Arches and ribs
sandstone pillar	2000	2500	0.15	Pillars
masonry vault	2300	2300	0.22	Vaults

Figure 71 Materials list and mechanical properties

Loading

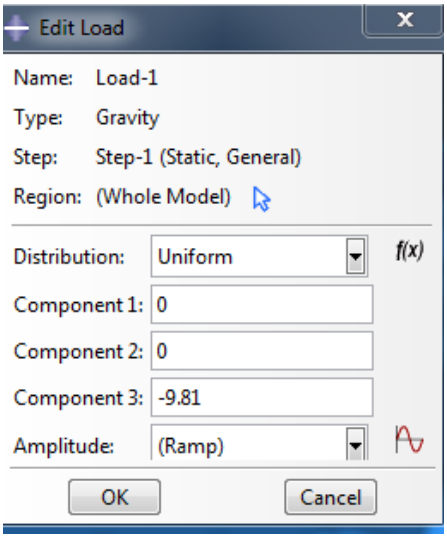

The next step is definition and assignment of loading system for the model in which must be analyzed. In this case study, we do just linear static analysis under the gravity force. Thus we need just to define the uniform gravity load in the –z direction. The acceleration of the earth is considered 9.81 m/s^2.

Figure 72 loading definition

4.2. Definition of boundary condition

Definition of the boundary condition must be done according to the connection of the parts with ground as a rigid and fixed body. In this model, just external walls and pillars are connected to the ground, consequently all the bottom base surface of the pillars and external walls are selected and assigned as the boundary surfaces.

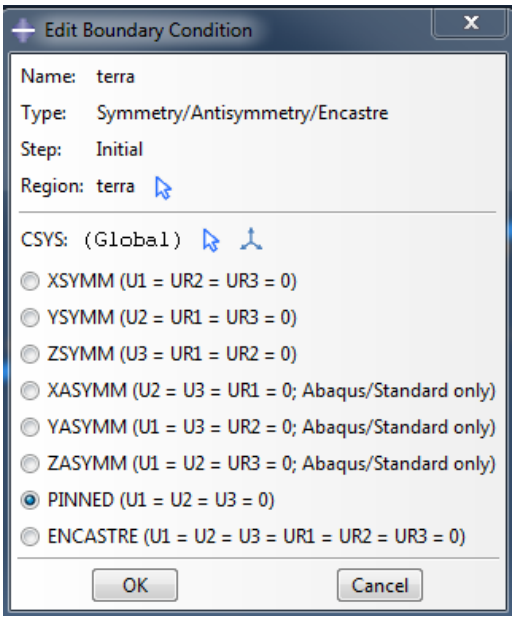

Figure 73 Boundary condition type window in Abaqus

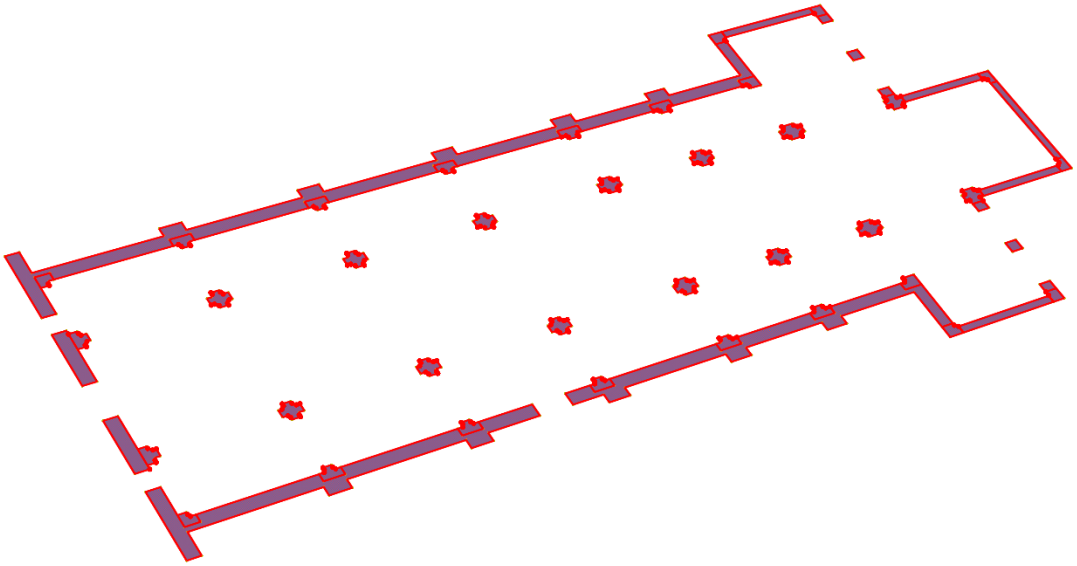

Figure 74 the selected surface from pillars and walls for boundary condition definition

4.3. Interaction definition

After definition and assignment of the materials for parts, now it is time to define interactions for determine connection type of the different parts. As arches, pillars and external walls are merged with together, so there is no need to define interaction between them, but for vaults and internal walls that are assembled separately, it is necessary to define interaction between the merged part and vaults and internal walls.

Definition of interaction between arches and internal walls

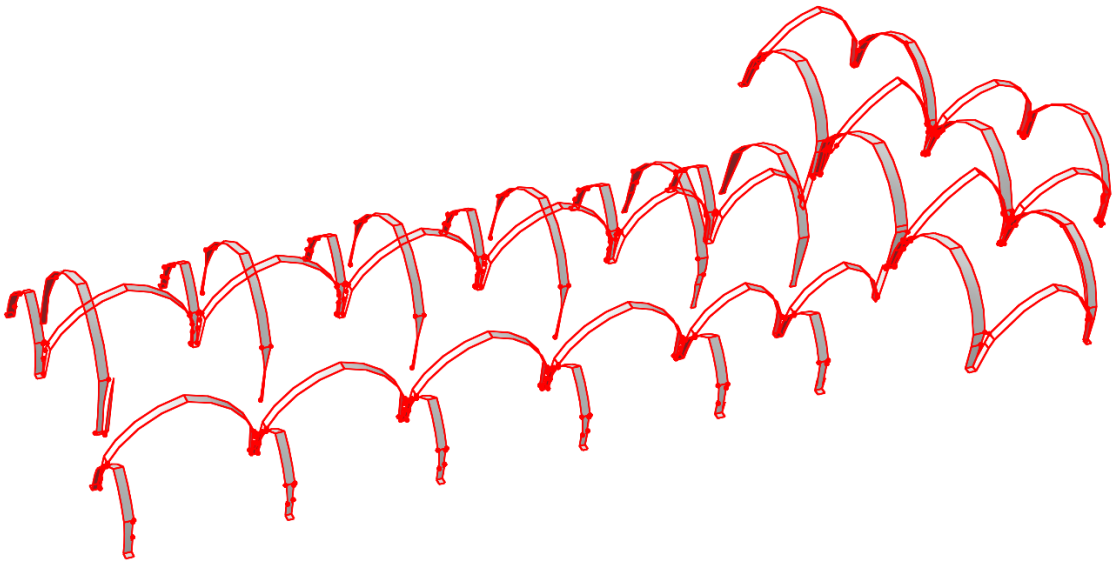

Figure 75 interaction between arches and internal walls

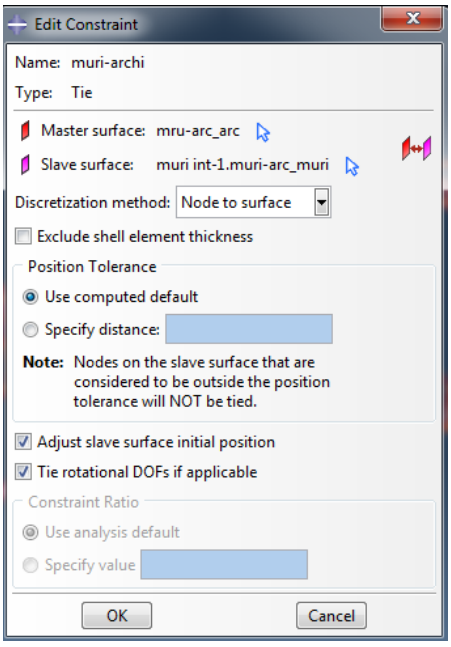

Figure 76 interaction window in Abaqus

In this case, the upper surfaces of the arches are selected as Master surface and the downer surfaces of the internal walls are selected as slave surface.

Node to surface is the discretization method in this definition.

All the nodes in the boundary zones are tied in the way that they cannot have any rotation respect to each other.

Definition of interaction between external and internal walls

Figure 77 interaction between external and internal walls

Definition of interaction between external and internal walls

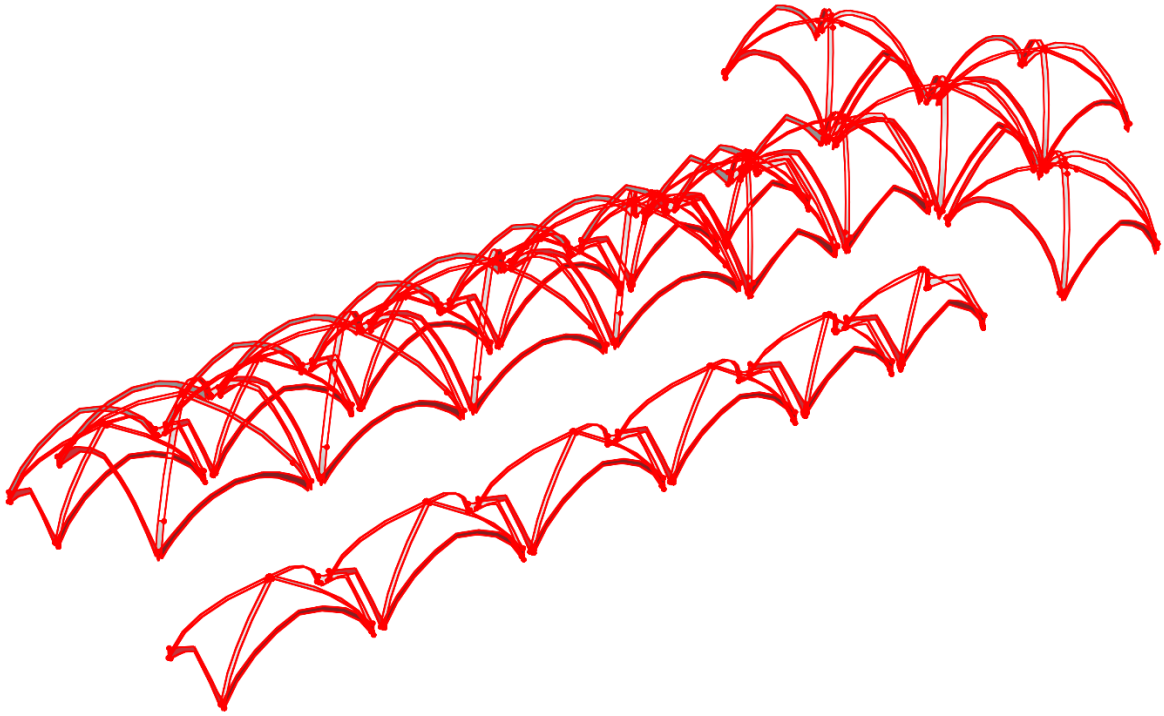

Figure 78 interaction between external and internal walls

4.4. The results of the analysis for the 80cm and 20cm seeding distance

The deformed shape of the model with the scale of 1000 is presented in the figures below. The deformed shape of both models, with seeding of 80cm and 20cm, are so similar and same displacement pattern happens in both models.

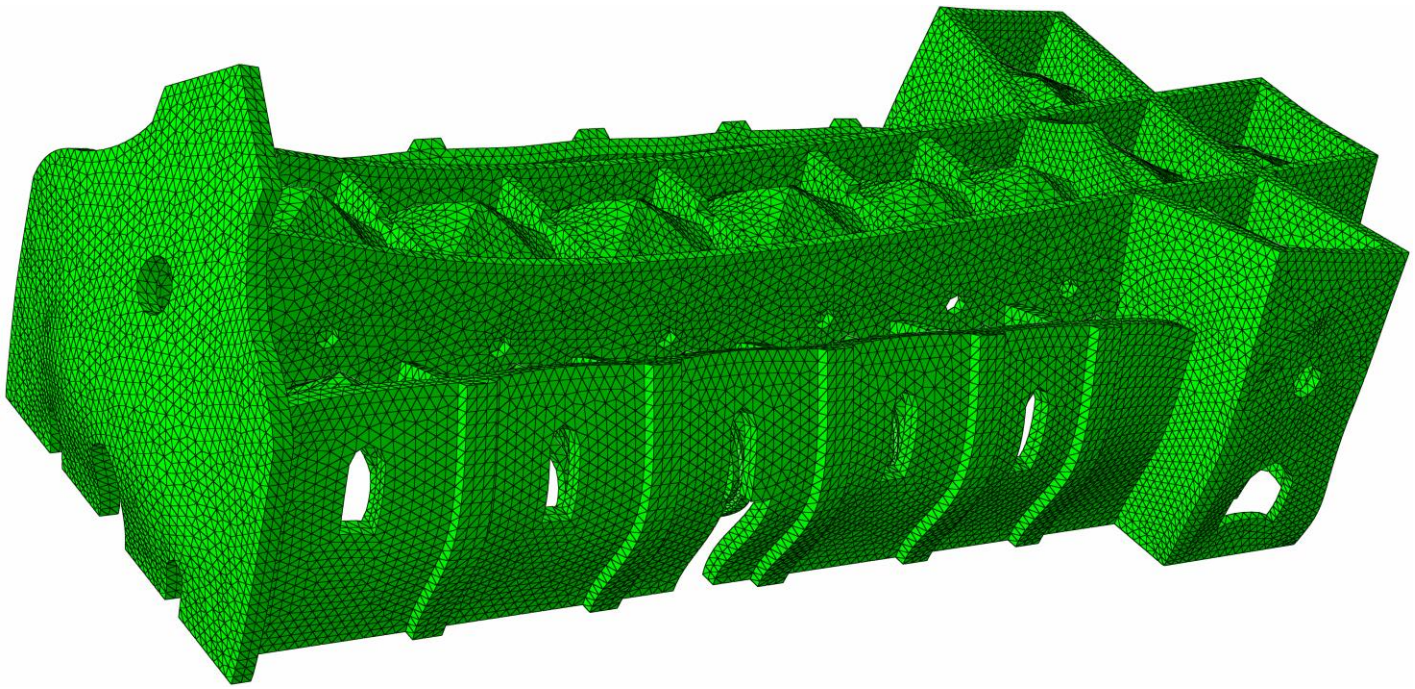

Figure 79 Deformed shape of the model for 80cm elements with scale factor of 1000

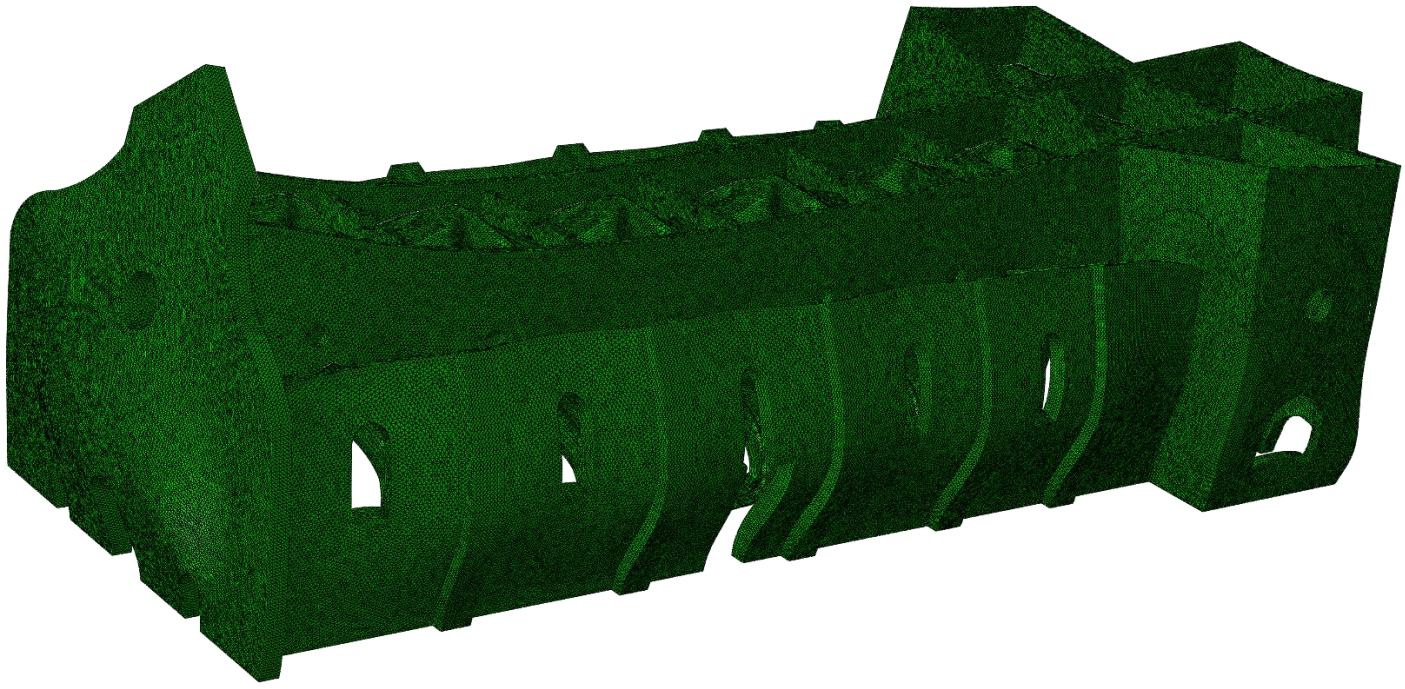

Figure 80 Deformed shape of the model for 20cm elements with scale factor of 1000

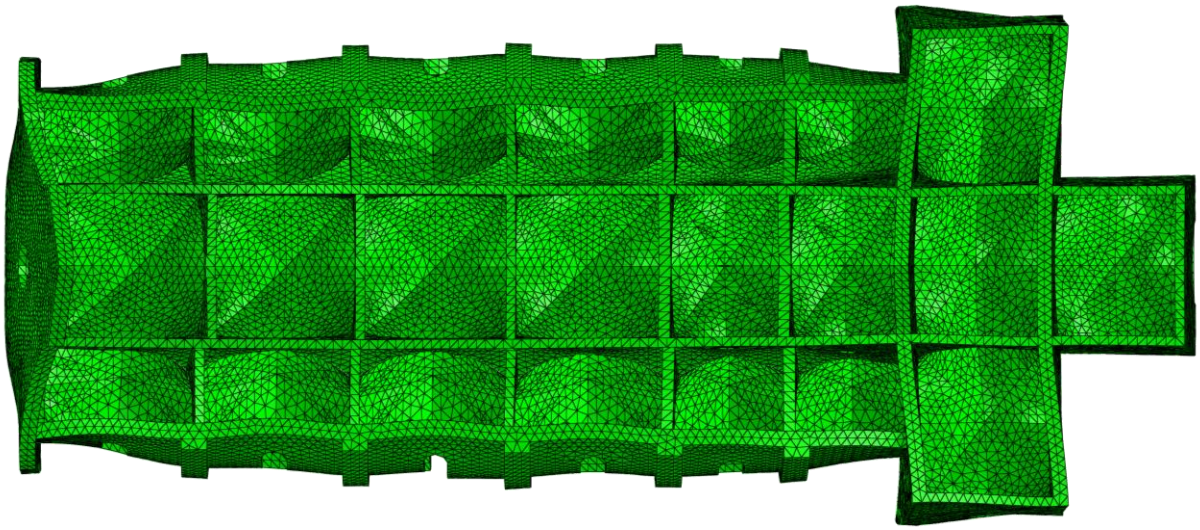

Figure 81 Deformed shape from vertical upper view with scale factor of 1000

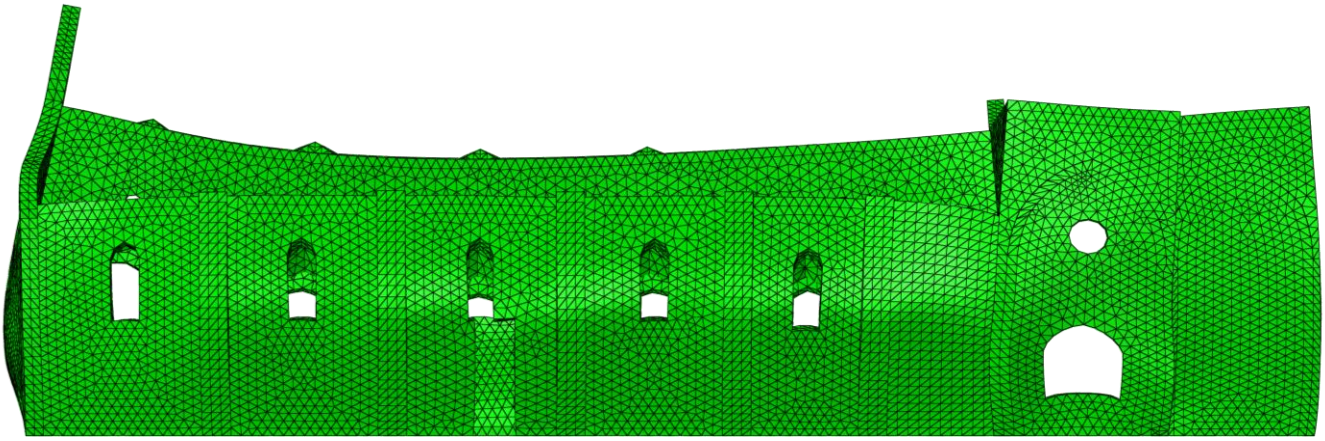

Figure 82 Deformed shape from eastern view with scale factor of 1000

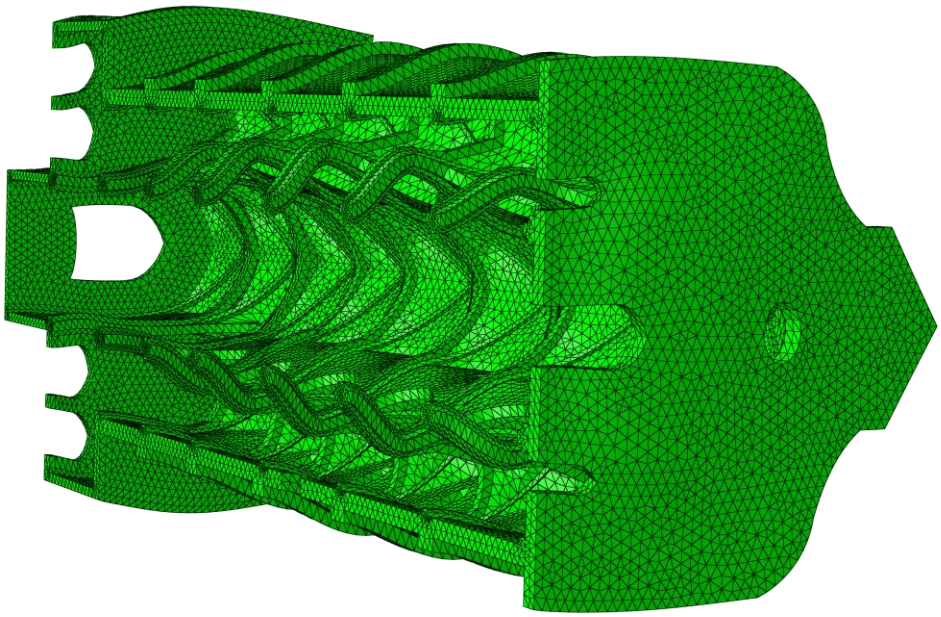

Figure 83 deformed shaped of the pillars

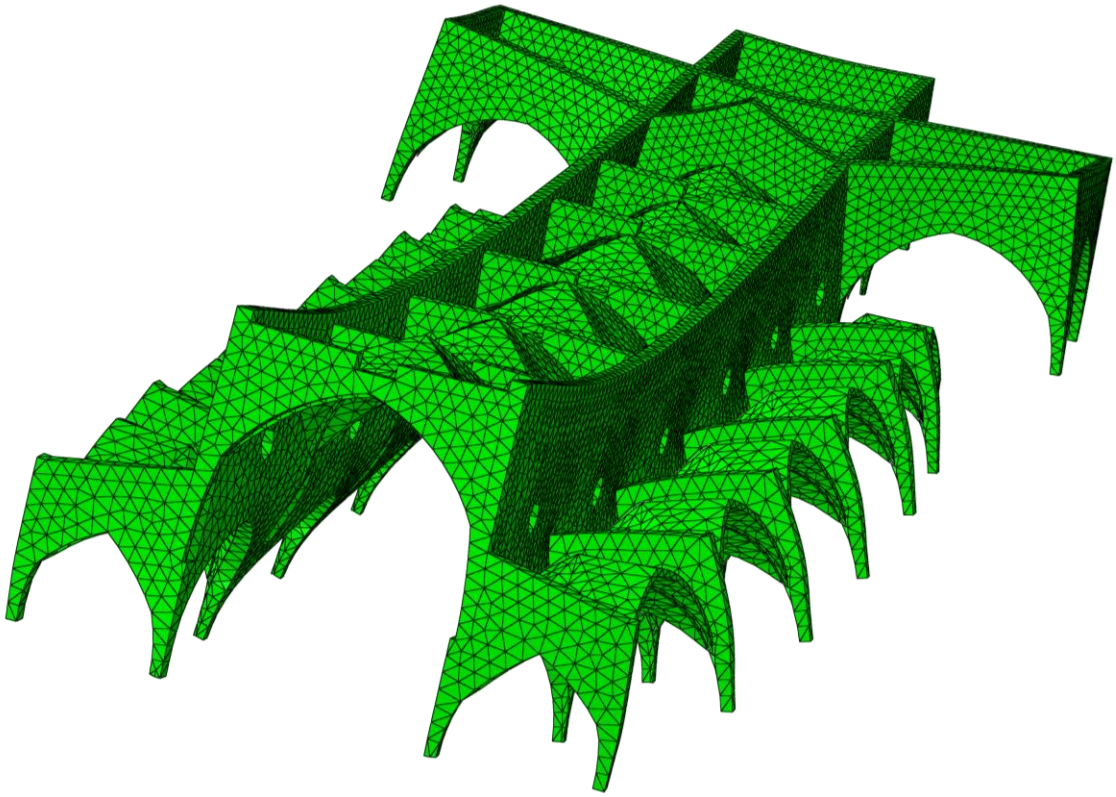

Figure 84 deformed shape of the internal walls

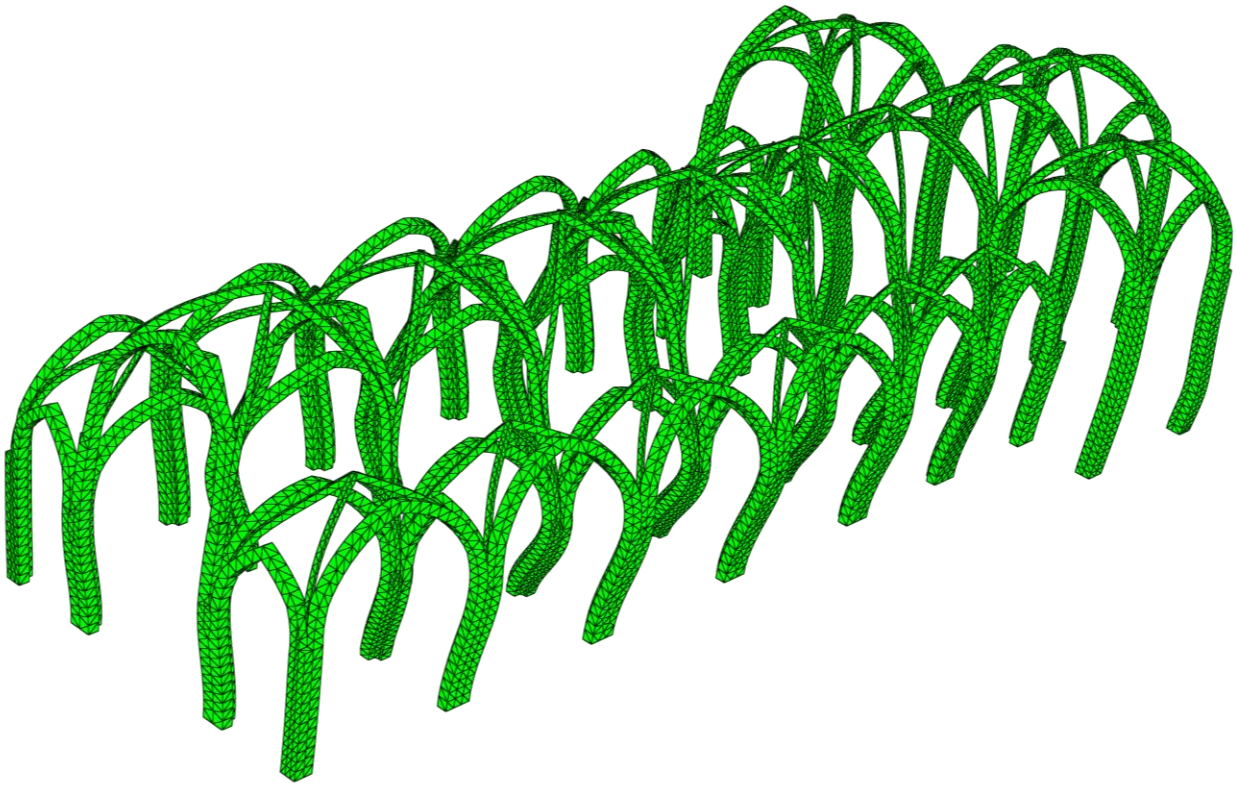

Figure 85 deformed shape of the arches and pillars

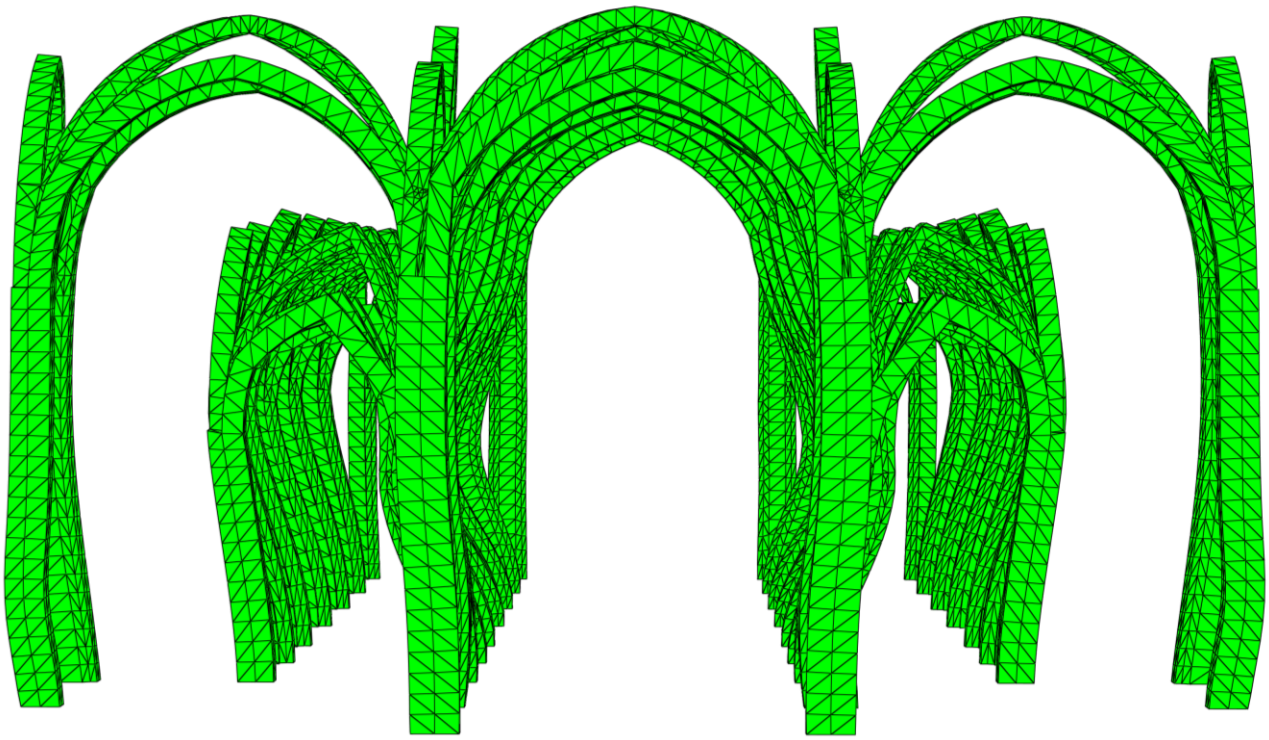

Figure 86 deformed shape of the arches and pillars from southern view

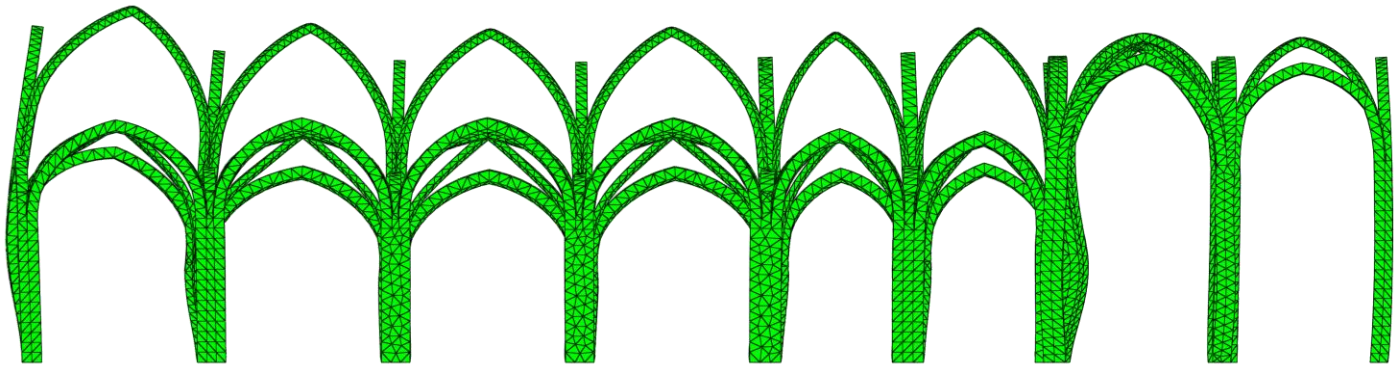

Figure 87 deformed shape of the arches and pillars from western view

According the deformed shapes, the central pillars of the nave and the external walls have the most deformation respect to other parts. The weight of the internal walls and vaults in the central bays can the most important factor of large displacements of the central pillars. All the pillars seem to be deformed symmetrically according to nave longitudinal axis.

4.5. Maximum principal stress of the elements

By considering that the maximum allowable stress in this masonry structure ($0 < \sigma_{max} < 0.2$ MPa), presentation of the maximum principal stress are limited between 0 and 0.2 MPa.

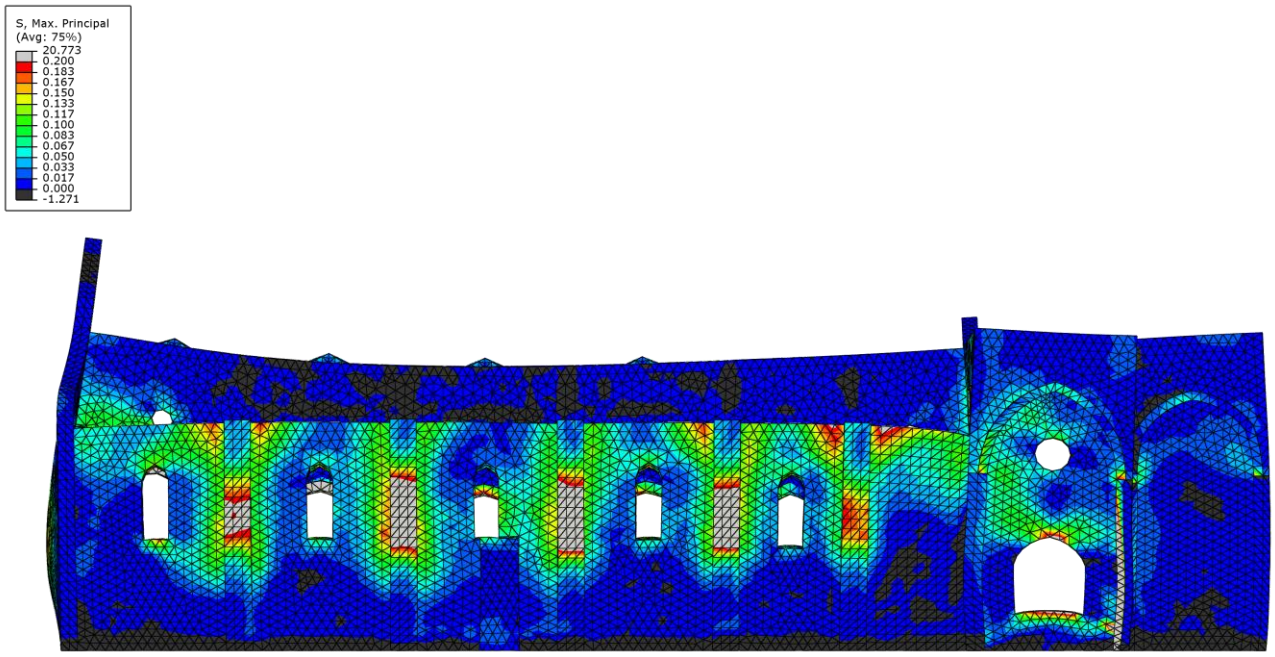

Figure 88 Maximum principal stress of the elements from western view with 80cm seeding

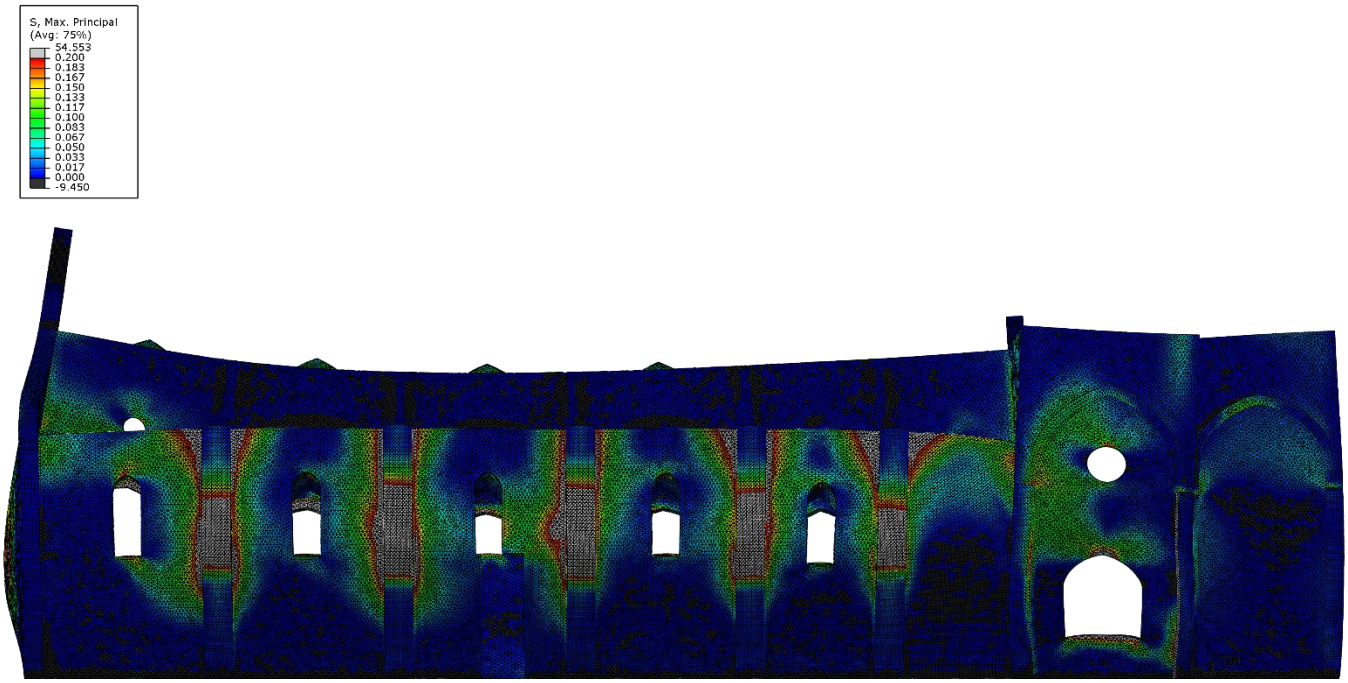

Figure 89 Maximum principal stress of the elements from western view with 20cm seeding

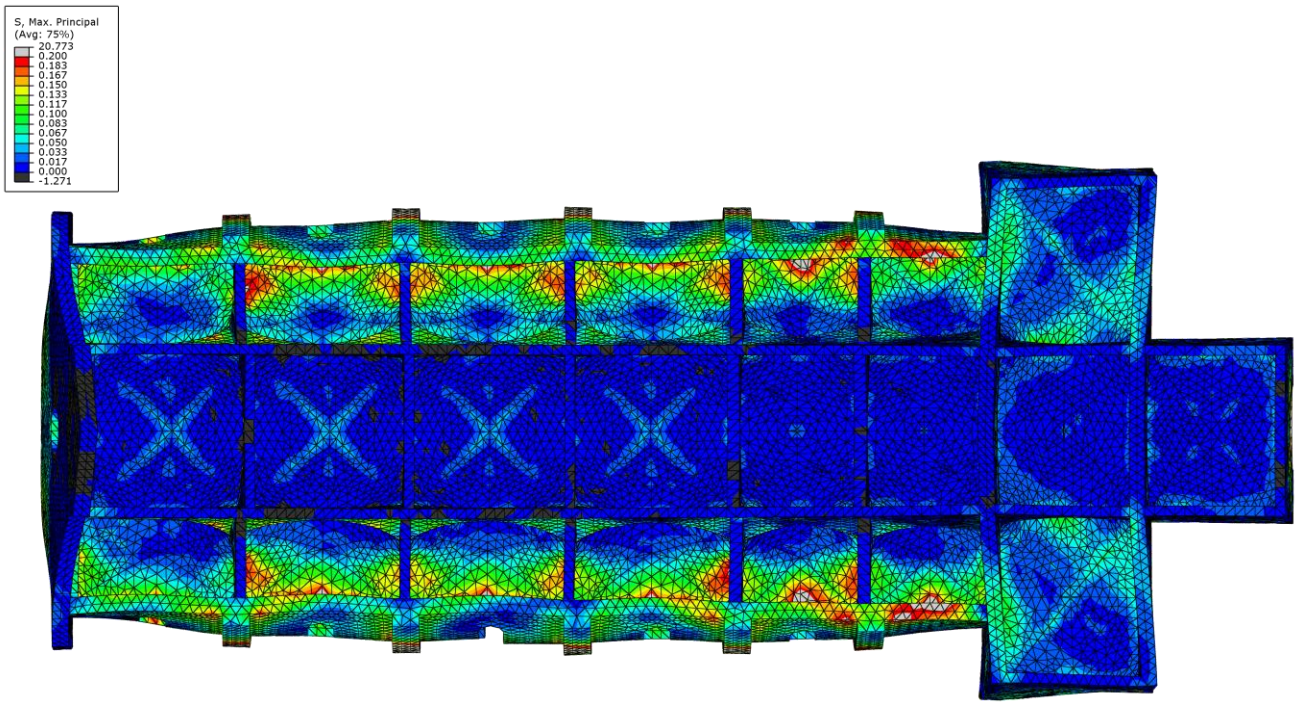

Figure 90 Maximum principal stress of the elements from upper view with 80cm seeding

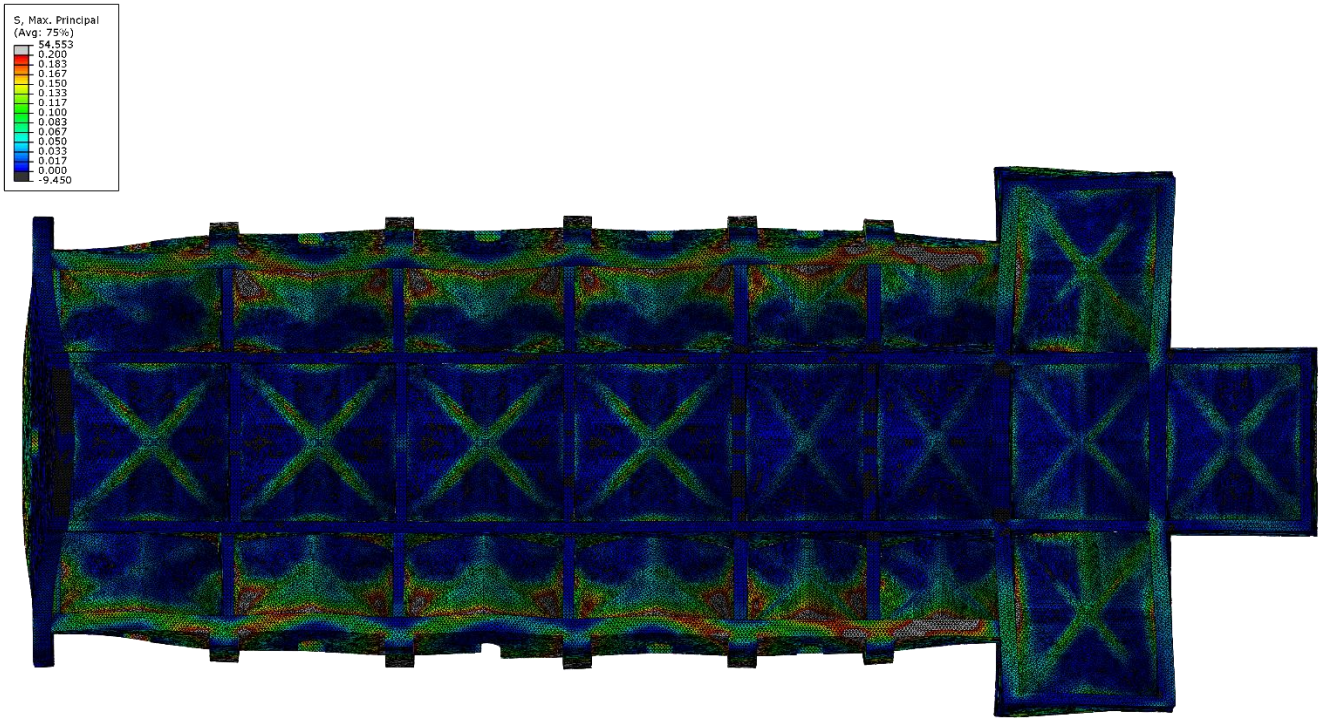

Figure 91 Maximum principal stress of the elements from upper view with 20cm seeding

Lateral bays have more critical condition in comparison to central and transept bays. It can happen because of large deformation of the external walls to that the lateral vaults are connected.

Also it is obvious, the vaults of middle bays in nave have higher maximum stress respect to other vaults of the central bays.

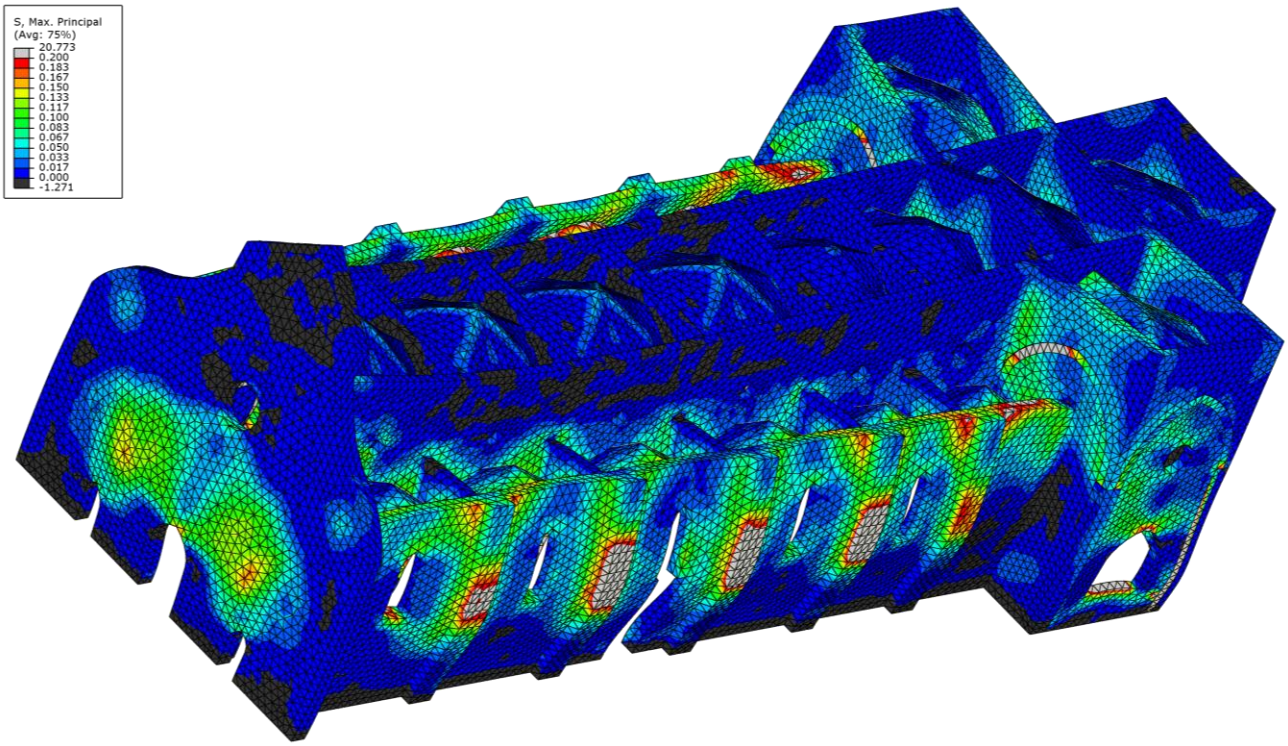

Figure 92 Maximum principal stress of the elements from perspective view with 80cm seeding

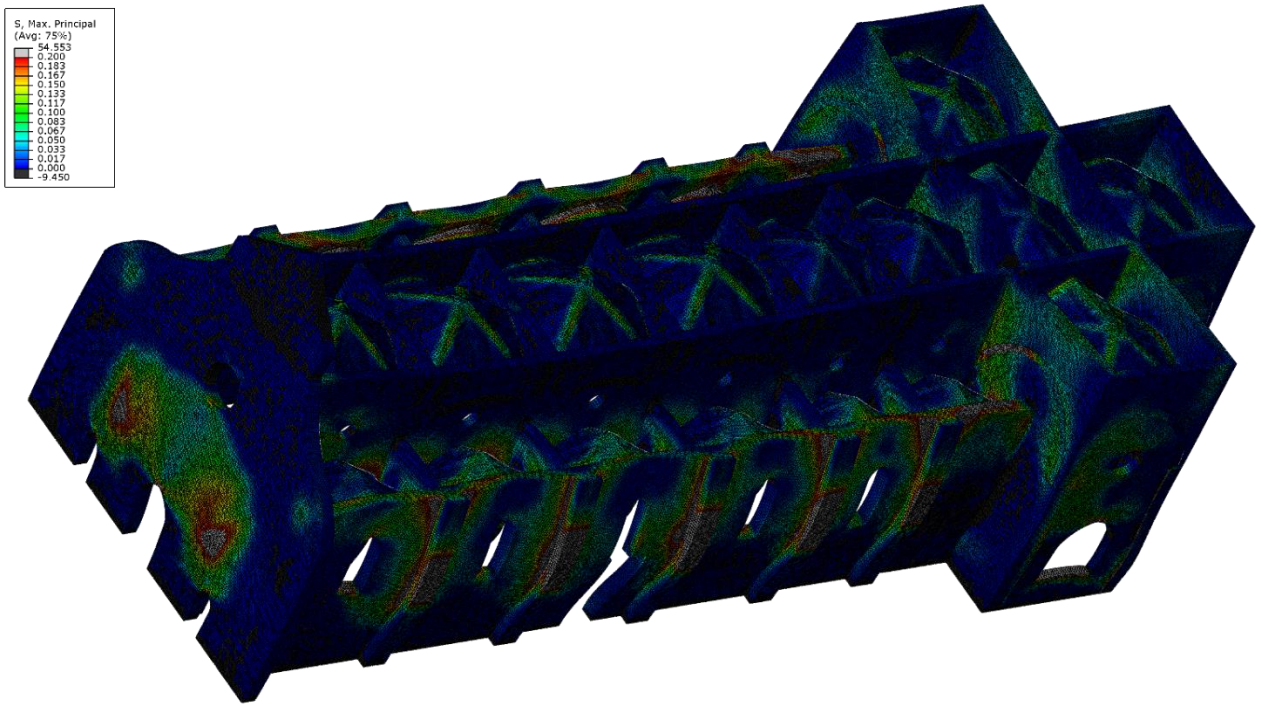

Figure 93 Maximum principal stress of the elements from perspective view with 20cm seeding

Both of the model show the existence of maximum principal stress more than 0.2 MPa in the plasters of the external walls. The reason can be occurrence of large deformation in exterior side of external walls.

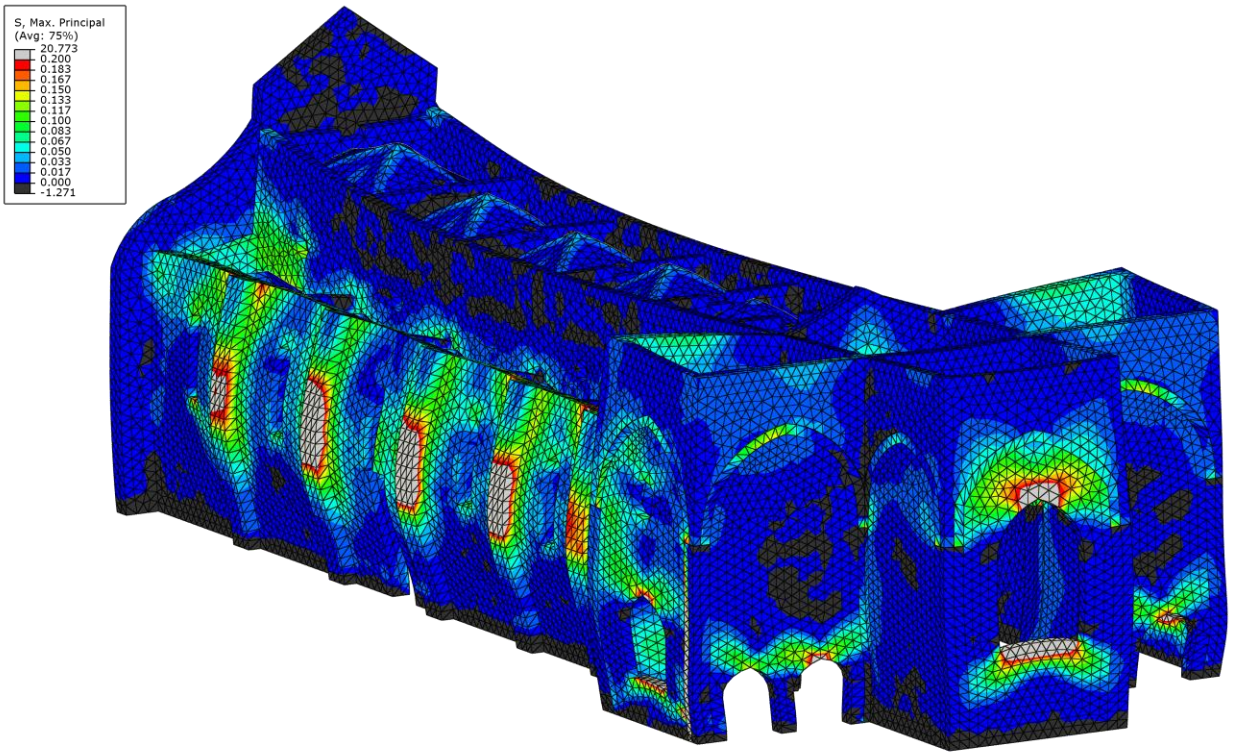

Figure 94 Maximum principal stress of the elements from northern view with 80cm seeding

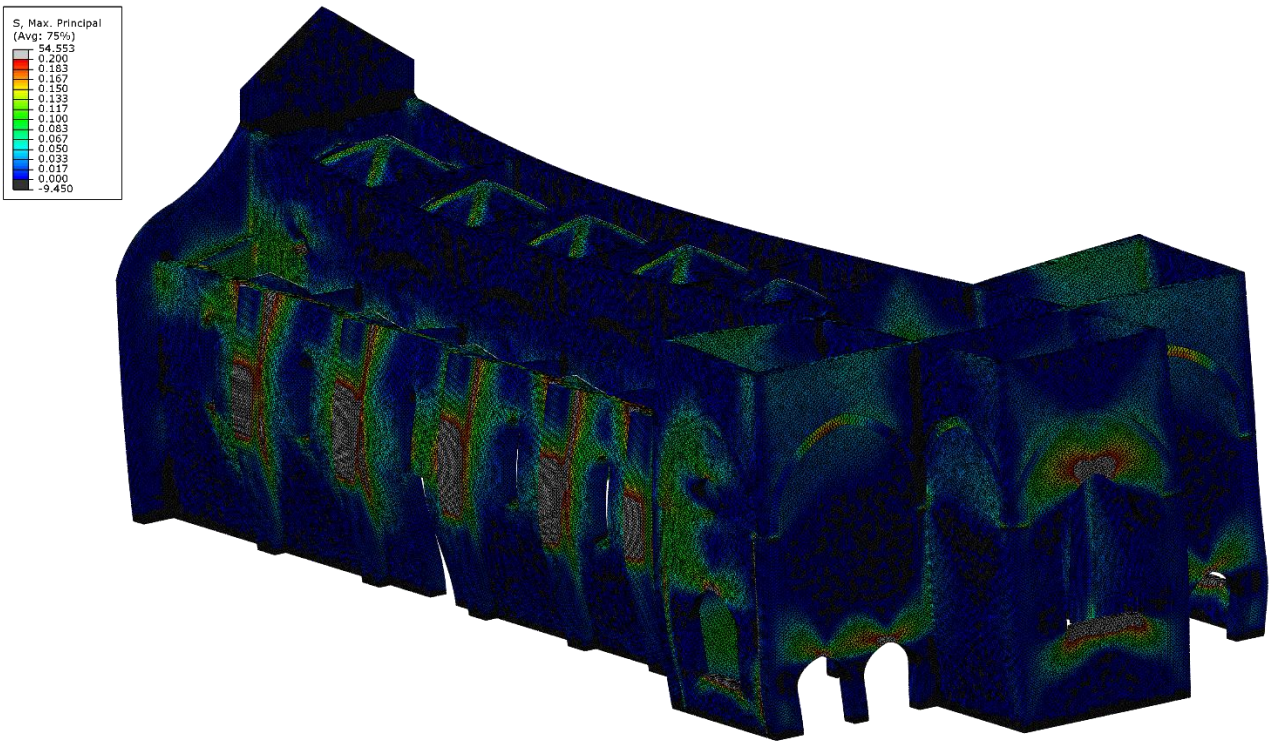

Figure 95 Maximum principal stress of the elements from northern view with 20cm seeding

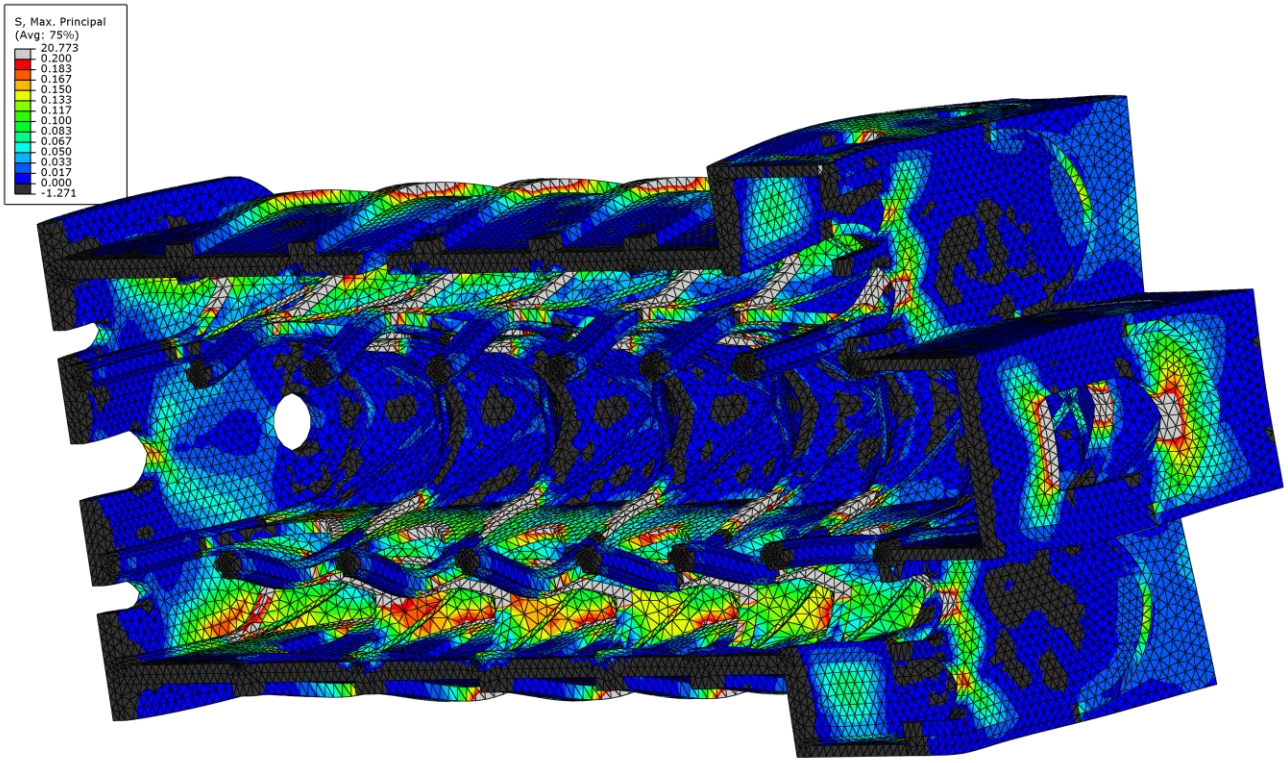

Figure 96 Maximum principal stress of the elements from lower view with 80cm seeding

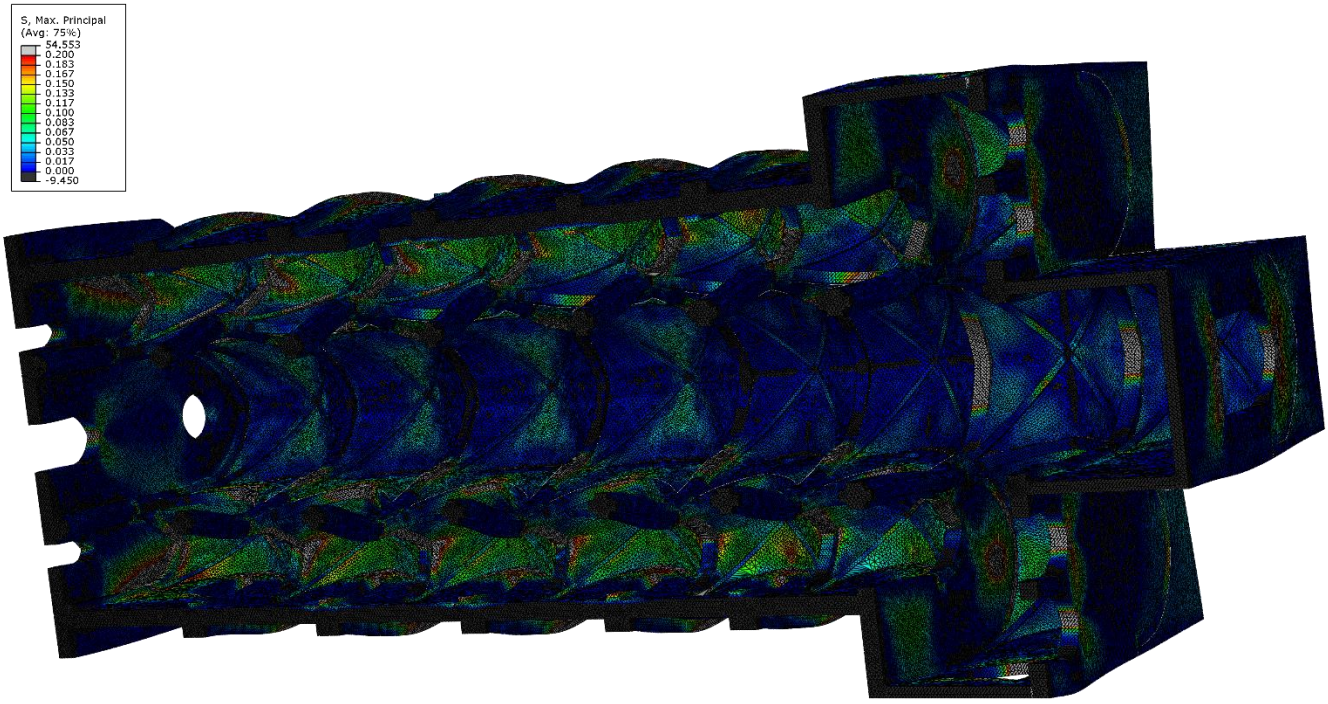

Figure 97 Maximum principal stress of the elements from lower view with 20cm seeding

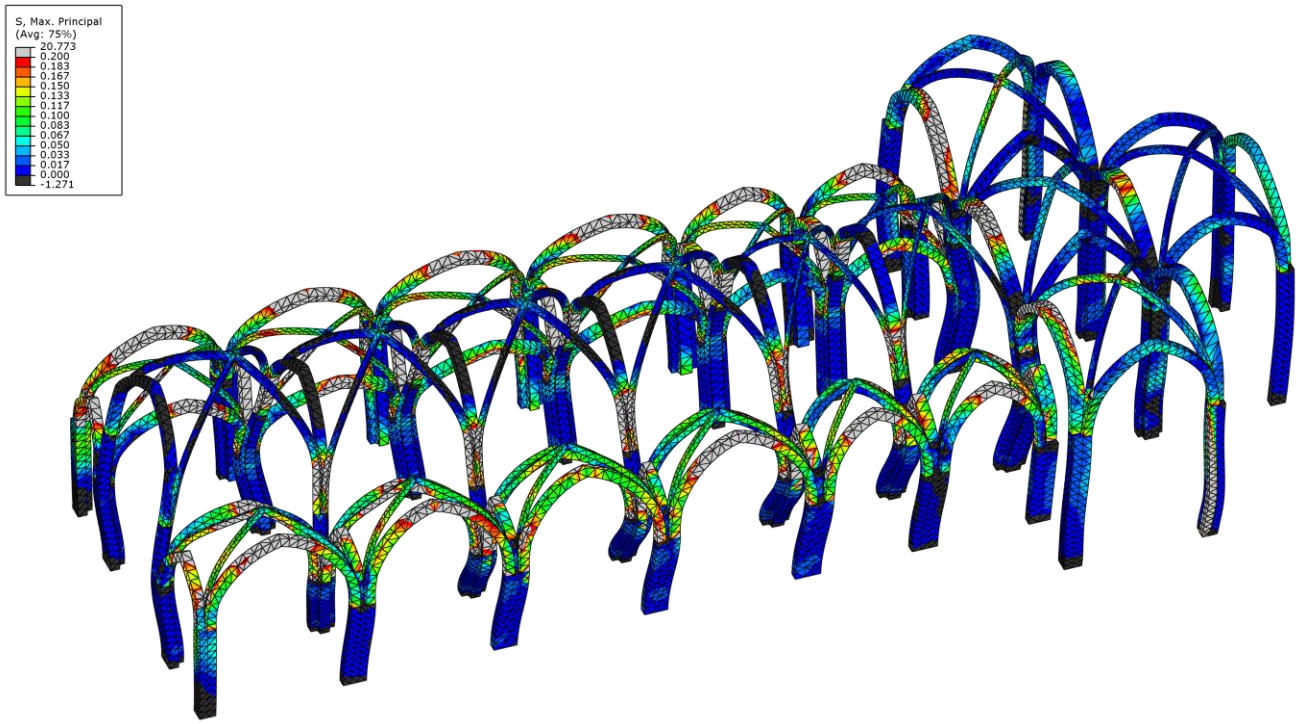

Figure 98 Maximum principal stress of the elements of arches and pillars with 80cm seeding

Figure 99 Maximum principal stress of the elements of arches and pillars with 20cm seeding

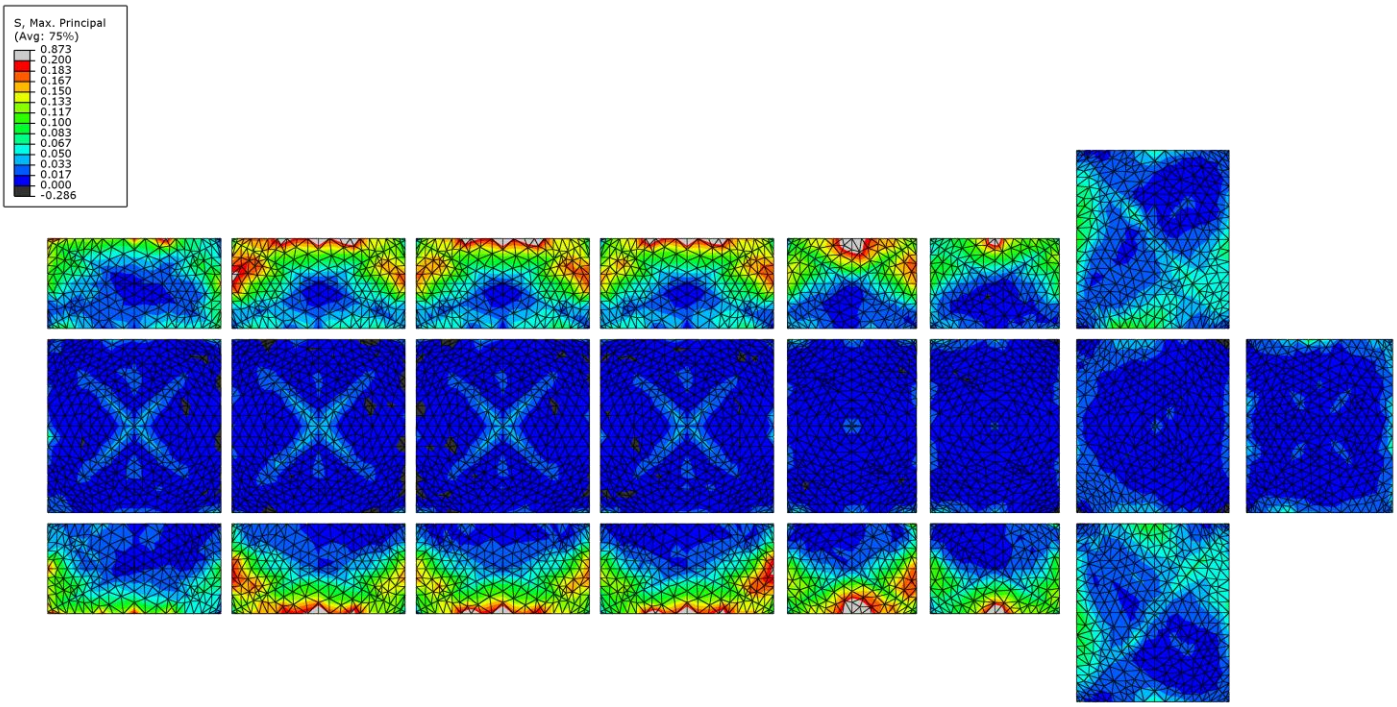

Figure 100 Maximum principal stress of the elements of vaults with 80cm seeding extrados

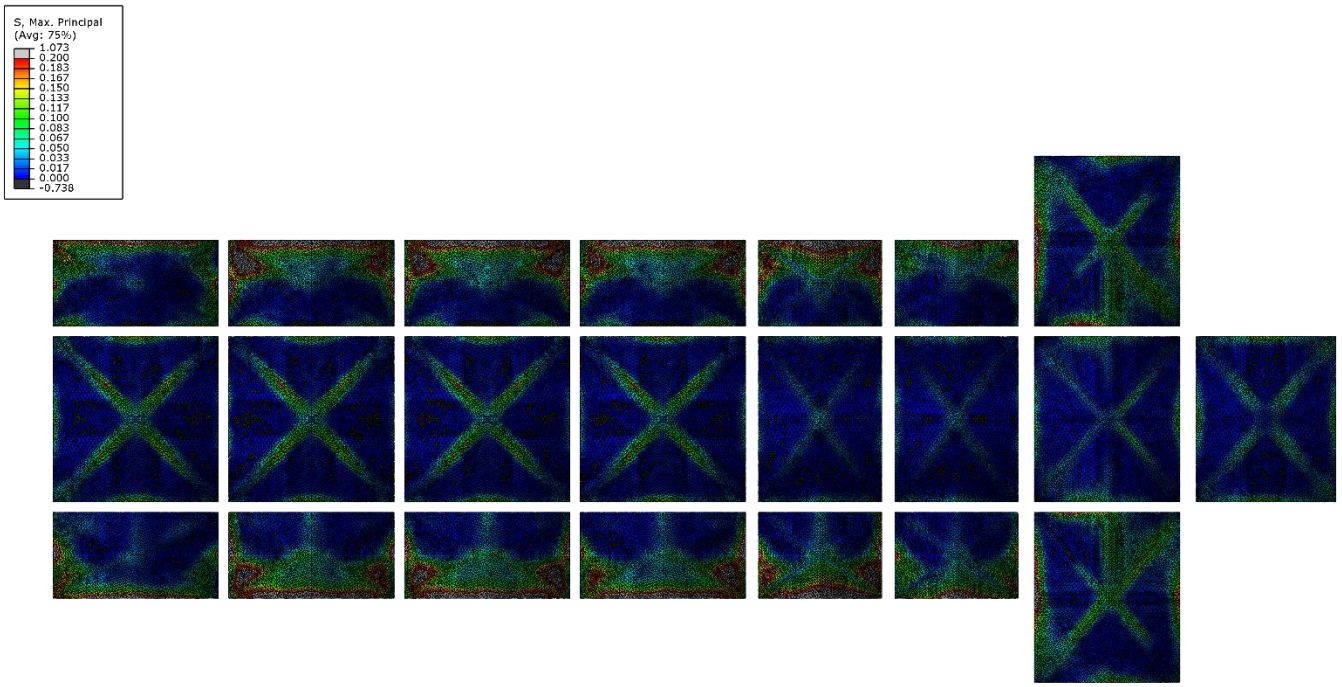

Figure 101 Maximum principal stress of the elements of vaults with 80cm seeding intrados

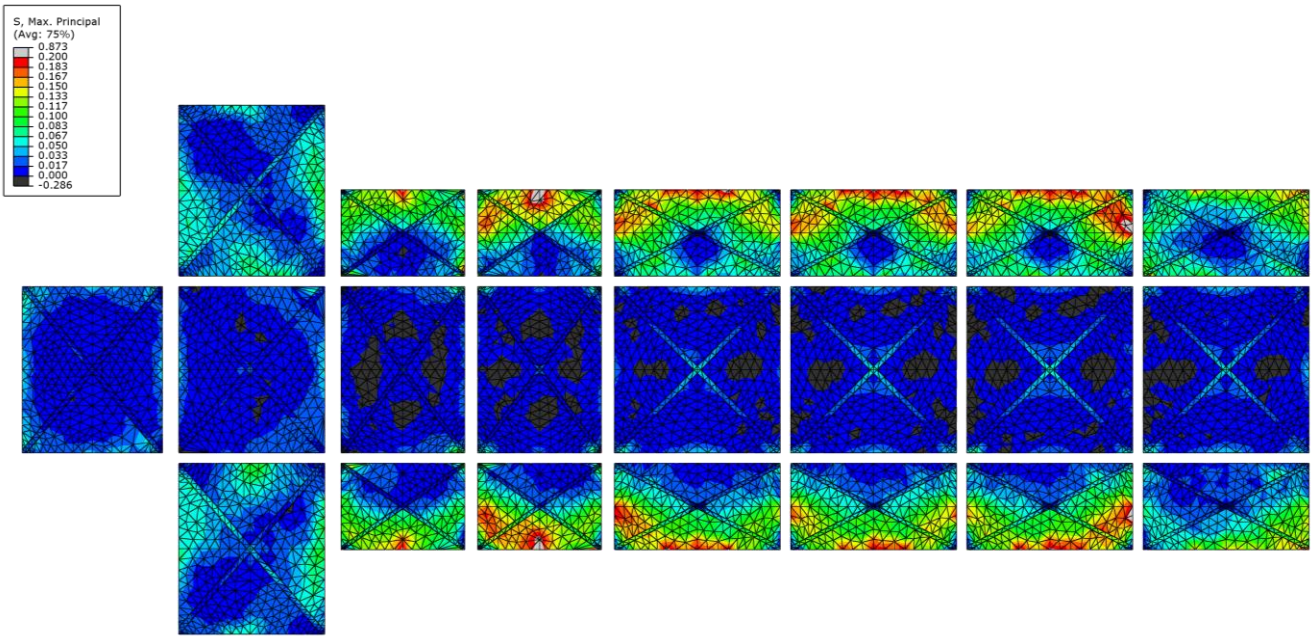

Figure 102 Maximum principal stress of the elements of vaults with 80cm seeding extrados

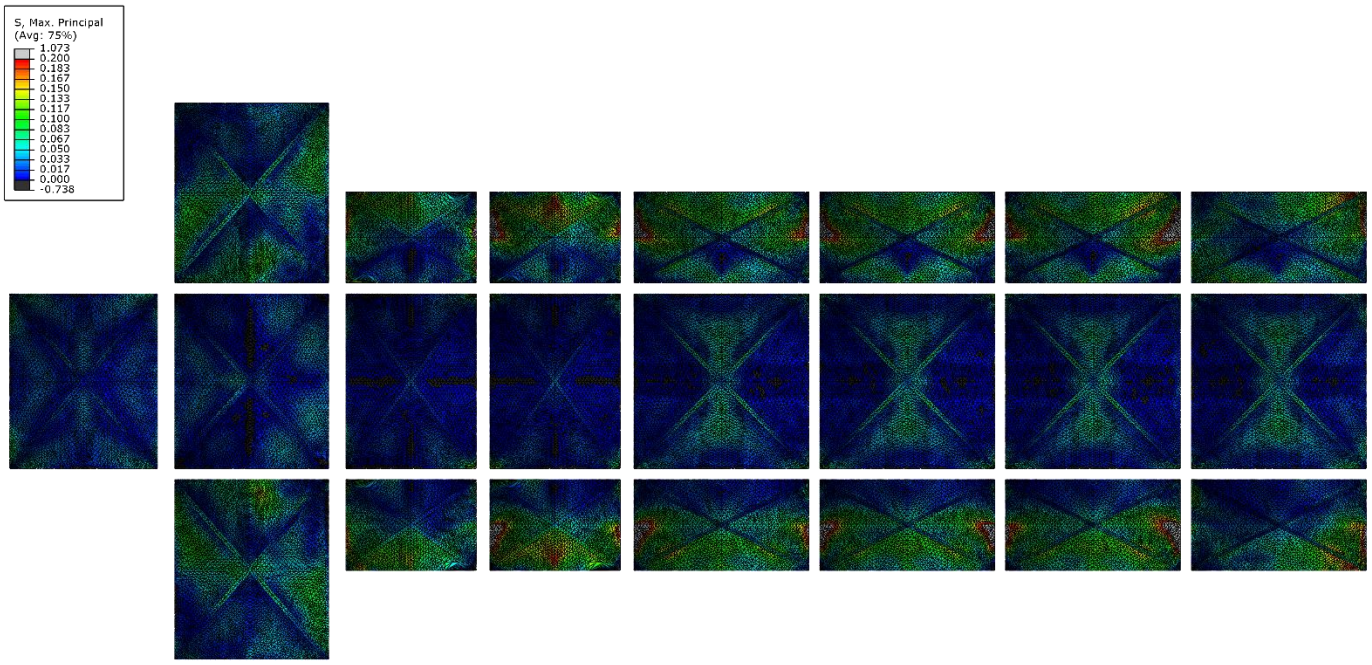

Figure 103 Maximum principal stress of the elements of vaults with 20cm seeding intrados

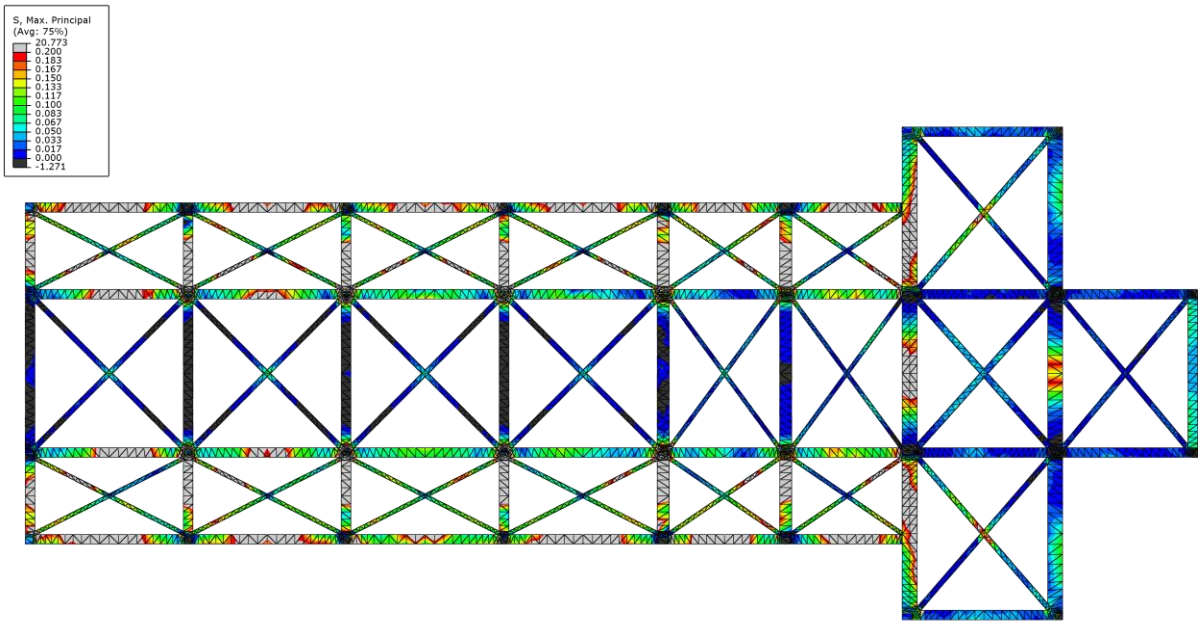

Figure 104 Maximum principal stress of the elements of arches with 80cm seeding extrados

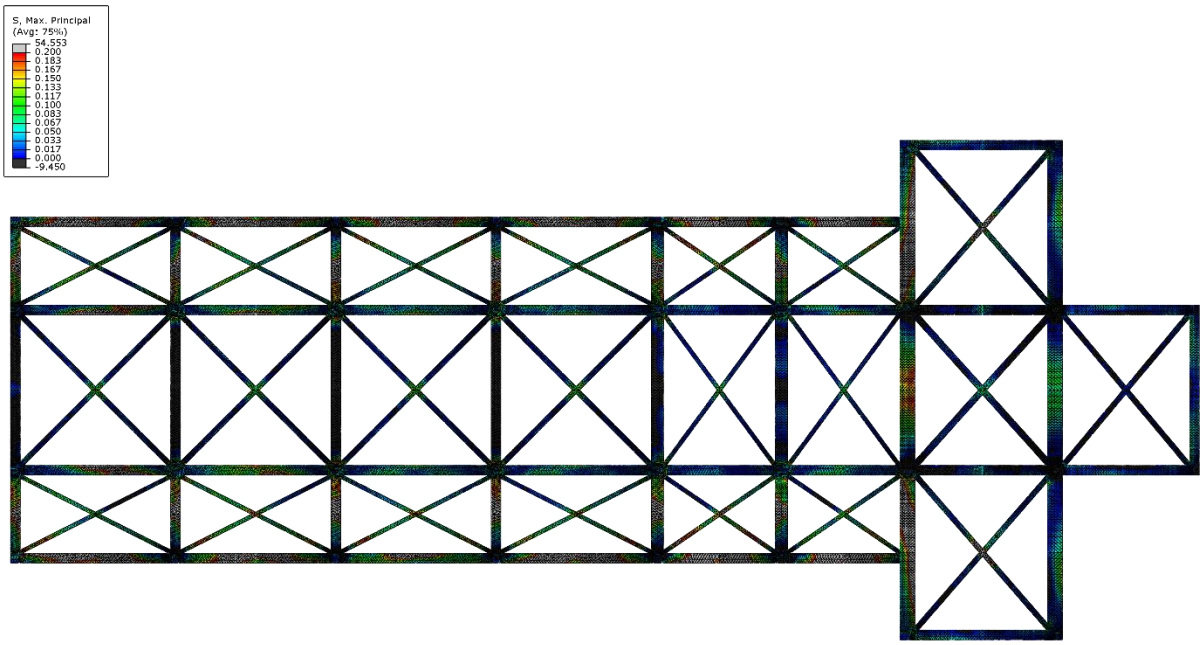

Figure 105 Maximum principal stress of the elements of arches with 80cm seeding intrados

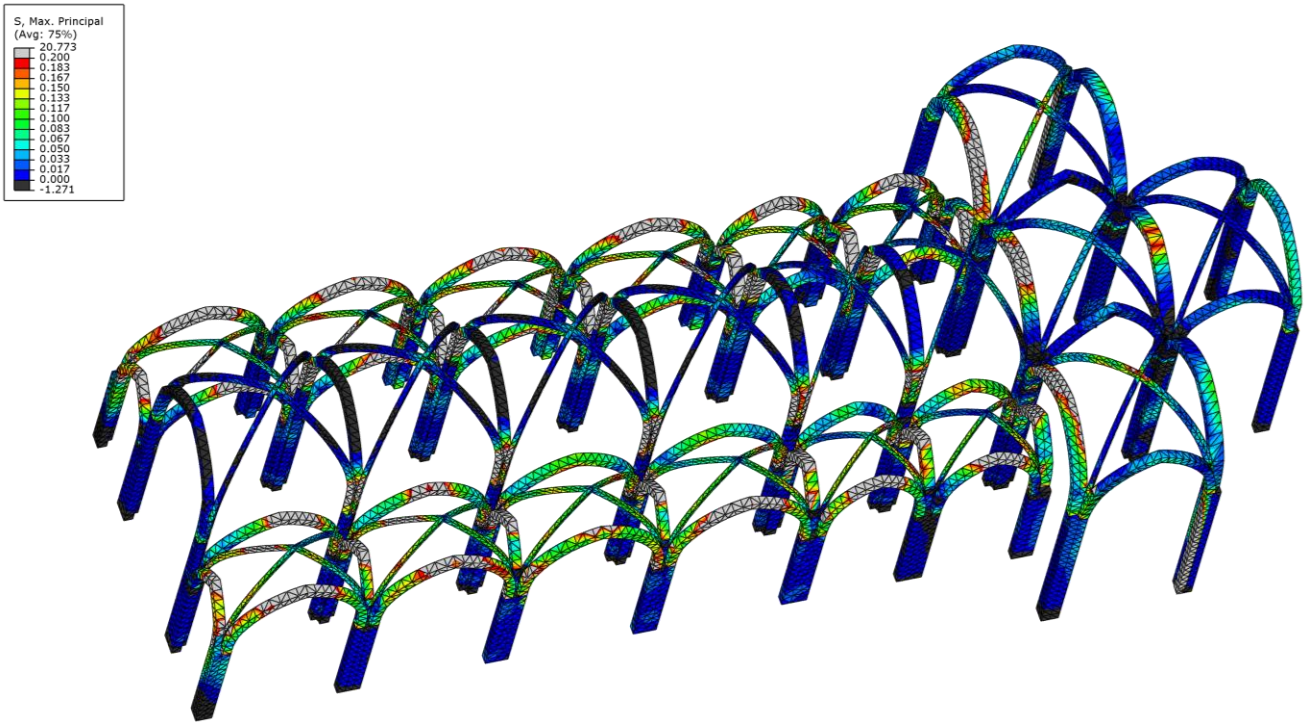

Figure 106 Maximum principal stress of the elements of arches and pillars with 80cm seeding

Figure 107 Maximum principal stress of the elements of arches and pillars with 20cm seeding

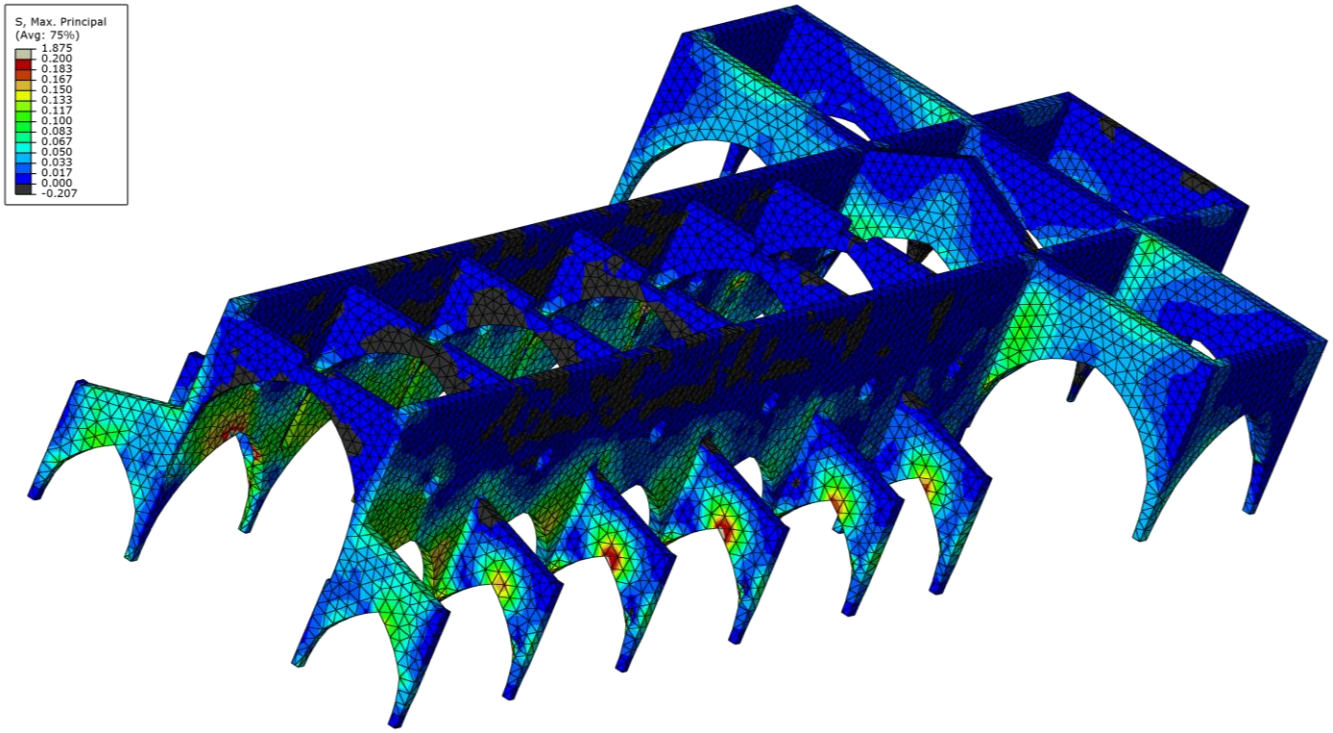

Figure 108 Maximum principal stress of the elements of internal walls and pillars with 80cm seeding

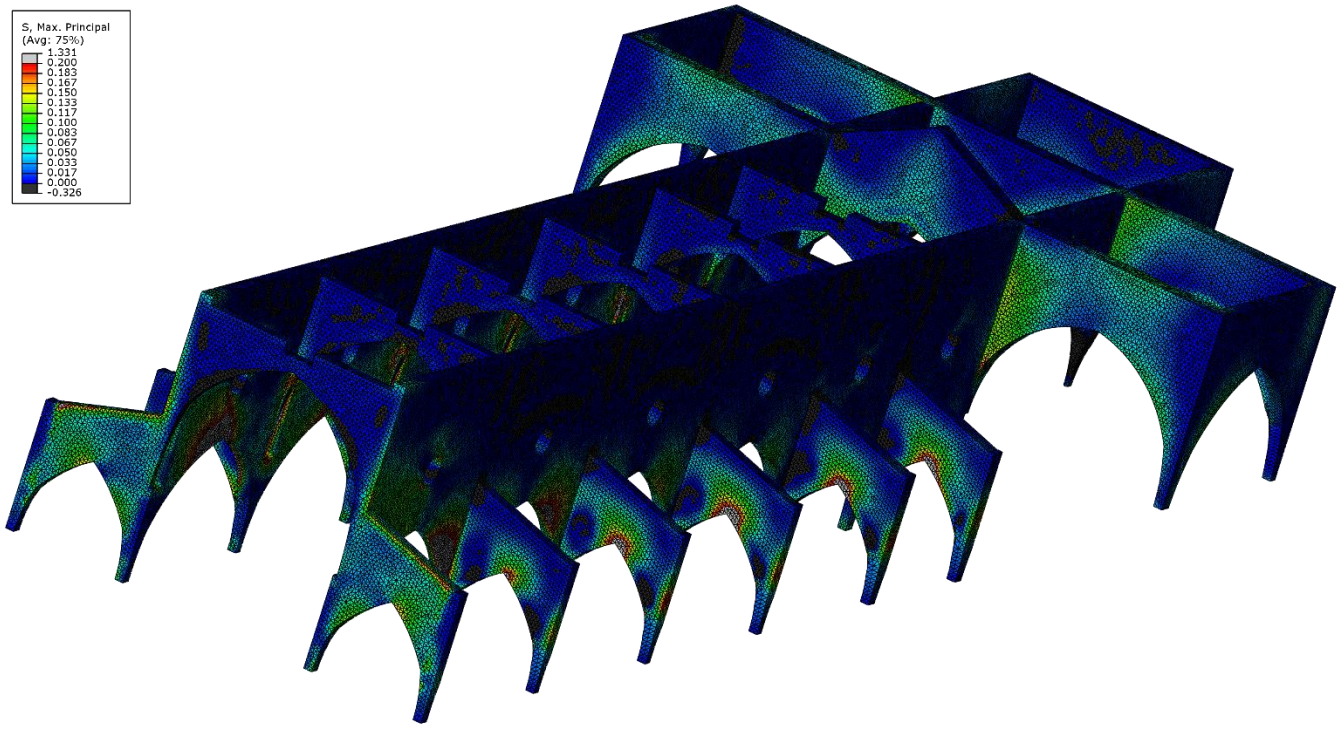

Figure 109 Maximum principal stress of the elements of internal walls and pillars with 20cm seeding

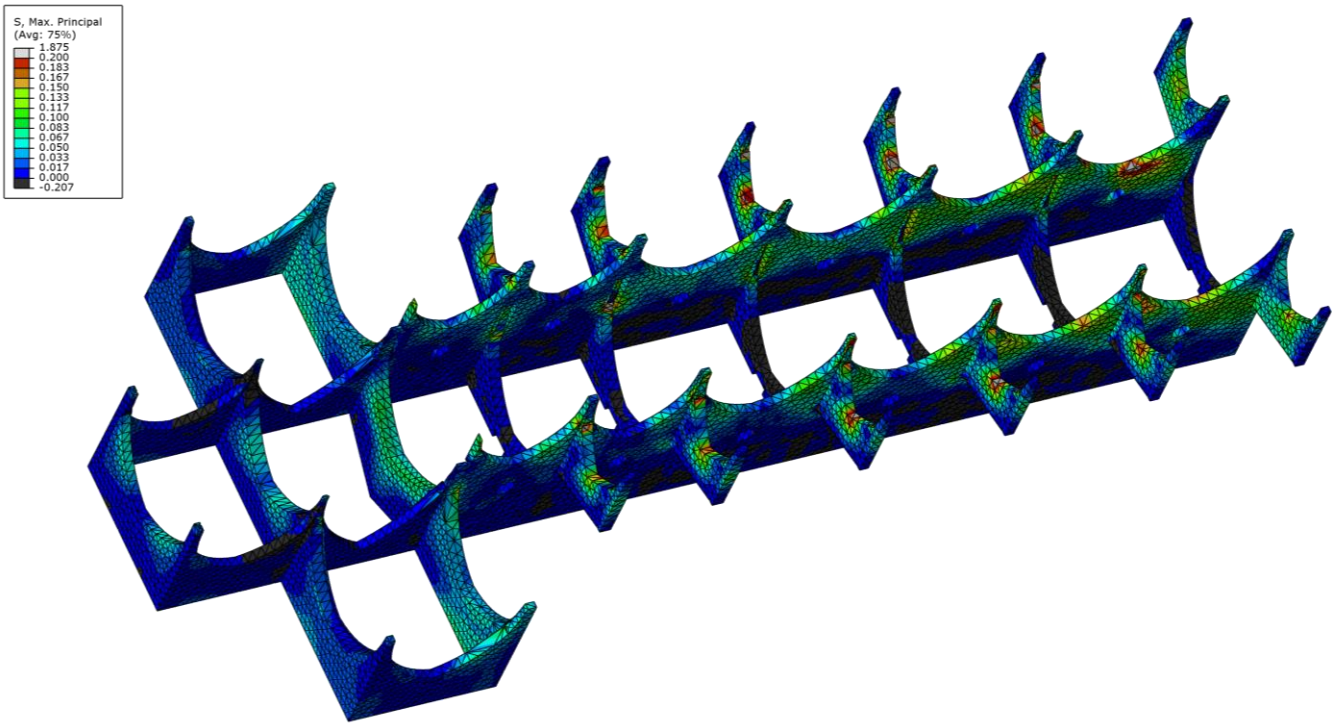

Figure 110 Maximum principal stress of the elements of internal walls and pillars with 80cm seeding

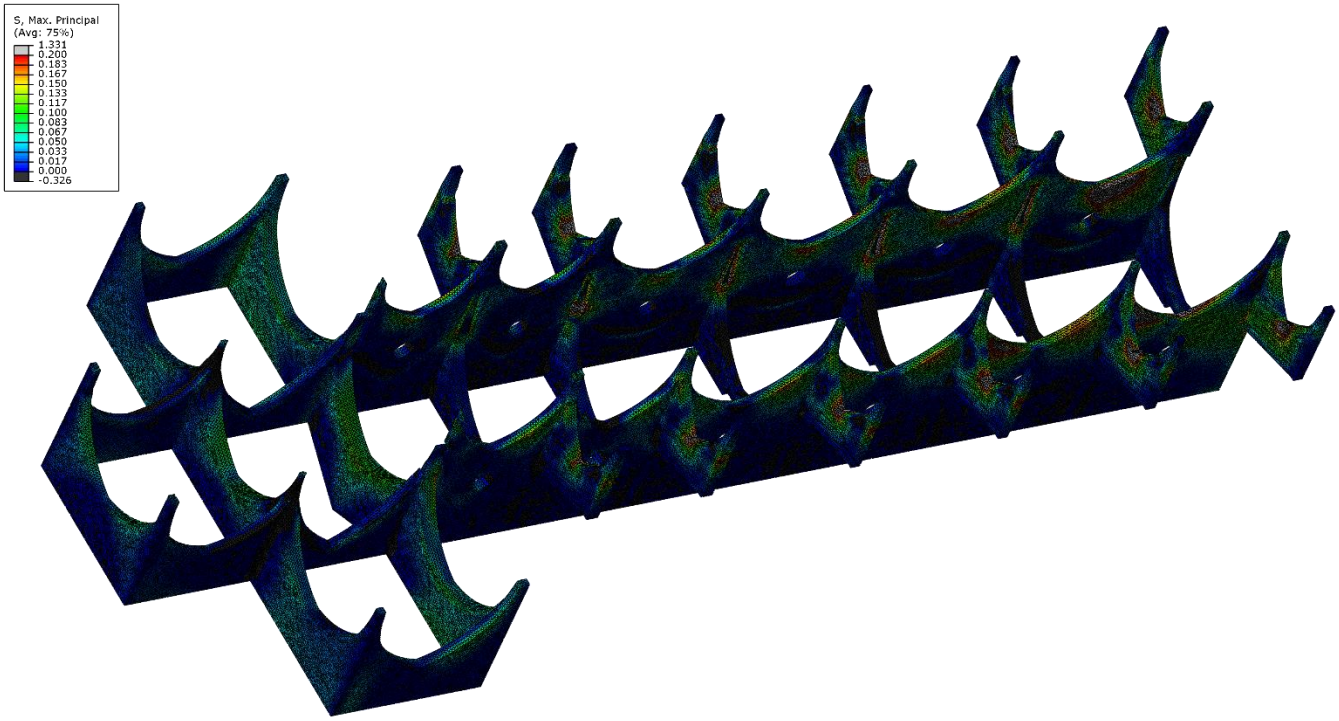

Figure 111 Maximum principal stress of the elements of internal walls and pillars with 20cm seeding

4.6. Elements displacement representation

In the following figures, the overall maximum values of the displacements are represented. The maximum values in both of models are happened on the vault of central bay no.4, as it seems to be the middle of the nave.

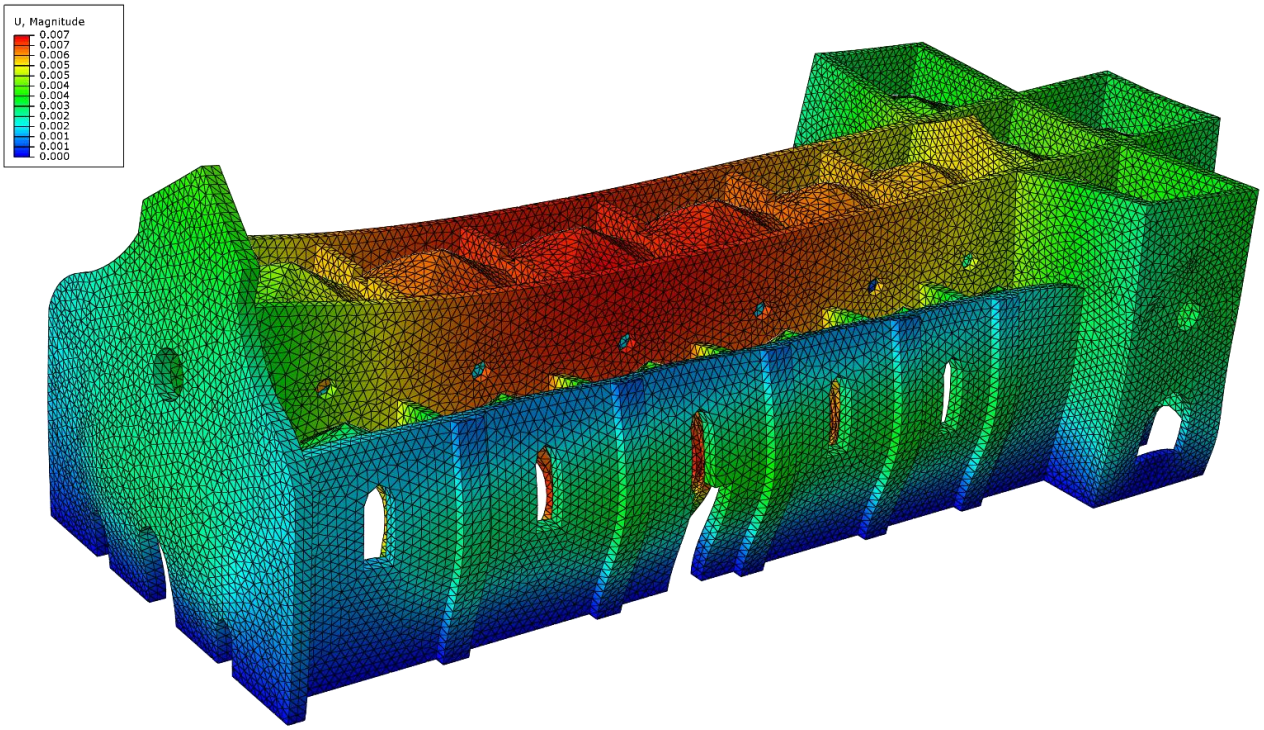

Figure 112 magnitude of elements displacement with 80cm seeding

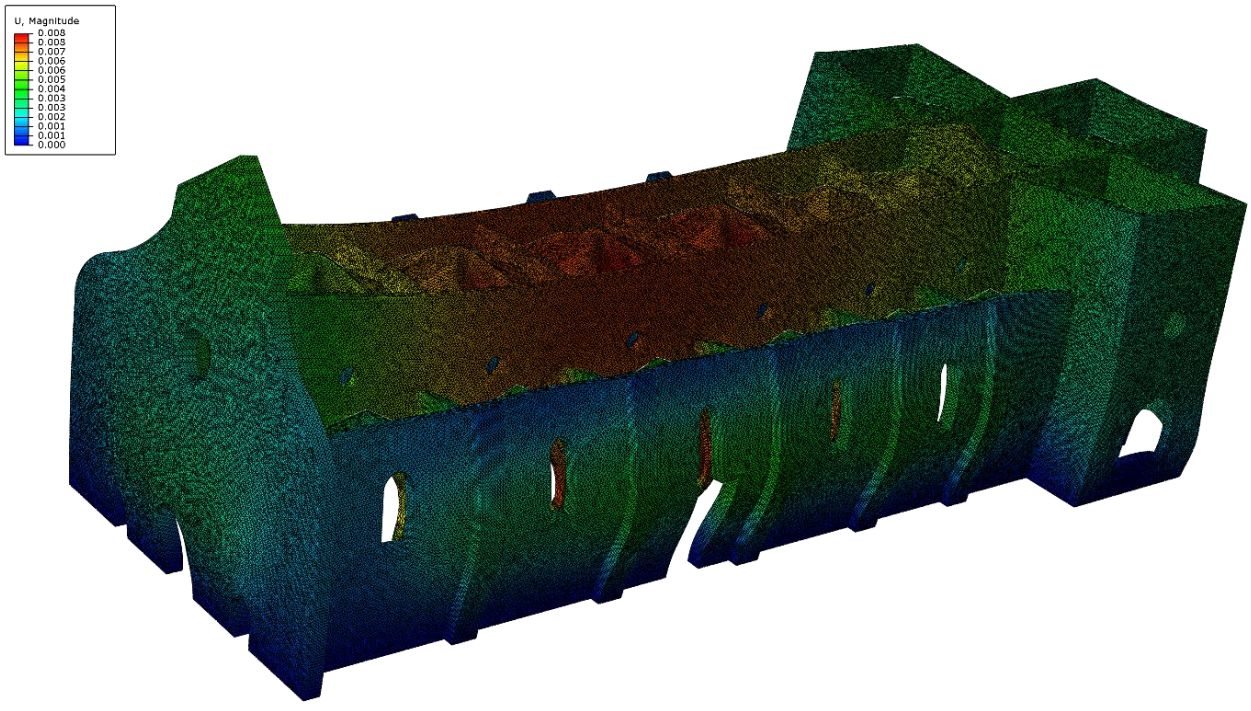

Figure 113 magnitude of elements displacement with 20cm seeding

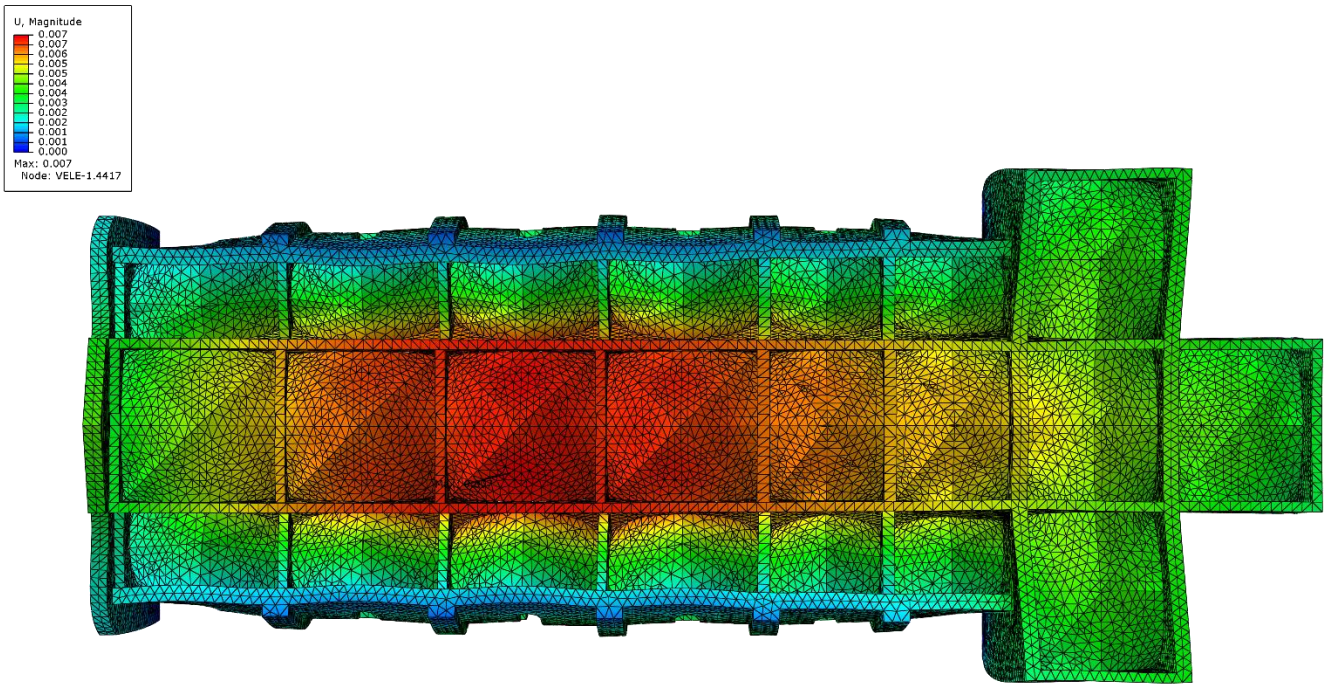

Figure 114 magnitude of elements displacement with 80cm seeding from up view

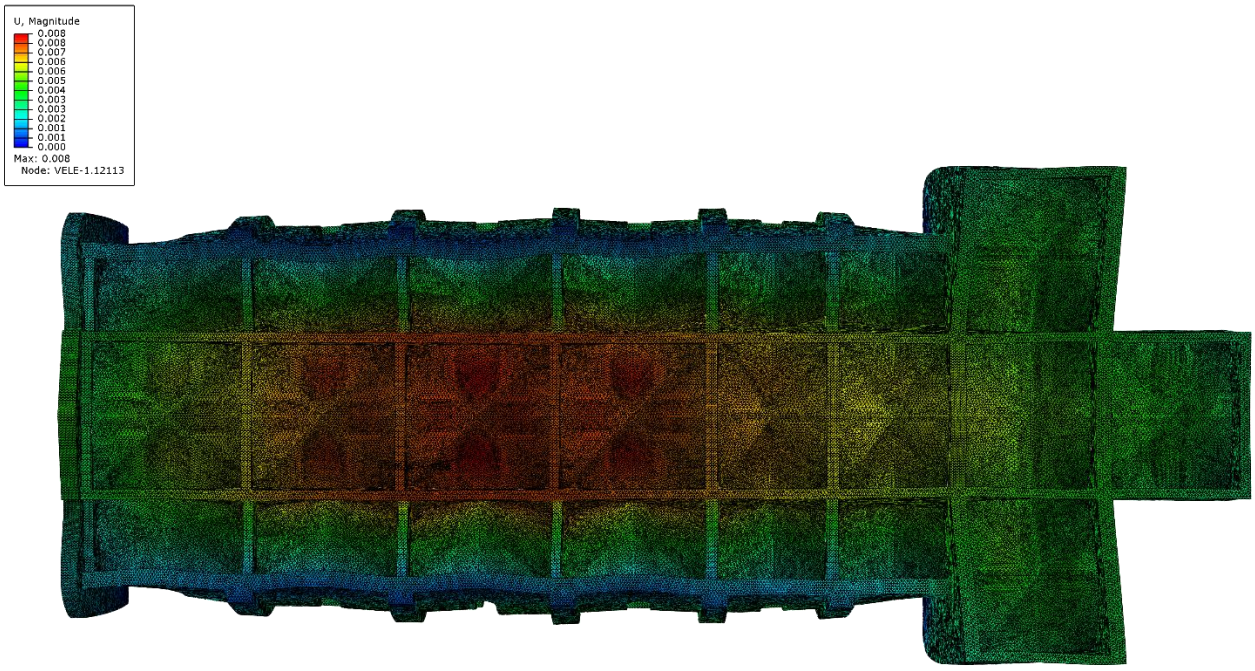

Figure 115 magnitude of elements displacement with 20cm seeding from up view

The maximum value of displacement in the model with 80cm elements is 0.007 meter and for another is 0.008 meter. There is about 15% of difference between the displacement value of the both model but there is no difference where they are happening in both model.

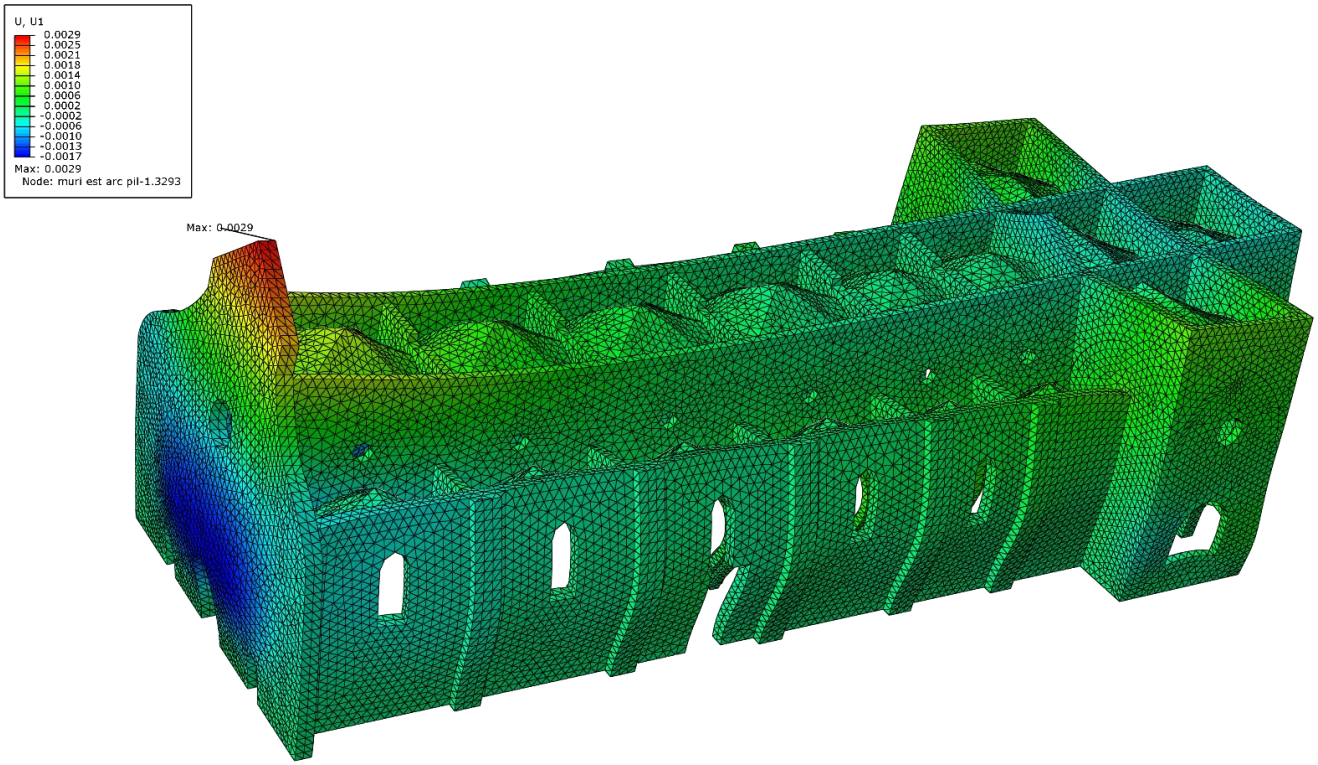

Figure 116 elements displacement in U1 direction with 80cm seeding

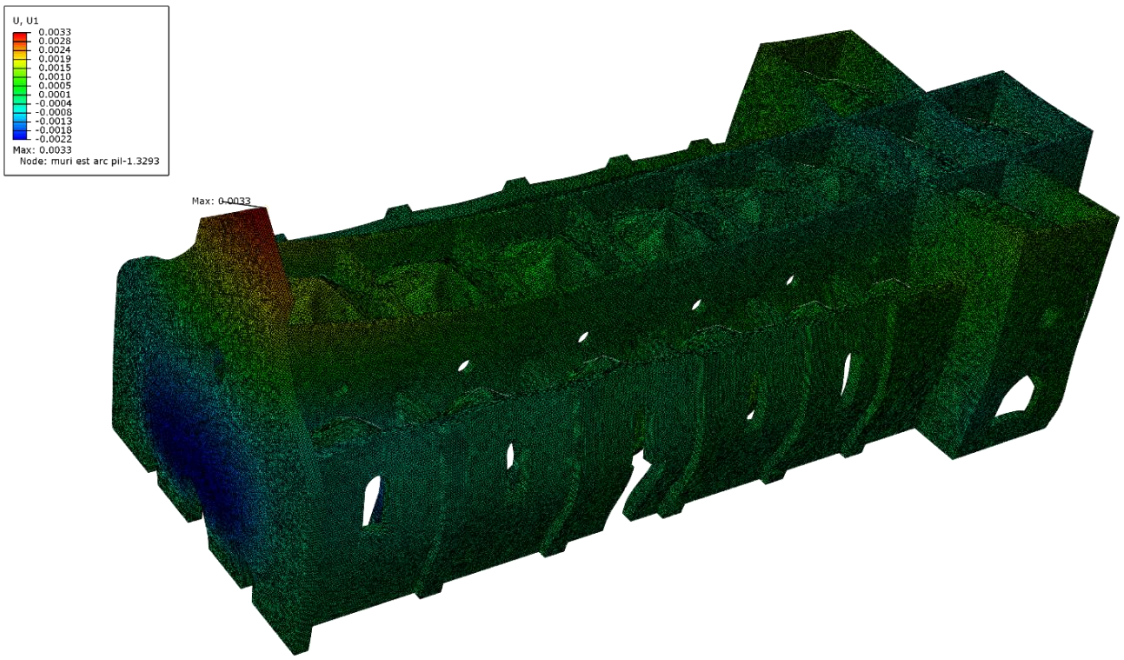

Figure 117 elements displacement in U1 direction with 20cm seeding

The maximum displacement in the longitudinal direction of the church (U1) in the model with 80cm meshing is 0.0029m and for the model with 20cm meshing is 0.0033m. As before, there is an increase of 10-15% in the value of the displacement but there is no difference in the location of the maximum value.

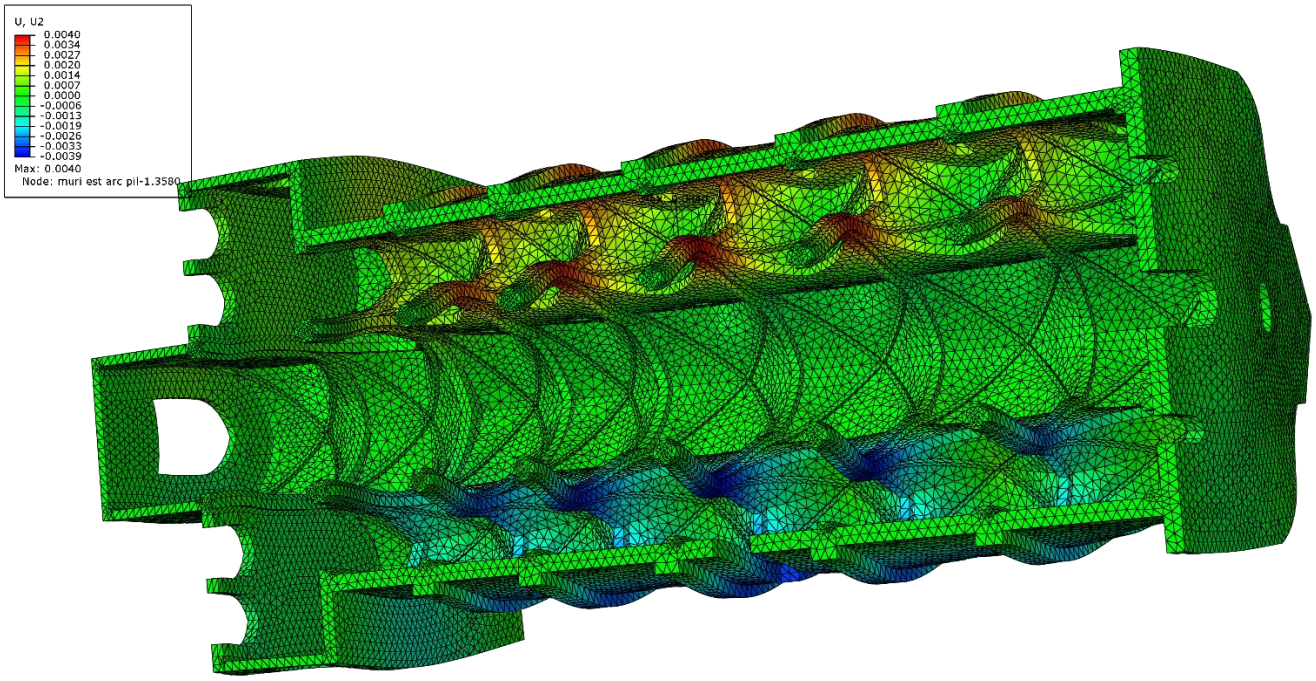

Figure 118 displacement in U2 direction with 80cm seeding

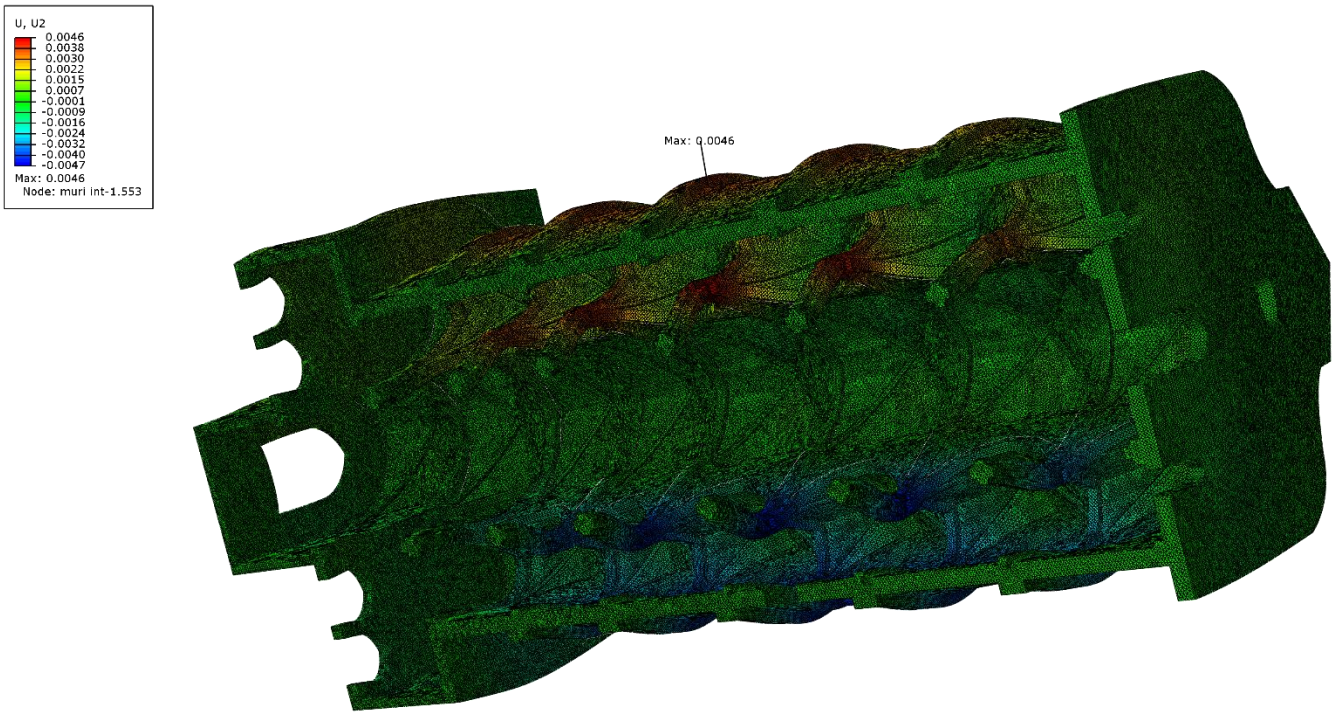

Figure 119 displacement in U2 direction with 20cm seeding

4.7. Comparison of the results with the previous analysis results

In these parts the results of the new model will be compared with the existing results of the previous 3D model with mono and bi-dimensional elements.

Maximum principal stress

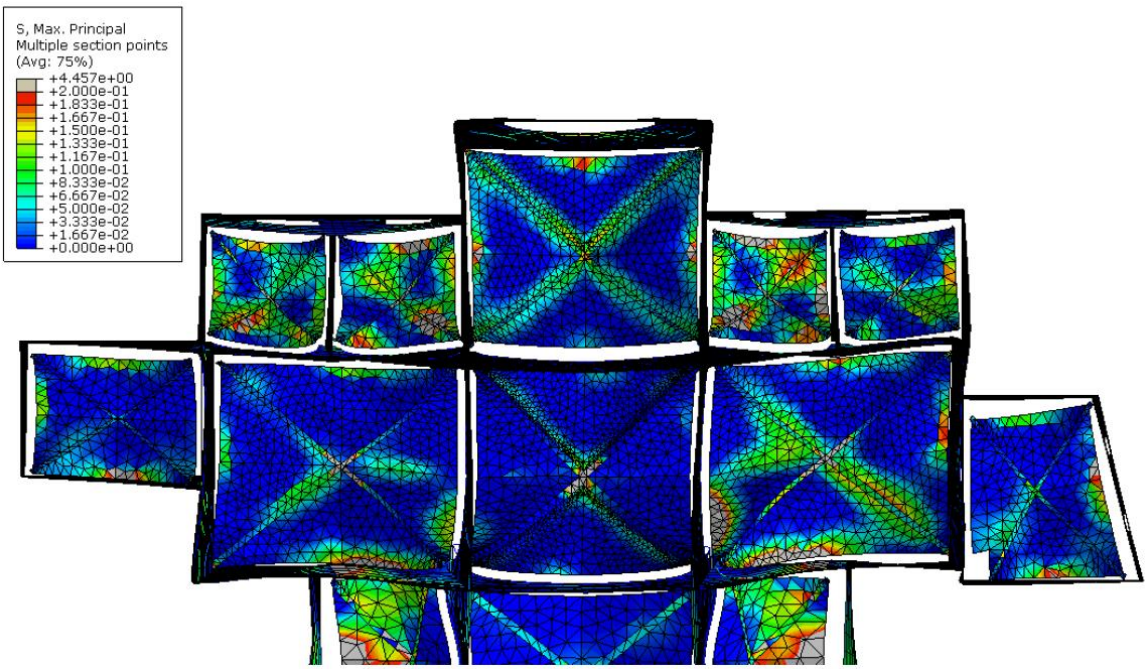

Figure 120 maximum principal stress of previous model

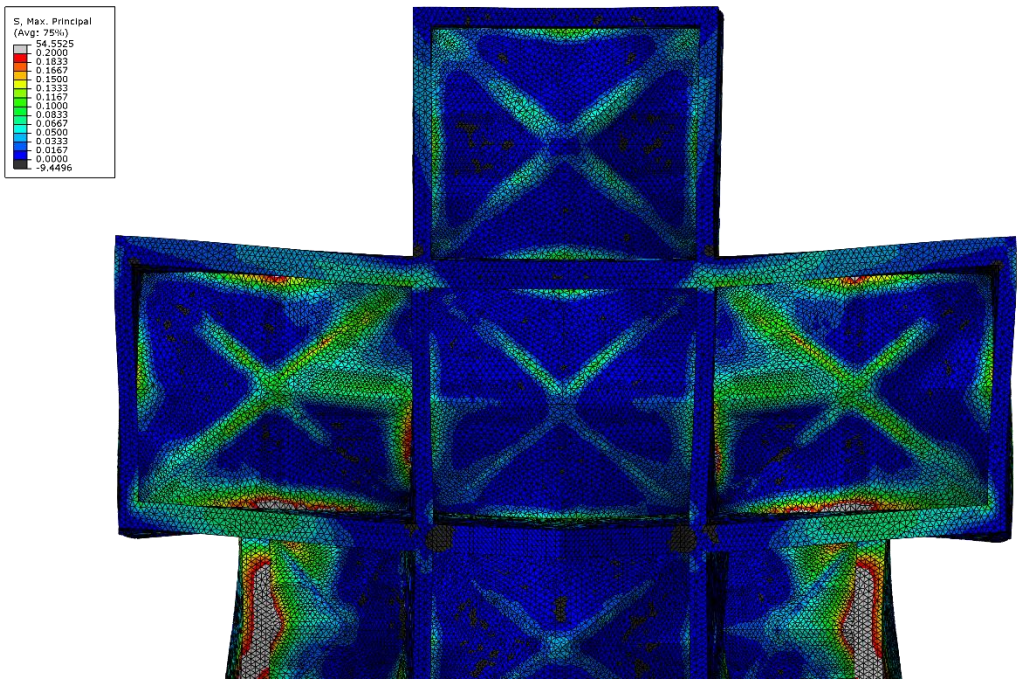

Figure 121 maximum principal stress of new model

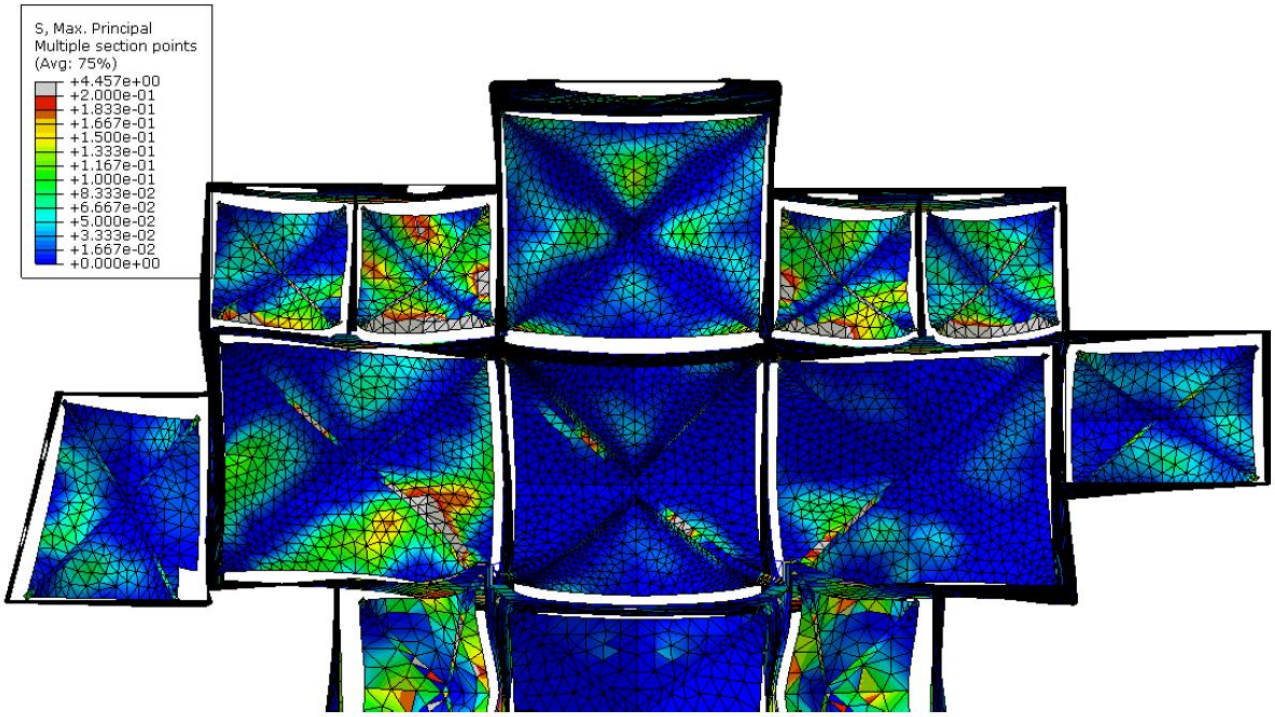

Figure 122 maximum principal stress of previous model intrados

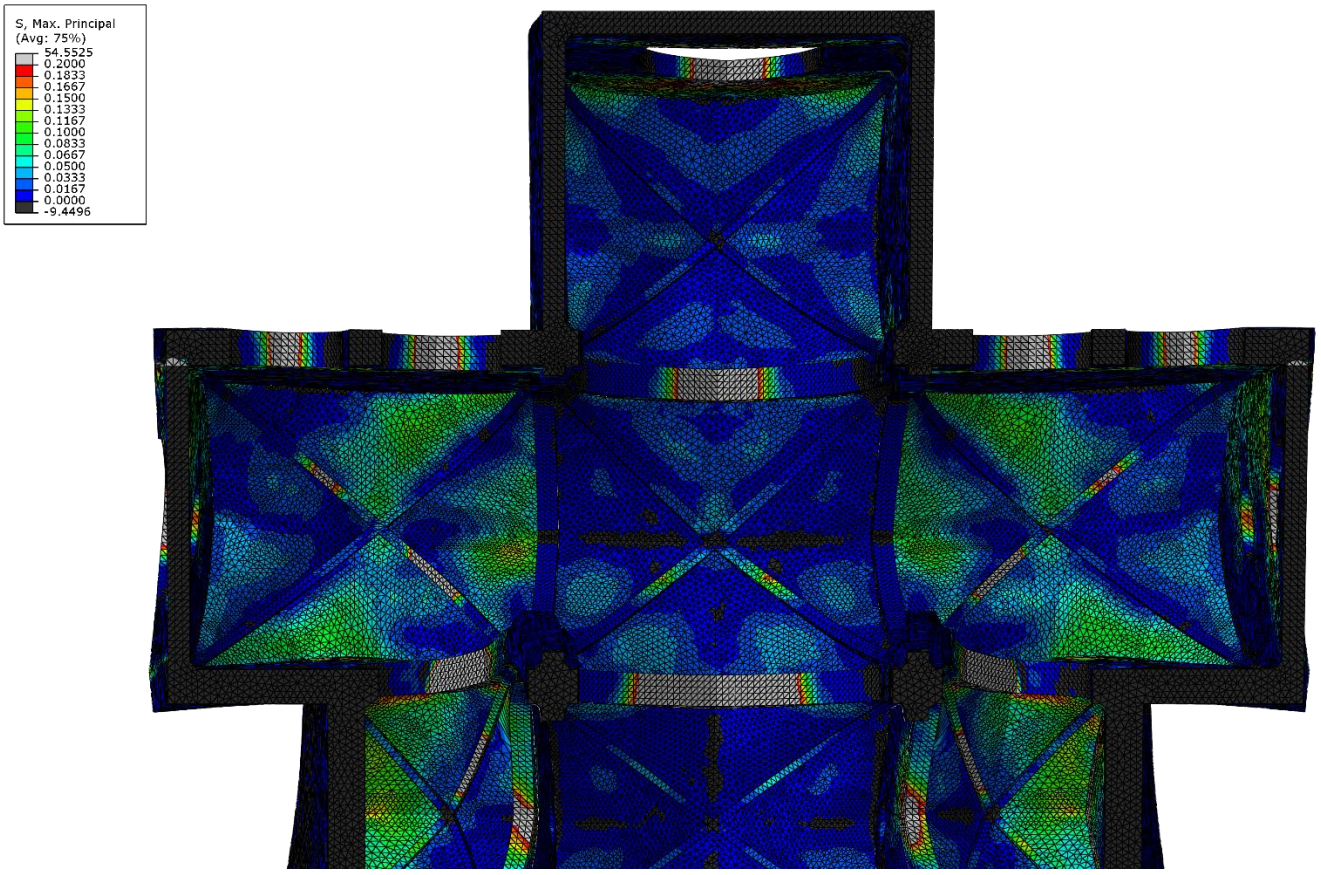

Figure 123 maximum principal stress of new model intrados

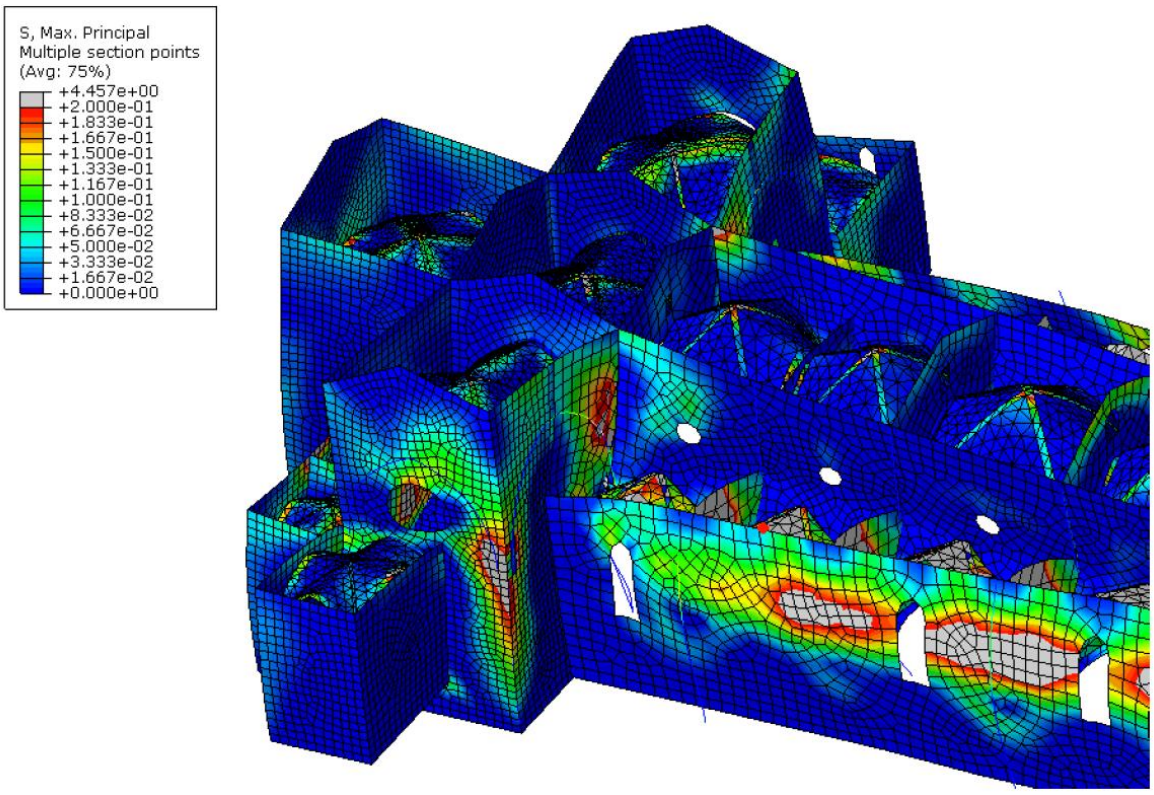

Figure 124 maximum principal stress for western part in previous model

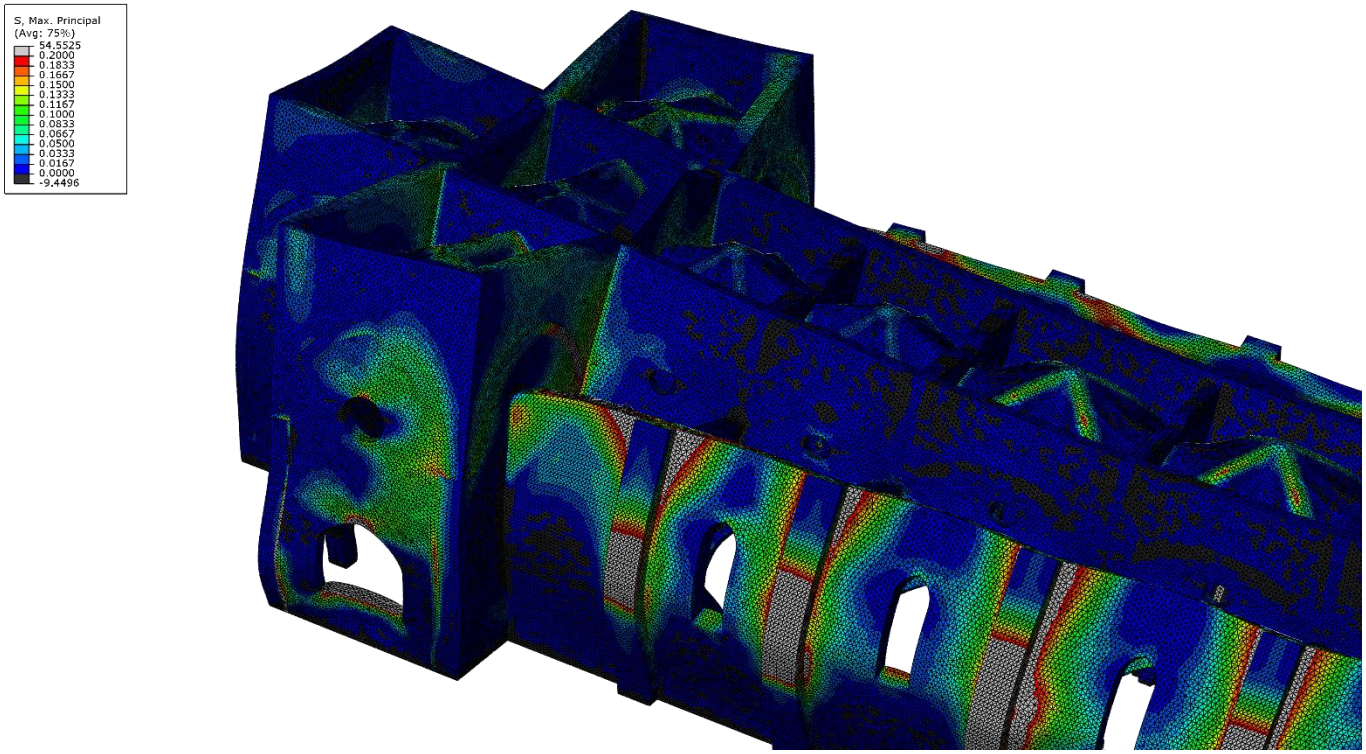

Figure 125 maximum principal stress for western part in new model

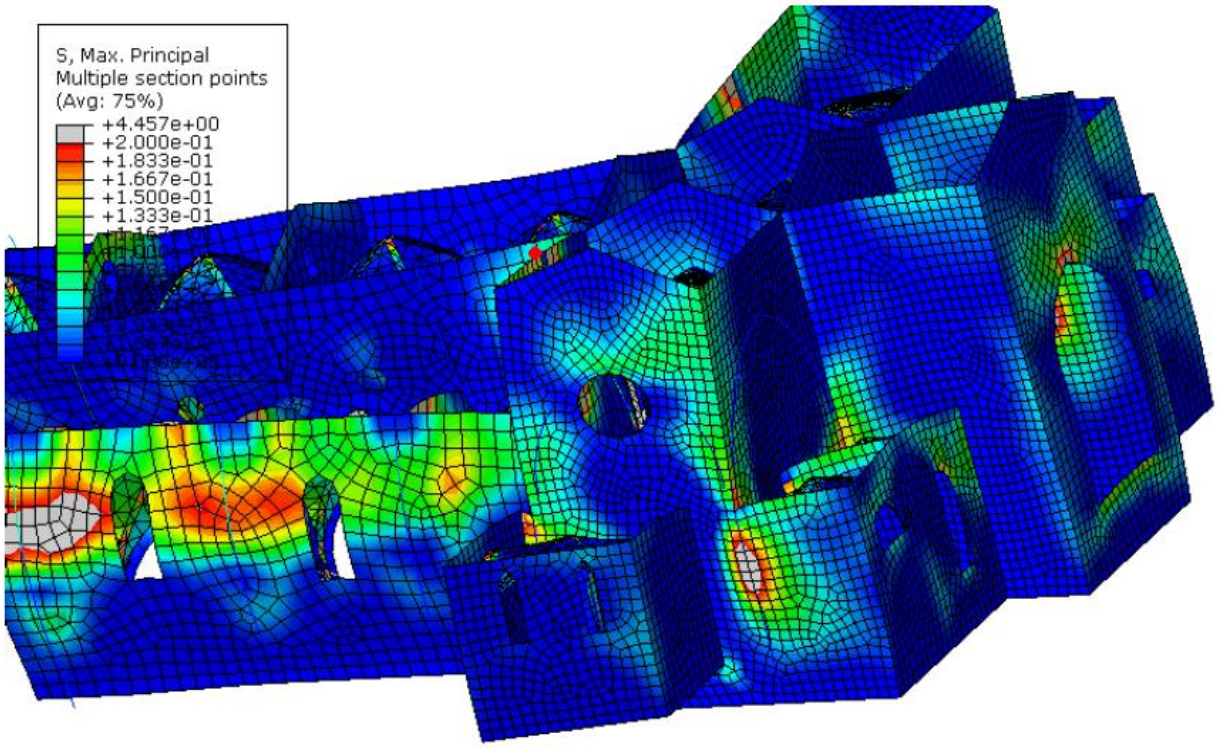

Figure 126 maximum principal stress for eastern part in previous model

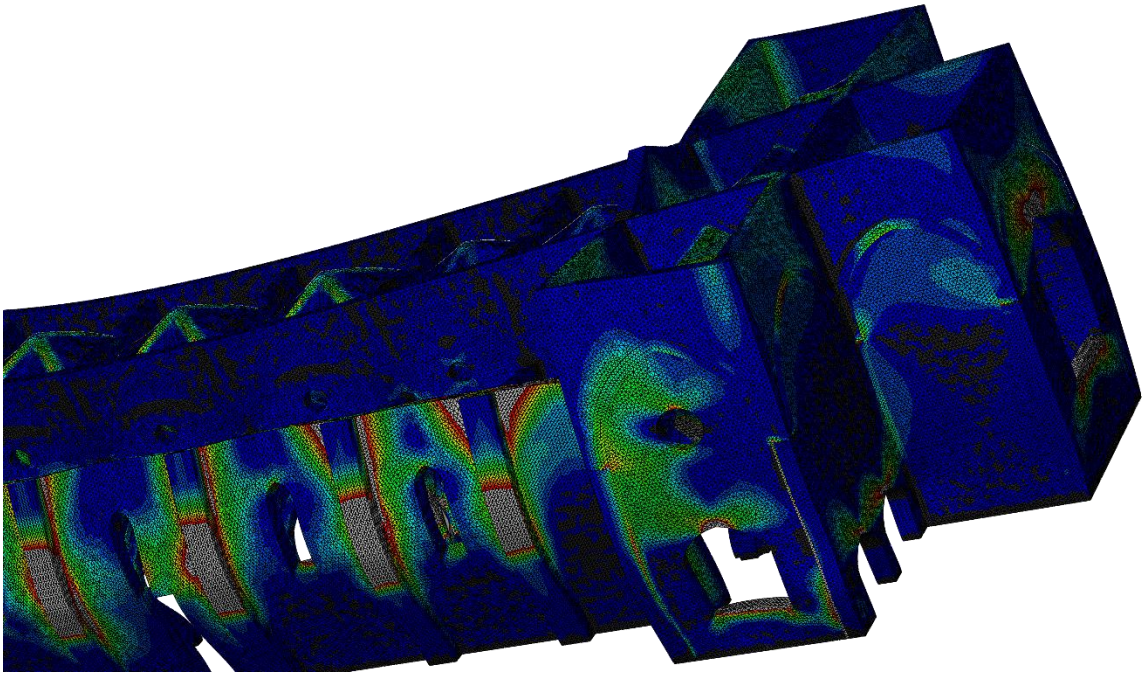

Figure 127 maximum principal stress for eastern part in new model

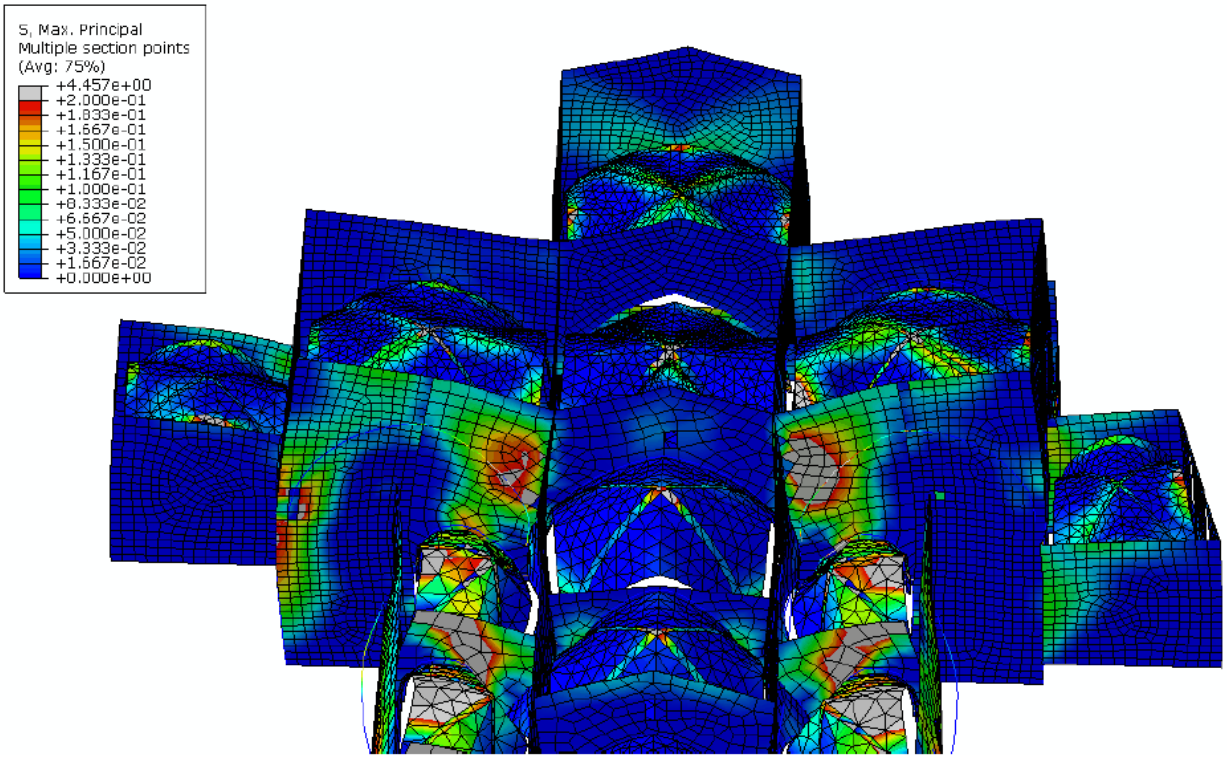

Figure 128 maximum principal stress for internal walls in previous model

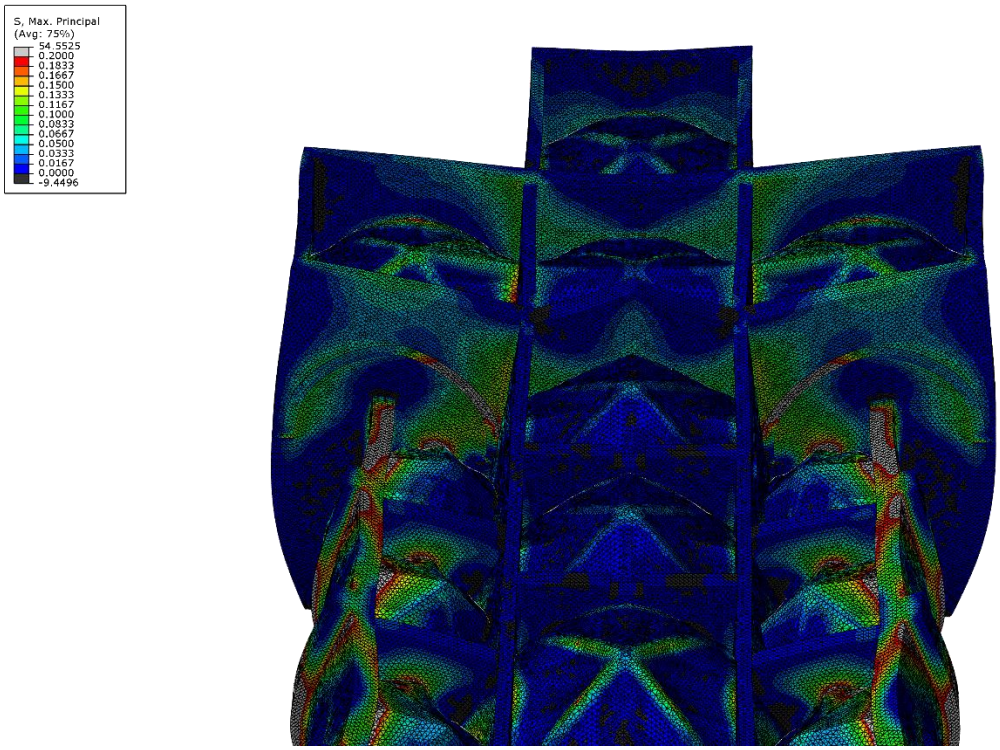

Figure 129 maximum principal stress for internal walls in new model

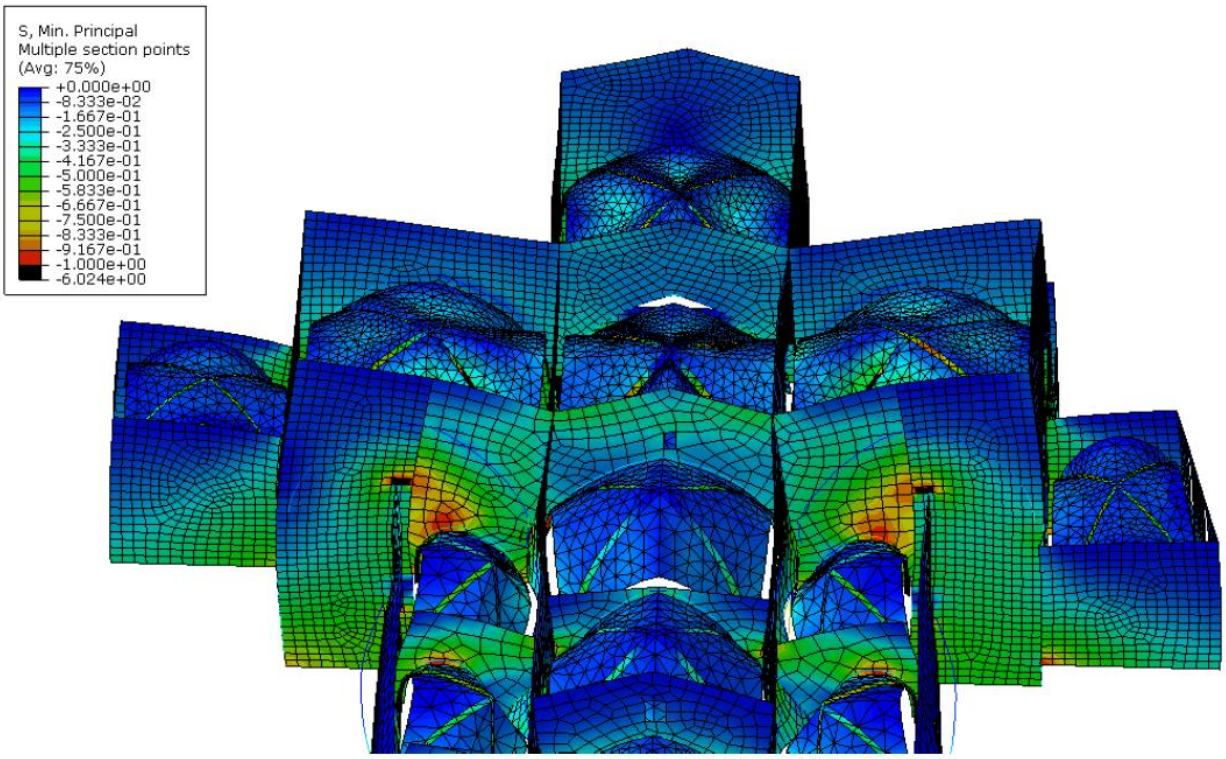

Figure 130 minimum principal stress for internal walls in previous model

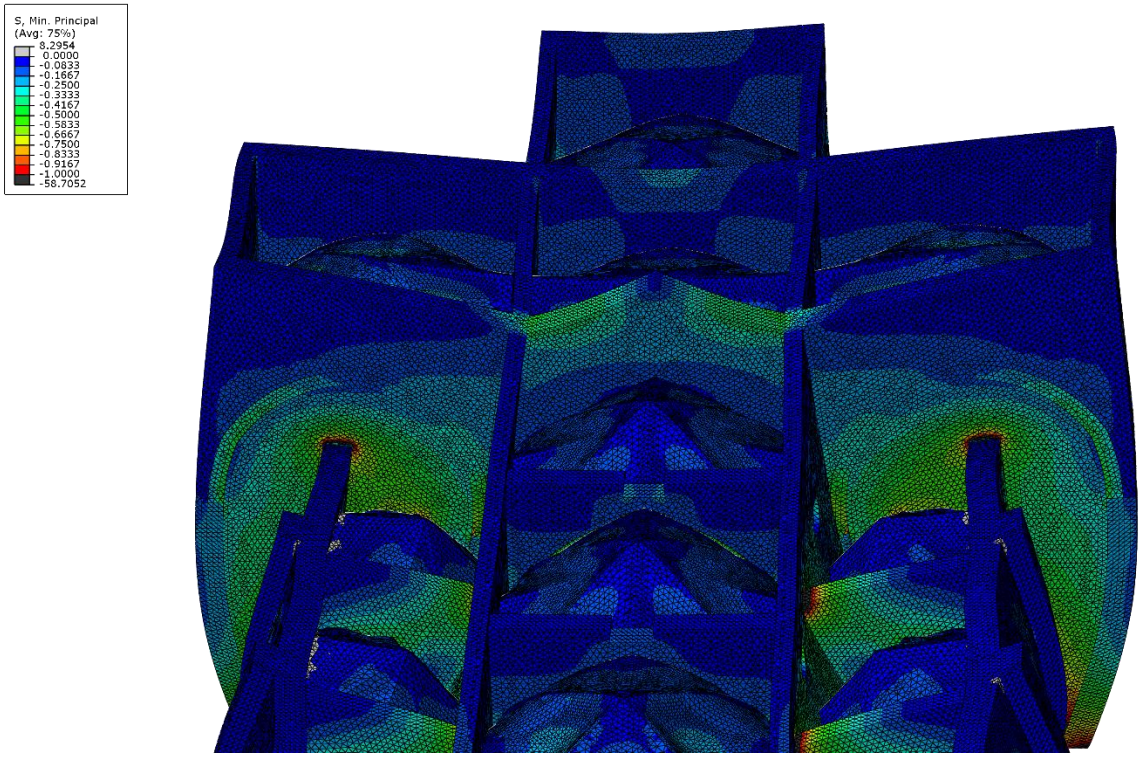

Figure 131 minimum principal stress for internal walls in new model

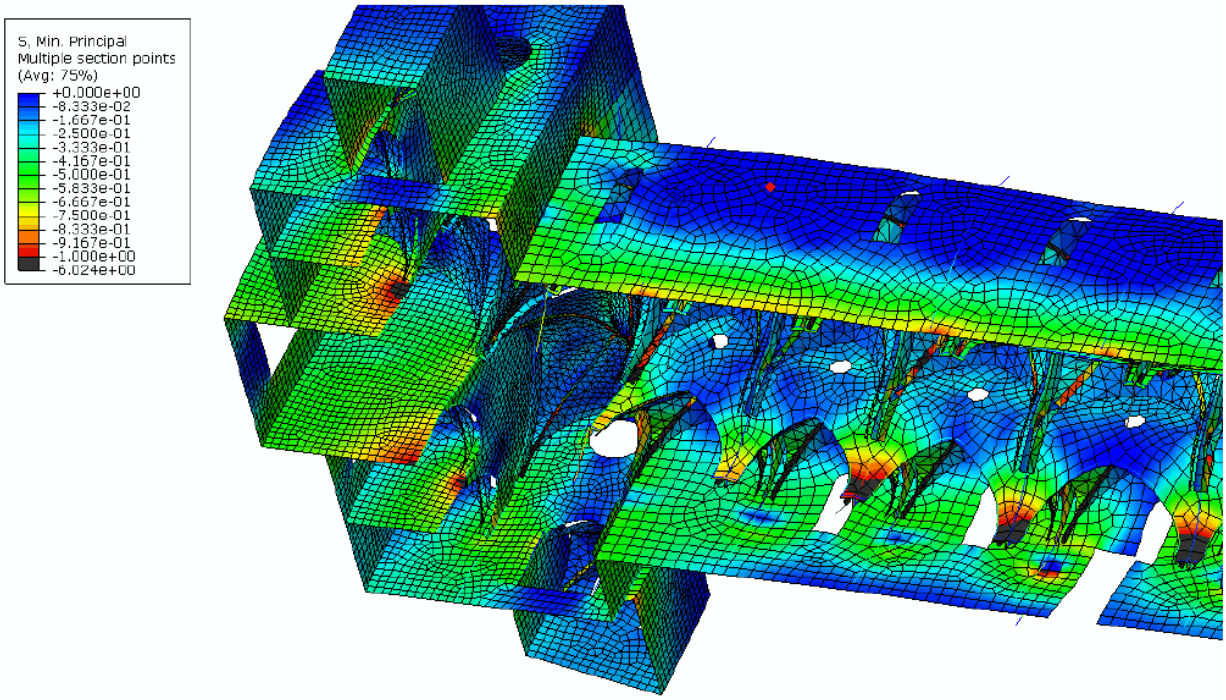

Figure 132 minimum principal stress for internal walls in previous model

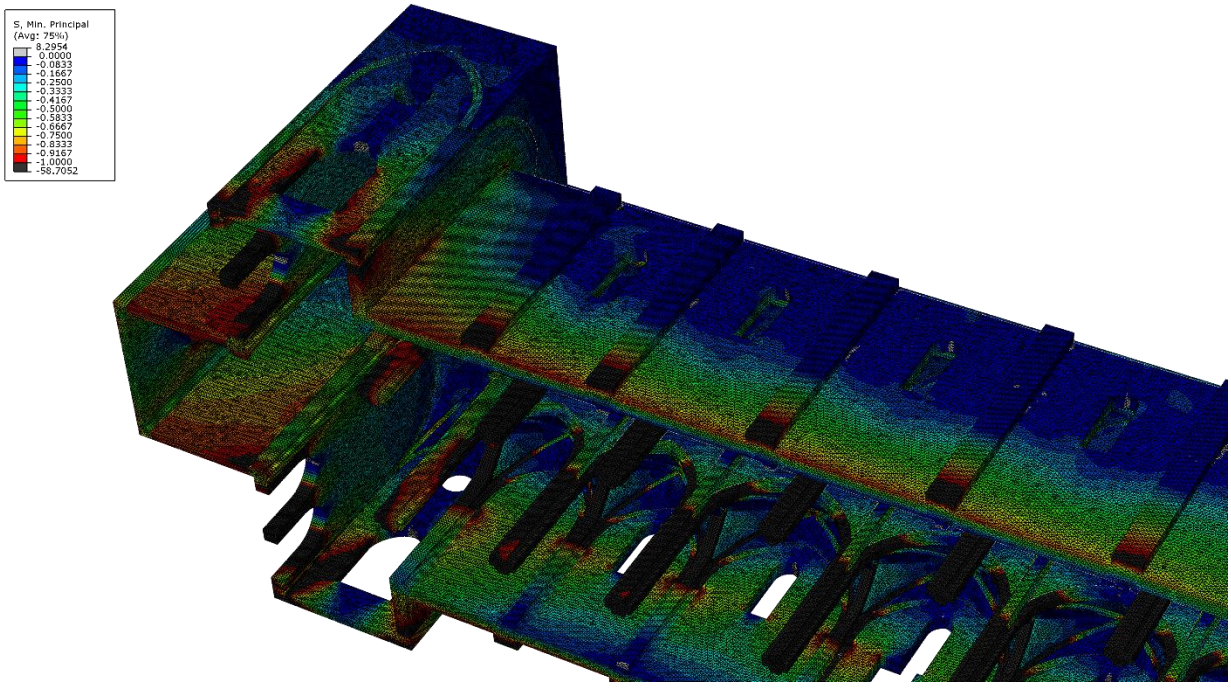

Figure 133 minimum principal stress for internal walls in new model

4.8. Comparison of the analysis results with existing crack pattern

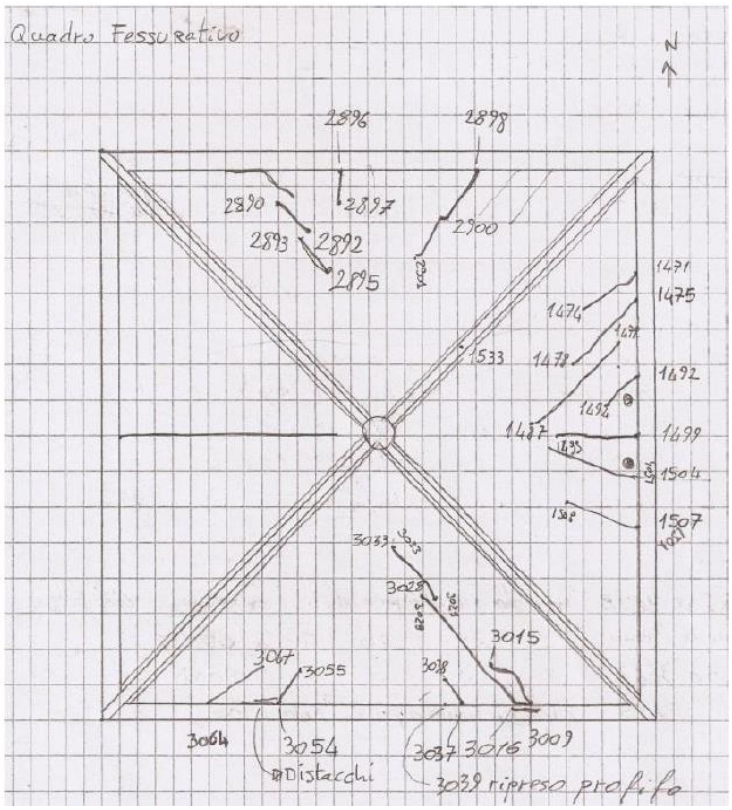

Figure 134 Crack pattern of the vault

The crack pattern of the transept vault is done by surveying the vault and measuring the length, depth and exact position of the cracks on the vault.

All the cracks occur near the lateral arches to which the vault are connected.

The zones in that two different parts with different materials are connected to each other, it is much probable to exist concentration of the stress. Consequently they are more likely to have some cracks in these areas.

By comparing the analysis results and crack pattern, a good correspondence is noticeable between the analytical and experimental results.

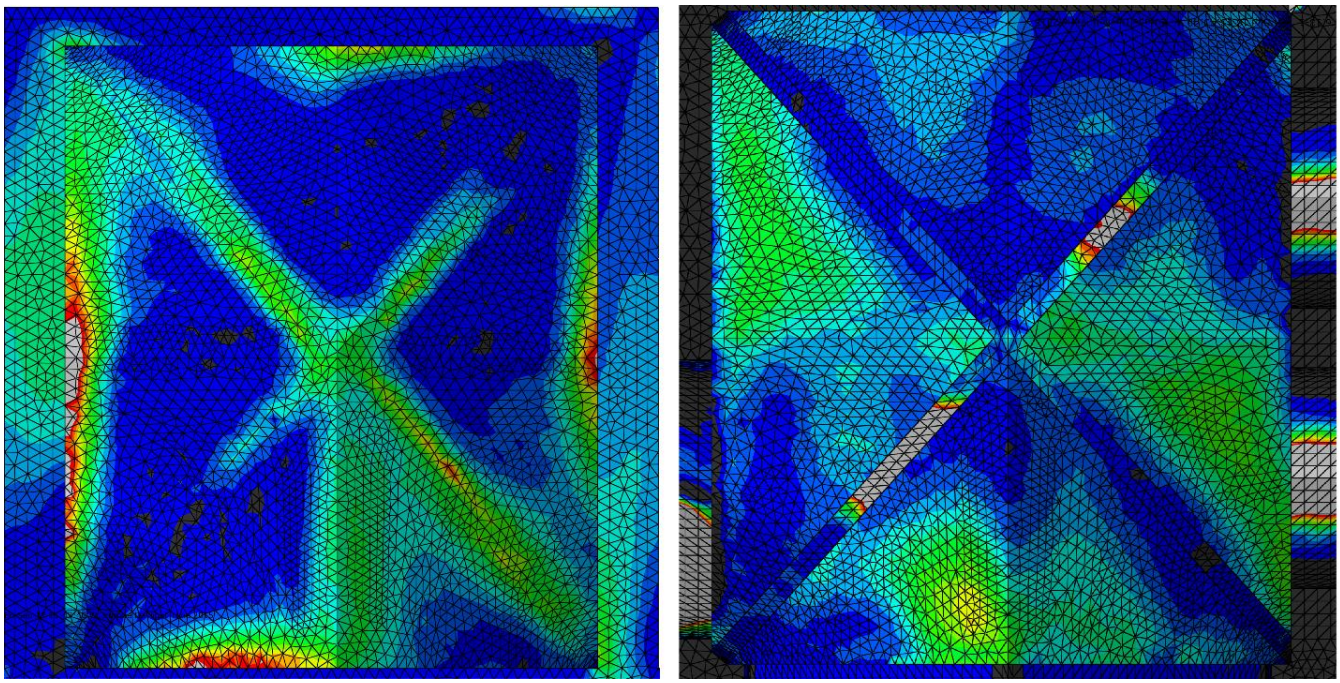

Figure 135 Maximum principal stress on the vault, extrados and intrados view

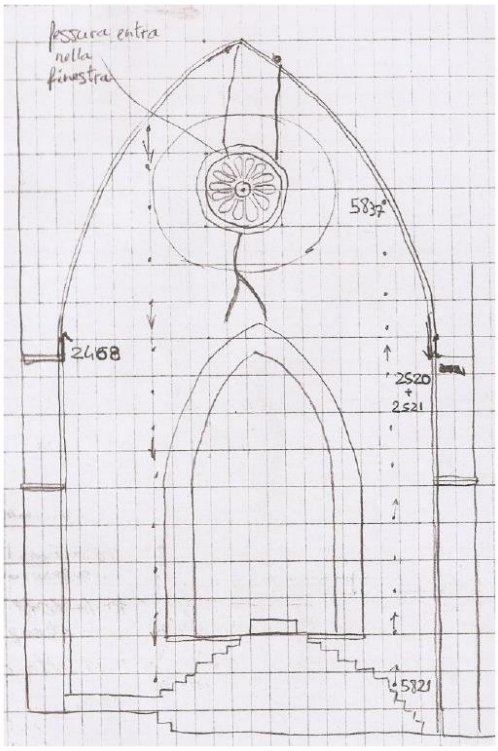

Existence of the cracks on the northeastern later wall of the transept is shown in figure 136. One of the cracks starts from upper cut out part and continuous until the lower cut out part.

Figure 136 Crack pattern of the northern east wall

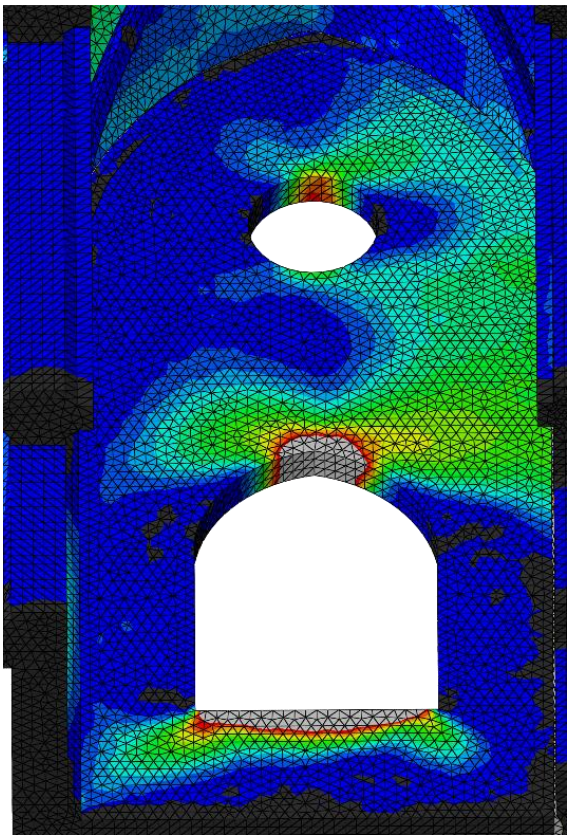

Distribution of the maximum stress on the northeastern lateral wall of transept, shows concentration of the stress in the zones near top of the cut out's arch, and also concentration of stress near the circular cut out part.

By comparing the both figures with together, it is seen a good correspondence between the crack pattern and the analysis results. Thus it can stated, the zones near cut outs are more prone to be cracked or to be in the path of crack propagation.

Figure 137 maximum principal stress

Conclusion

In this project 3D model of the church is designed in the way that is so similar and close to the real geometry of the model. Because of having a model with three-dimensional elements, it is possible to study and check the analysis results of any element and part of the model after accomplishing FEM analysis.

As the geometry of the new model and the system of loading are almost symmetric, so the analysis shows the existence of symmetry in terms of all the results, including displacements, maximum principal stress, minimum principal stress and other parameters.

By comparing the analysis results of the model with seeding of 80cm and the models with seeding of 20cm, it is obtained that there are higher maximum displacement values in all U1, U2 and U3 directions in the model with 20cm elements respect to the model with 80cm elements. The increase in the maximum displacement values is about 10-15%.

The middle part of the nave can be considered the most deformed part in both of the models. The external walls are also very deformed at the middle of the plasters. They supposed to be the most critical part of the church in terms of the maximum principal stress.

In previous thesis project, the generation of the model is done with the external walls having 2.35 meter of thickness which is much thicker than the walls of the new model having 1.35 meter of thickness. As a consequence, the external walls in the new model have more critical conditions compared to previous model.

There is always a concentration of the stress in the zones in which the parts are connected to each other. In some cases because of assignment of the different material to different parts, even if deformation is continuous, there are very different values of the stresses in these zones.

There is a good correspondence between experimental Crack pattern of the vaults and the distribution of maximum principal stress obtained from analysis results. Considering the locations of the maximum stress on the vault, the critical zones for occurrence of the crack can be predicted. Also the analysis results of the north eastern wall, are corresponded with the real pattern of the existing crack on the wall.

By considering the results of the maximum principal stress of the model, the zones in which there are cut outs, they are highly probable to occur cracks around the cut outs.

Recommendations for further research

This thesis project has raised more questions in need of further researches. Thus, it is recommended that further research be undertaken by taking these considerations into account:

- Designing the cross sections of the ribs and arches according the real shapes of these elements.
- By defining the seismic parameters and loading, performing static and dynamic seismic analysis too.
- By increasing the knowledge of the construction process, determining which parts have interaction with other parts, and also which type of the interaction describes the best real condition of the structure.
- There are some geotechnical and on site parameters which are strongly affecting the safety factor and the structural condition of the church. So it is recommended to do some on site experimental tests to get more knowledge about important parameters, for example to measure the settlements of the pillars bases and external walls, in the case there are noticeable values of settlements, try to consider these effects in the analysis too.
- Some pillars are not completely vertical cause of out-of-plump phenomena occurrence over the years. By taking into account these parameters in the model or in the analysis procedure, more real and accurate results can be obtained.

References

- Binda, L., Boothby, T., Condoleo, P., Cardani, G, Cantini, L., and Smith, E., 'Santa Maria Novella and the Development of a Florentine Gothic Structural System', Proc. Int. Symp. On Studies on Historical Heritage (SHH-07), Antalya, Turkey, September 17-21, 2007.
- Boothby, T., Binda, L., and Smith, E., 'Structural and Historical Assessment of Santa Maria Novella, Florence, Italy', Proc. 10th North American Masonry Conference, St. Louis (MO), USA, June 3-6, 2007.
- Smith, E.B., 'Santa Maria Novella e lo sviluppo di un sistema gotico italiano', In 'Arnolfo di Cambio e la sua epoca: Costruire, scolpire, dipingere, decorare', Atti del Convegno Internazionale di Studi, Firenze-Colle di Val d'Elsa, 7-10 marzo 2006, Vittorio Franchetti Pardo (Ed.), Rome : Viella, 2006, 289-298.
- Erdogmus, E., Boothby, T.E., and Smith, E.B. 'Structural appraisal of the Florentine gothic construction system', Journal of Architectural Engineering, 13(1) (2007) 9-17.
- Lourenço, P.B., 'Computations on historic masonry structures', Progress in Structural Engineering and Materials, 4(3) (2002) 301-309.
- Studies on historical heritage Santa Maria Novella and the development of a Florentine Gothic structural system L. Binda, T.E. Boothby, P. Condoleo, G Cardani, L. Cantini, E.B. Smith
- On Site Assessment of Concrete, Masonry and Timber Structure SACoMaTiS 2008 L. Binda, M.Di Prisco, R. Felicetti
- Erdogmus, E. Structural Appraisal of the Florentine Gothic Construction System, Ph.D. Dissertation, The Pennsylvania State University, July 2004.
- Polesano, Leonardo, Santa Maria Novella: Indagini sulle volte della basilica. Tesi di Laurea Trienalle. Politecnico di Milano, Facoltà di Architettura, 2007.Smith, Elizabeth Bradford.
- Santa Maria Novella e lo sviluppo di un sistema gotico italiano. In Arnolfo di Cambio e la sua epoca: Costruire, scolpire, dipingere, decorare. Atti del Convegno Internazionale di Studi, Firenze-Colle di Val d'Elsa, 7-10 marzo 2006, Vittorio Franchetti Pardo, ed., Rome : Viella, 2006, pp.289-298.
- Final Project Report Santa Maria Novella, Florence, Italy prepared by: Thomas E. BoothbyDepartment of Architectural Engineering the Pennsylvania State University 104 Engineering Unit at University Park, PA 16803-1416, USA.
- Simulia, Abaqus Analysis User's Manual, Providence RI (2011).
- Simulia, Abaqus/CAE User's Manual, Providence RI (2011).
- Simulia, Abaqus Example Problems Manual, Providence RI (2011).
- Simulia, Abaqus Theory Manual, Providence RI (2011).

– *Basilica di Santa Maria Novella a Firenze: Modellazione Geometrica e Analisi strutturale del Transettoproject, Relatore: Prof. Alberto Taliercio, Correlatrice: Arch. Paola Condoleo, Candidato:Andrea Manini*.

– *Maple: Programming, Physical and Engineering Problems Paperback – February 2, 2006 by Victor Aladjev (Author), Marijonas Bogdevicius (Author), chapter 2: Application of Maple for solution of engineering-physical problems.*

List of Figures